EE213. Microscopic Nanocharacterization of Materials
Lecture 12. 2016

Scanned Tip Microscopies
a. Scanning Tunneling Microscopy
b. Atomic Force Microscopy
c. Near Field Optical Microscopy
d. Scanning Conductance Microscopy

Today, final paper topic due by midnight
(list top three choices)
March 1, final paper rough outline due

Final Paper

1. Paper: due last day of class

2. Topic should be about a particular microcharacterization technique and comparison with at least one other method. From topics covered in course outline.

3. You must discuss the spatial resolution characteristics and limits.

4. Abstract or summary of each paper listed as references.
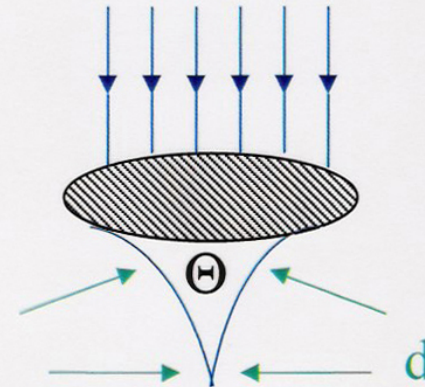
5. Discuss typical application use, briefly.

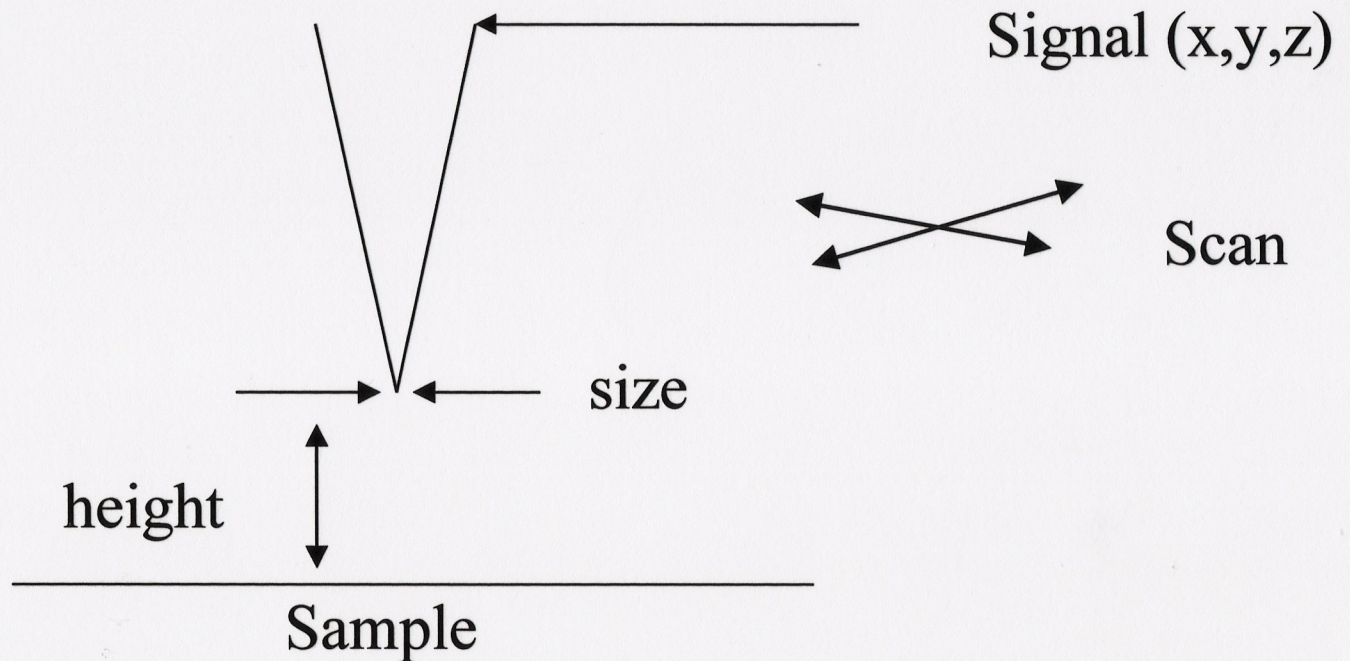# Microscopy Through the Centuries

$$d = \text{constant} \cdot \frac{\lambda}{n\sin\Theta}$$

To get better resolution:

1) Reduce λ
   electrons, xrays
2) Increase $n\sin\Theta$
   better lenses, "oil"
3) Decrease constant
   confocal
4) Take away lenses
   near field
   scanned tip

Scanned Tip Microscopy

Signal (x,y,z)

Scan

size

height

Sample

- **_Resolution is a function of size, height and mechanism used_**

    - *no lenses are used*

    - *Far field optics is not involved*

<u>lensless microscopies</u>

"scanned tip" or "scanned probe" microscopy

generic: SPM //

Scan a "tip" over a surface.
lateral resolutions a convolution of:

1) tip size
2) height of tip above surface
3) interaction process

further away from surface, the poorer the lateral resolutions.

In gen'l, SPM is a surface (or near-surface) technique

key technical element: — control tip position with
resolution ≤ tip size.

— piezo·electrics ///

show list/   a plethora of methods:
             we will discuss some (not all)

show
delatalk
pix adverted

— 1ST gen'l use of this method was the "surface profiler" —
         had ~ μm lateral resolutions, nm vertical resolutions
              just drag W tip across a surface.

DEKTAK 150
SURFACE PROFILER

The industry leader in performance, repeatability and application versatility

Dektak 150 Surface Profiler NEW

High performance repeatability, versatility and value in a single system

Industry-leading performance, repeatability, and standard scanning range size are all built into the Dektak 150 Surface Profiler – the culmination of four decades of stylus profiler technology innovations.

The Dektak 150 Surface Profiler offers a variety of configurations and add-on options for superior repeatability, programmability, low-force characterization, and detailed analysis. For power, performance, and reliability, there has never been a more complete profiler at a better price.

Established types of scanning probe microscopy

- AFM, atomic force microscopy [1]
  - Contact AFM
  - Non-contact AFM
  - Dynamic contact AFM
  - Tapping AFM
- BEEM, ballistic electron emission microscopy[2]
- CFM, chemical force microscopy
- C-AFM, conductive atomic force microscopy[3]
- EFM, electrostatic force microscopy[4]
- ESTM electrochemical scanning tunneling microscope[5]
- FMM, force modulation microscopy[6]
- KPFM, kelvin probe force microscopy[7]
- MFM, magnetic force microscopy[8]
- MRFM, magnetic resonance force microscopy[9]
- NSOM, near-field scanning optical microscopy (or SNOM, scanning near-field optical microscopy)[10]
- PFM, Piezoresponse Force Microscopy[11]
- PSTM, photon scanning tunneling microscopy[12]
- PTMS, photothermal microspectroscopy/microscopy
- SECM, scanning electrochemical microscopy
- SCM, scanning capacitance microscopy[13]
- SGM, scanning gate microscopy[14]
- SICM, scanning ion-conductance microscopy[15]
- SPSM spin polarized scanning tunneling microscopy[16]
- SSRM, scanning spreading resistance microscopy[17]
- SThM, scanning thermal microscopy[18]
- STM, scanning tunneling microscopy[19]
- SVM, scanning voltage microscopy[20]
- SHPM, scanning Hall probe microscopy[21]
- SXSTM synchrotron x-ray scanning tunneling microscopy

from Wikipedia

SIGNAL (X,Y,Z)

scan

TIP SIZE

HEIGHT

SAMPLE
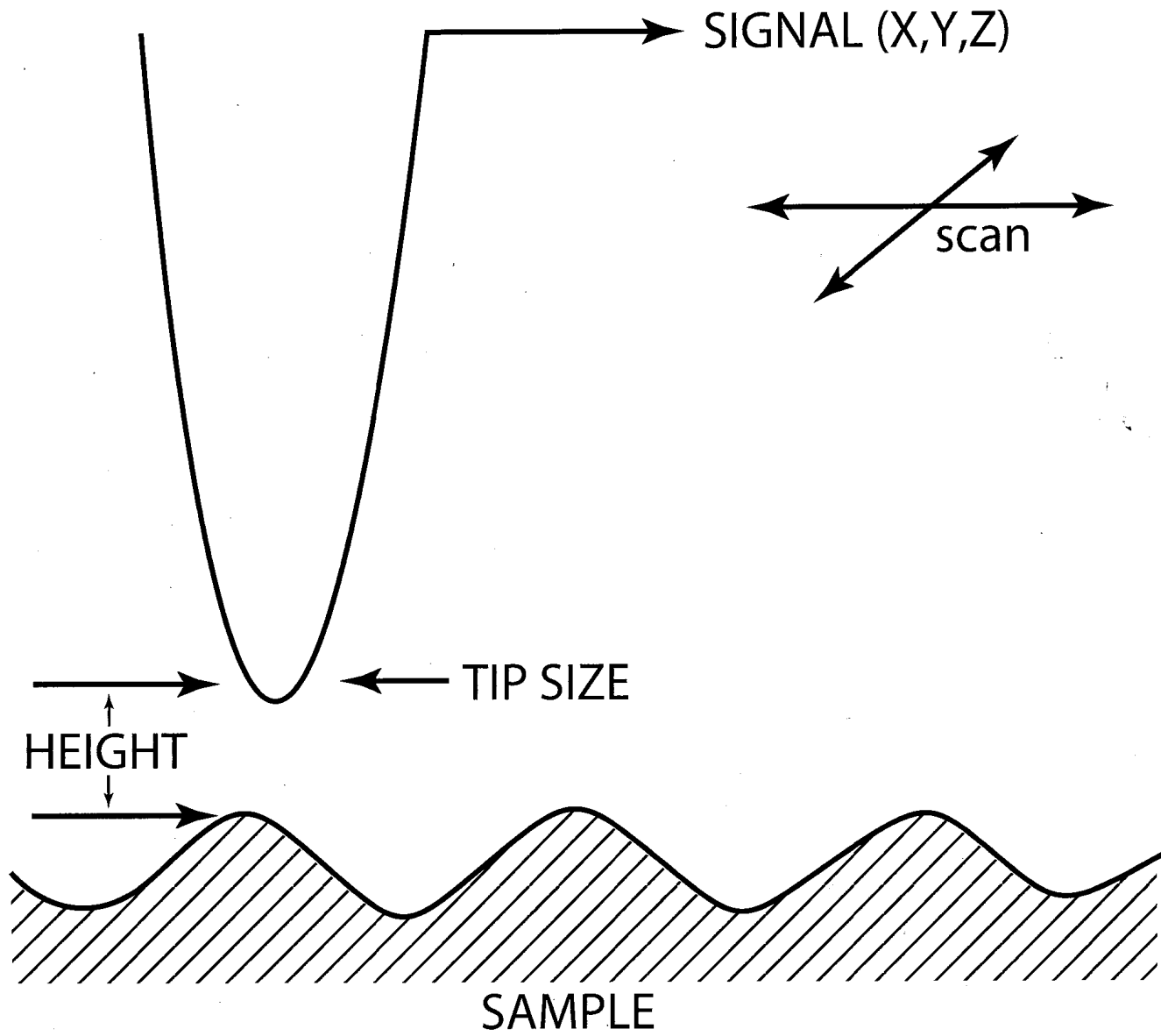
the advent of reproducible piezo elec stages
led to the scanning tunneling Ulmge by
Binnig and Rohrer in the 1980's and the STM
proliferation —
   But the principle of using QM tunneling at
the nm scale and below is actually due to
Russell Young/
          /R.D. Young, Rev Sci. Instr. 37(3). 1966. p 275-278

→ called "field emission ultramicrometer" ←
technology kept resolution to 10nm
— NBS killed project

taken up again by Binnig & Rohrer in early 1980's.
⎰ G.H. Binnig, H. Rohrer and, Ch. Gerber   ⎱
⎱ and E. Weibel (1982). APL. 40. 178-80   ⎰
⎱   "   (1982). Phy Rev Lett. 40. 178-80 ⎰

good older STM review:
         P.K. Hansma and J. Tersoff (1987)
              J. Appl. Phy. 61. R1-23.
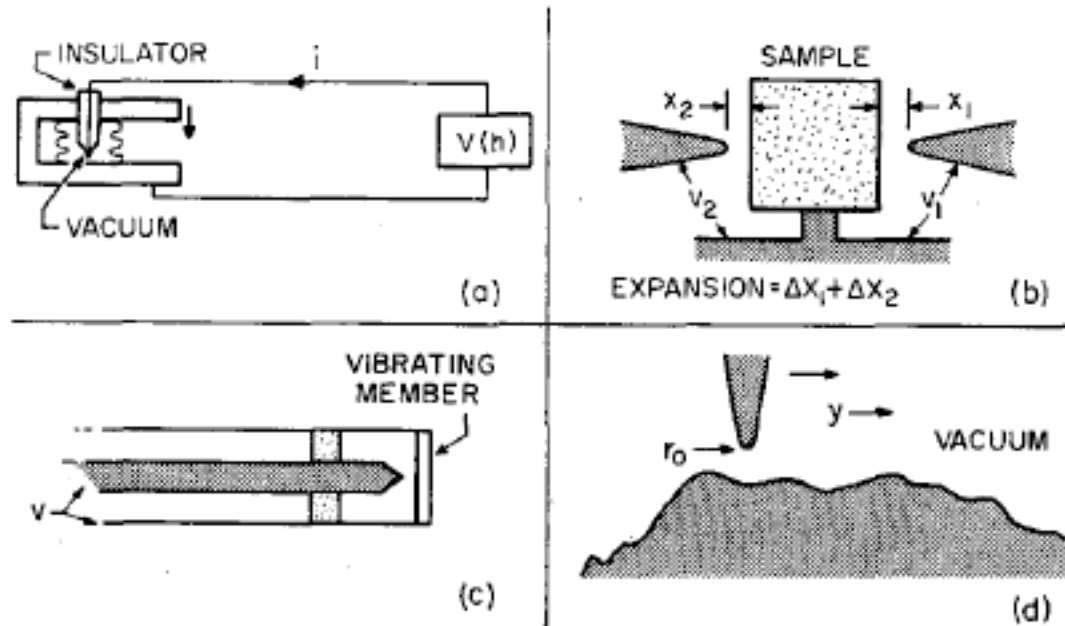
FIG. 5. Applications of field emission ultramicrometer; (a) strain gauge, (b) differential thermal expansion cell for small samples (c) mechanical vibration sensor, and (d) surface profile delineator.

R.D.Young, Rev. Sci. Instr. 37(3). 1966.pp.275-278.

Scanning Tunneling Mlwpy (STM)

Principles of general SPM

2 modes of operation

[ƒ pzyo]

1. use pzyo to keep tip at constant height, s from surface — pzyo voltage then is modulated with variations in height due to interaction (f(ht))

or 2. keep pzyo voltage constant, interaction signal changes as tip-sample distance changes.

for STM:
- monitor piezo voltage that moves tip up/down.
- monitor "tunneling" current between tip-sample.

doc camera
pic of tunnely

consider 1D tunneling between 2 plane electrodes — $\left(\dfrac{V}{\text{between}}\right)$

$$\boxed{I(\vartheta) \propto e^{-2KS}} \quad \text{where } S \text{ is dist. between}$$

$$K = \frac{2\pi}{h}\sqrt{2m\varphi}$$

where K is the decay constant for the electron wave function in the gap and Φ is local work function. (effective)

∴ for typical Φ ≅ 4eV (like in W)

E_{F1} ϕ_1 V ϕ_2 E_{F2} s

TIP
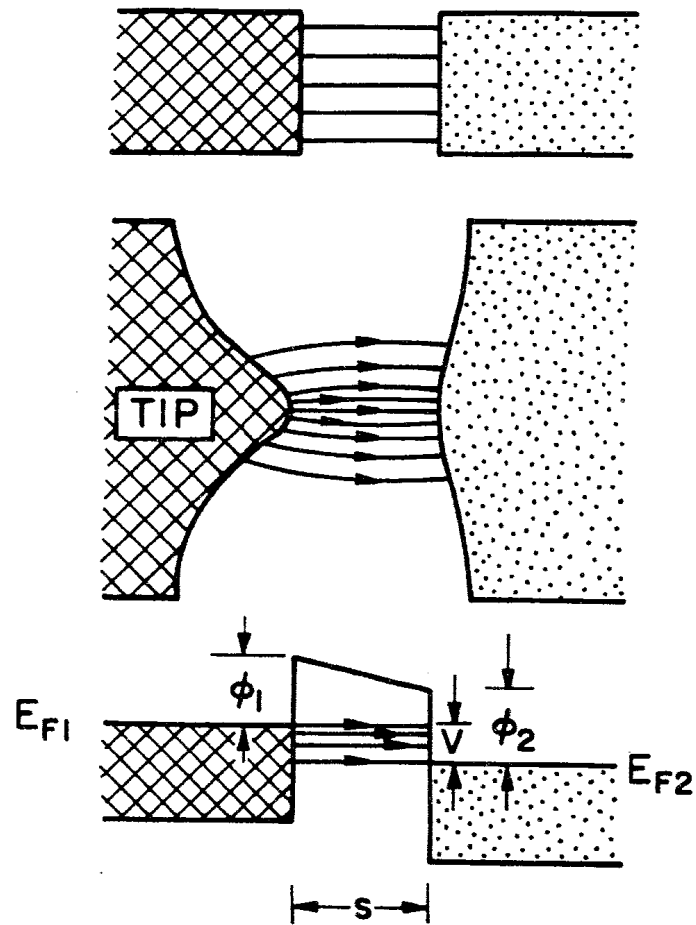
STM schematic of tunneling

we get $K = \frac{2\pi}{h}\sqrt{2m\varphi} \cong \frac{1}{Å} = 1 Å^{-1}$ ///

∴ for every decrease in gap s by 1Å
I ~~decreases~~ increases by e^2 / almost order of mag!

— thus, in "const. height" mode
one keeps voltage on tip fixed – (should be const. V mode)
as tip scans in xy, gap dist. changes,
thus I gets modulated by ~~its~~ surface topog

— in const. current mode, one changes voltage on
piezos to keep dist to sample constant
(ie tips moves up & down to track sample)
so I = constant. then that voltage modulation
related to topography.

NOTE // simple picture not exactly correct at
atomic resolution. ie, if we have an
atomically sharp tip scanning across
a "irregated plane" of atoms.
it is not clear what is "s" ——

moreover, tunneling involves states
at Fermi level — so "local density of states"
these affect tunneling current
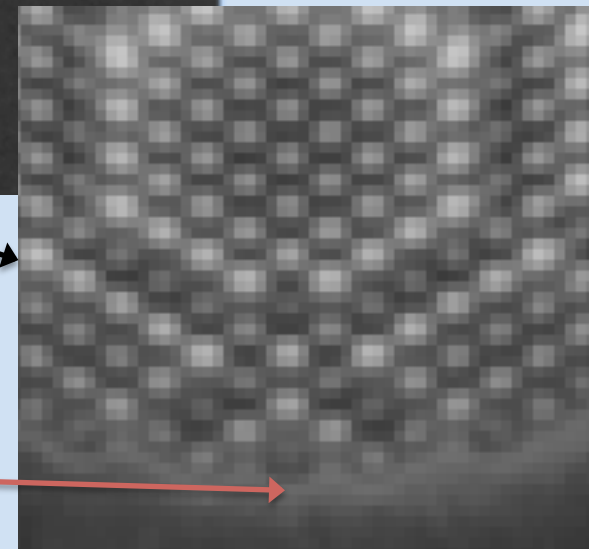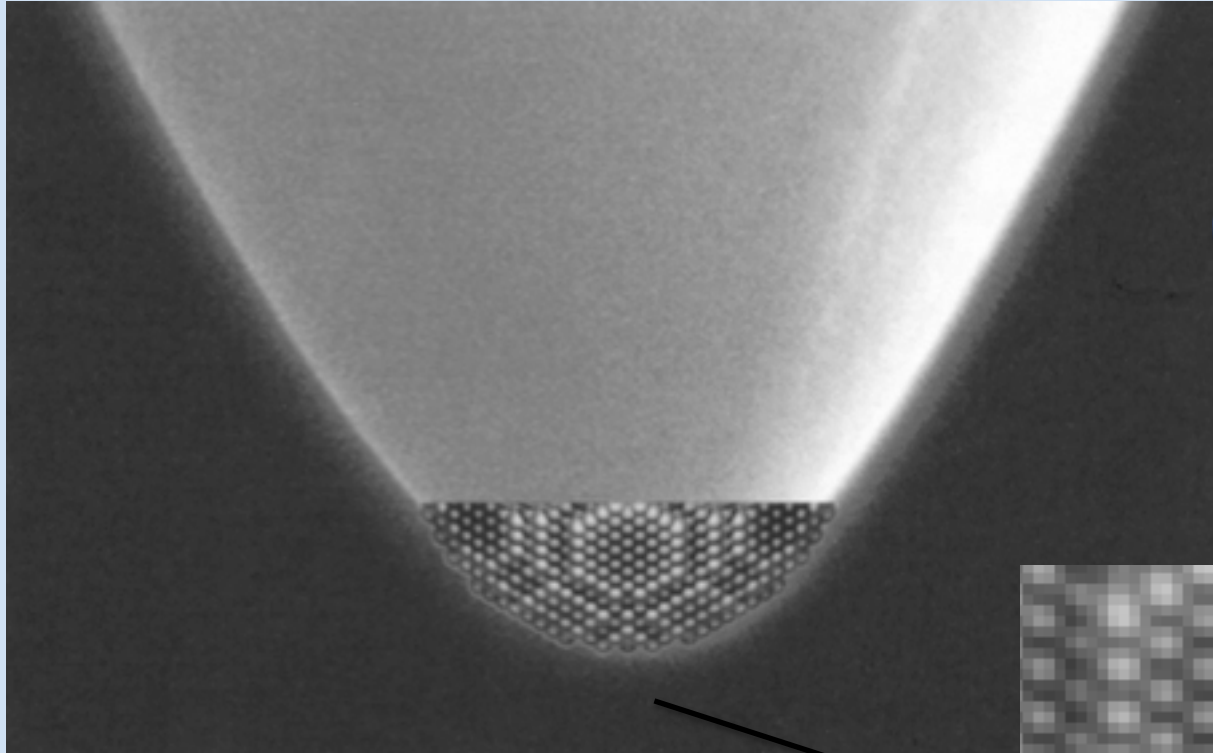— complex elec. structure / real 3D problem

cont
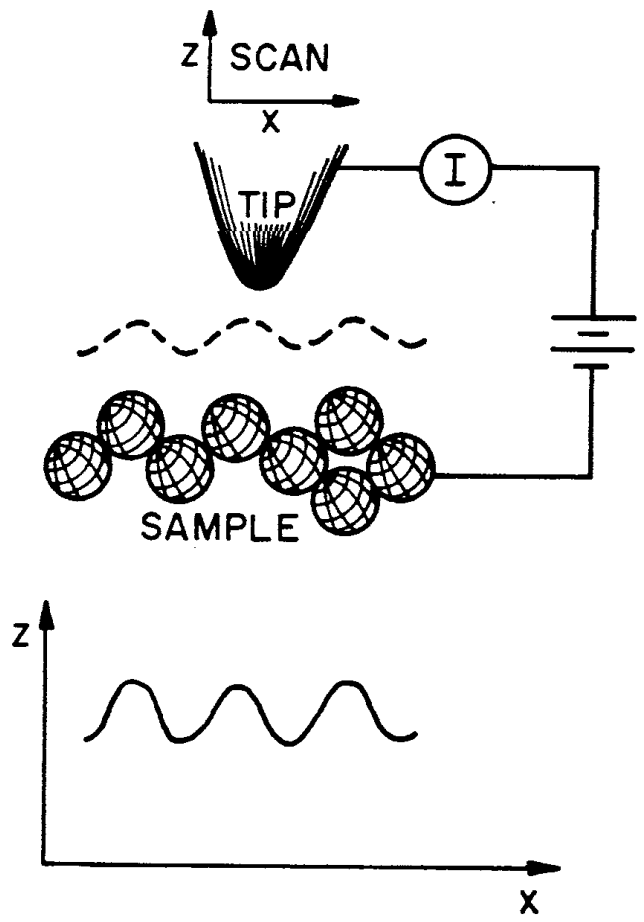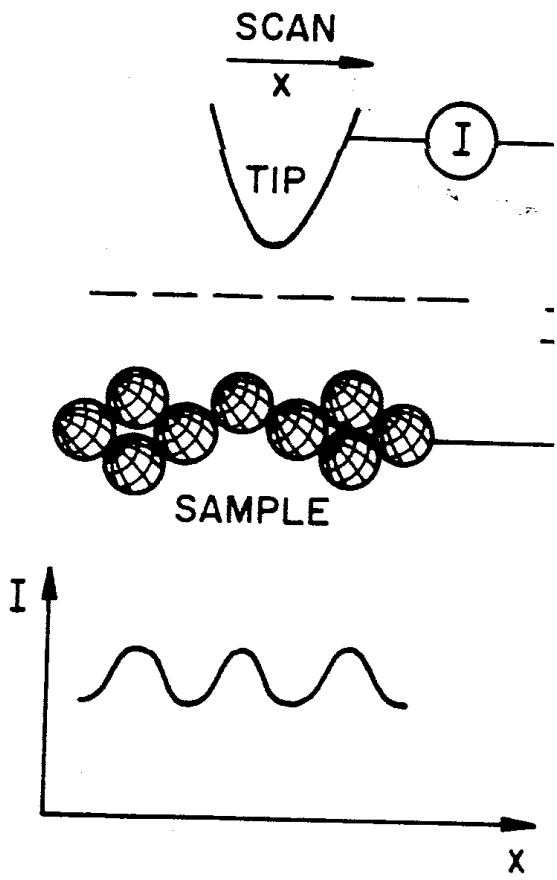
figure 2. common STM operational modes

Field Emission Tip

Single atom protrusion

..so in real world, how do we interpret the "tunneling" image?

when "tip" is a single atom or a cluster of a few then tip maps out a constant local surf density of states — ie we approximate image as a "topog" map.
      see example of calculations

const. I mode // keeps s constant by changing V_{piezo}
    ∴ need feedback —
    assuming avg. Φ is constant, then for
    resolutions > nm, this is essentially a
    topog. map.

const. height mode (ie V_{piezo}= const)
    current changes as s changes
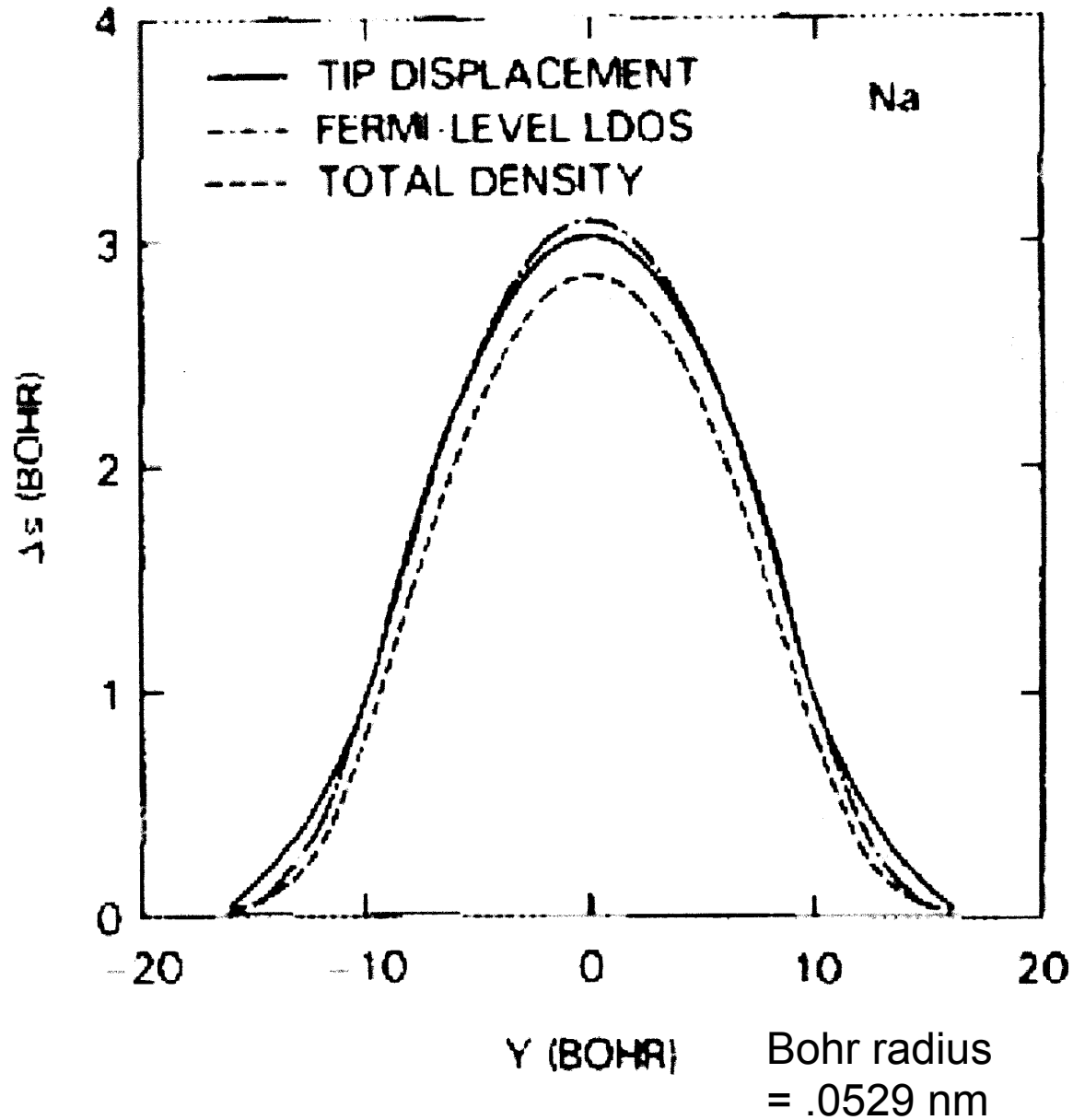   but no don't need feedback — ∴ can scan
    faster! BUT doesn't work on rough surface!
       crash!
    thus this is limited to "smooth" surfaces

$$I = const. e^{-2ks}$$

so STM like SEM in that image interpretation
at zeroth order is easy — but you need
to be careful
    pt to note: since $k = \frac{2\pi}{h}\sqrt{2m\Phi}$
    variations in Φ look like variations in s
       but

from Hansma & Tersoff

if V between tip and sample $\ll \varphi$ then

tunneling current density
$$J = \frac{2\pi e^2}{h} \frac{KV}{4\pi^2 S} e^{-2KS}$$

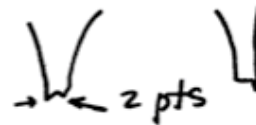where $K = \frac{2\pi}{h} \sqrt{2m\varphi_{EFF}}$, $\varphi_{EFF} = \frac{1}{2}(\varphi_S + \varphi_{TIP})$

NOTE: $K \neq K(V)$ as long as $V \gg \varphi_{EFF}$

if that is not the case
then exponential factor is V dependent

ie, to separate out S variations from
φ variations you need more than
1 measurement
— get at this by dI/dV measurements etc
at each pt as well

NOTE: tip is crucial for interpretation

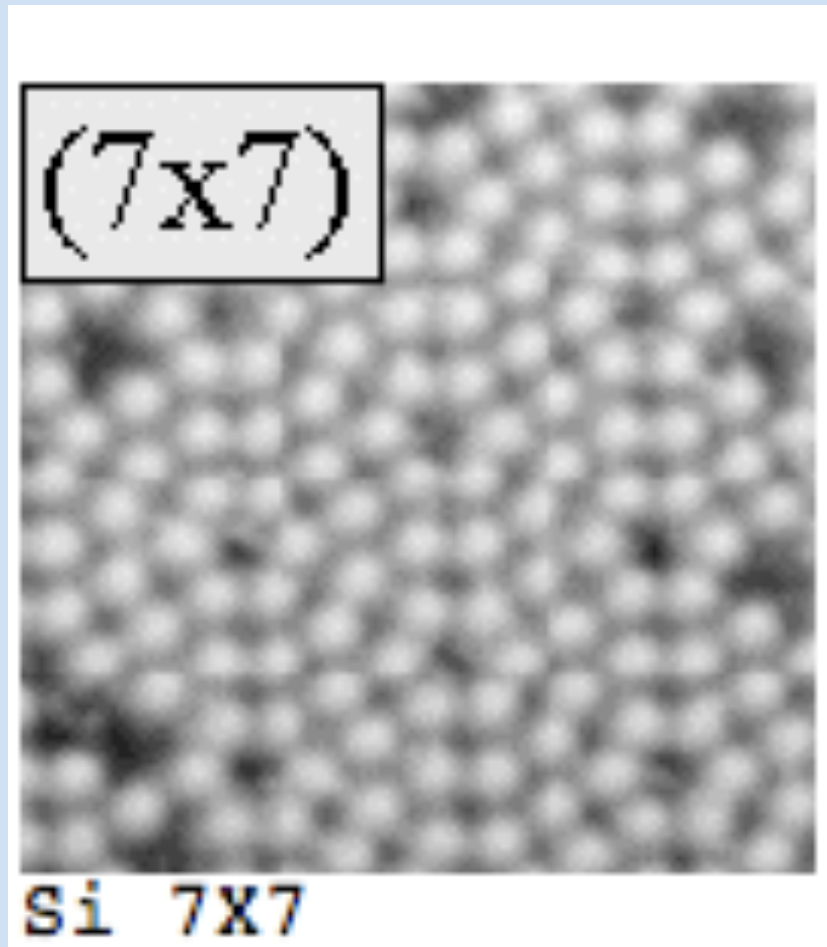eg if it looks like this
one gets confusing
imaging $\rightarrow$ 2 pts

since can get variation in φ as:
$$\frac{d(\ln I)}{dS} \propto \frac{d}{dS}(-2KS) \propto \sqrt{\varphi}$$ oscillate
lot of tip
by ΔV_{piezo}

STM tutorial

(7x7)

Si 7X7

www.fkp.uni-erlangen.de/methoden/stmtutor/stmpge.html
T. Fauster
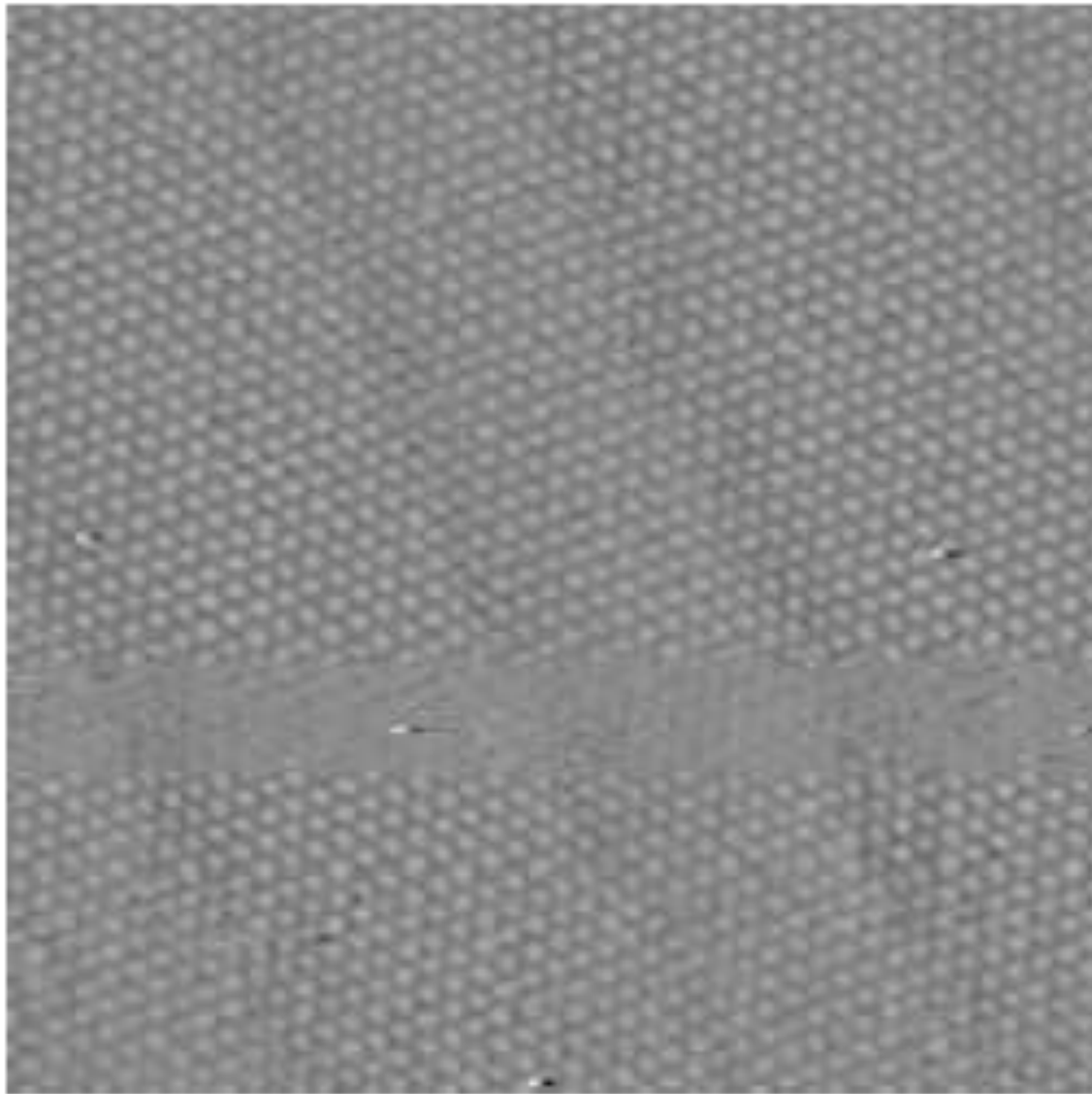
Atomic resolution of Au(111)

S

www.fkp.uni-erlangen.de/methoden/stmtutor/stmpge.html

STM (cont):

disadvantages/
— best with "smooth" samples
— best with conducting samples
— if used in air or water, interpretation
  gets complicated.

can get around some of those probs
with AFM/atomic force μscope

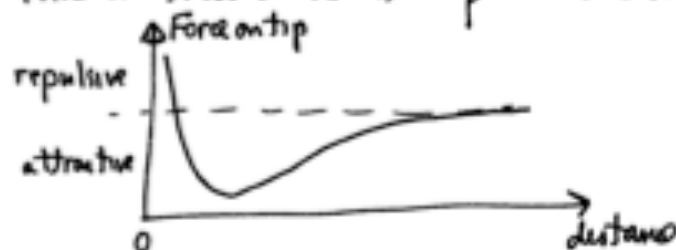ref: G. Binnig, C.F. Quate and Ch. Gerber (1986). Phys Rev Lett. 56, 930 [1]

// — sharp tip mounted on cantilever
   — laser focused on back of cantilever
   — back of cantilever reflects light to split photodiode
   —— Optical lever // ~ 10^3-10^4/1
      to monitor tip displacements (Hooke's law

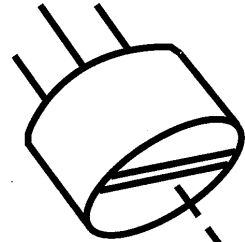several modes to look at the forces on
the cantilever.   distance
                                    F = -kS

Look at force curve as tip nears sample
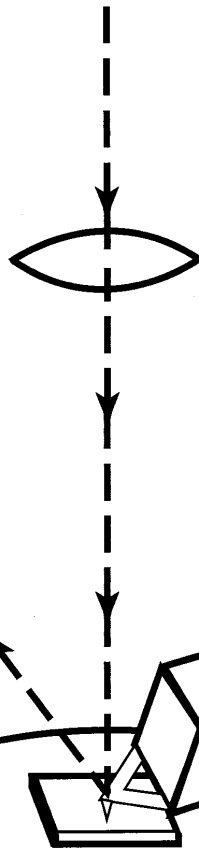

repulsive / attractive — Force on tip vs distance, 0
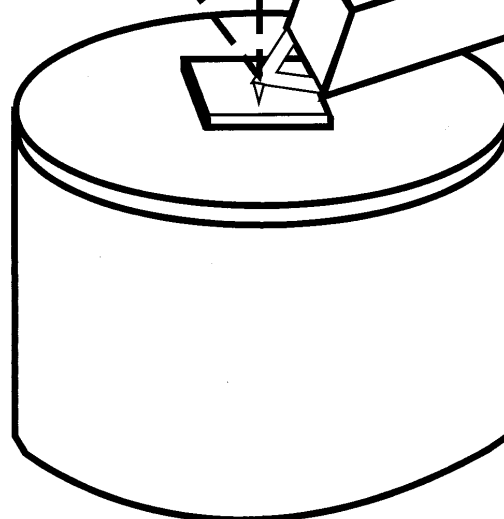
Atomic Force Microscope

LIGHT

PHOTODIODE

LENS

CANTILEVER

Binnig, Quate and Gerber.
Phys.Rev.Lett. 56.930 (1986)

XYZ TRANSLATOR

xyz translator

STM (cont):

disadvantages/
— best with "smooth" samples
— best with conducting samples
— if used in air or water, interpretation
gets complicated.

can get around some of those probs
with AFM/atomic force μscope

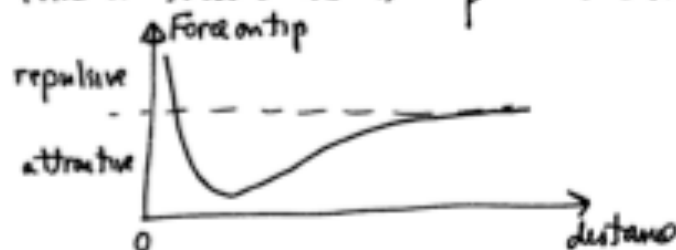ref: G. Binnig, C.F. Quate and Ch. Gerber (1986). Phy RevLett. 56: 930 [1]

// — sharp tip mounted on cantilever
— laser focused on back of cantilever
— back of cantilever reflects light to split photodiode
— optical lever //~$10^8 - 10^9$/1
to monitor tip displacements (Hooke's law

several modes to look at the forces on
the cantilever.   distance
                                        $F = -kS$

Look at force curve as tip nears sample

Force on tip
repulsive
attractive
0   distance

Tip is in hard contact with the surface; repulsive regime

Tip is far from the surface; no deflection

Tip is pulled toward the surface - attractive regime

Force

0

Probe Distance from Sample (z distance)

ration

properties of the "cantilevers" and tips for AFM.

spring const

$$F = -K\delta$$

1. want max. defl. for minimum. force
   soft spring, low k
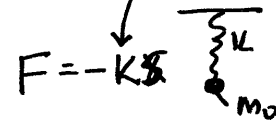
2. want min sensitivity to bldg. vibrations (20-100 Hz)

3. resonant freq. $f_0 = \frac{1}{2\pi}\left(\frac{K}{M_0}\right)^{1/2}$
   should be high.
   10's kHz or more

   effective mass that
   loads spring
   (ie, the tip)

   ∴ reduce K
   reduce M_0 further to keep $\left(\frac{K}{M_0}\right)$ large.
   ($< 10^{-10}$ kg).

— limits of AFM on force detection:
thermomechanical noise //

$Q = \omega/\delta\omega$

bandwidth

force noise, $F = (4K [k_B T] B / Q \omega_0)^{1/2}$

spring
const.

thermal
energy

qual factor

res-freq

hi Q
low T
hi ω_0

Tip is in hard contact with the surface; repulsive regime

Tip is far from the surface; no deflection

Tip is pulled toward the surface - attractive regime

Force

0

Probe Distance from Sample (z distance)
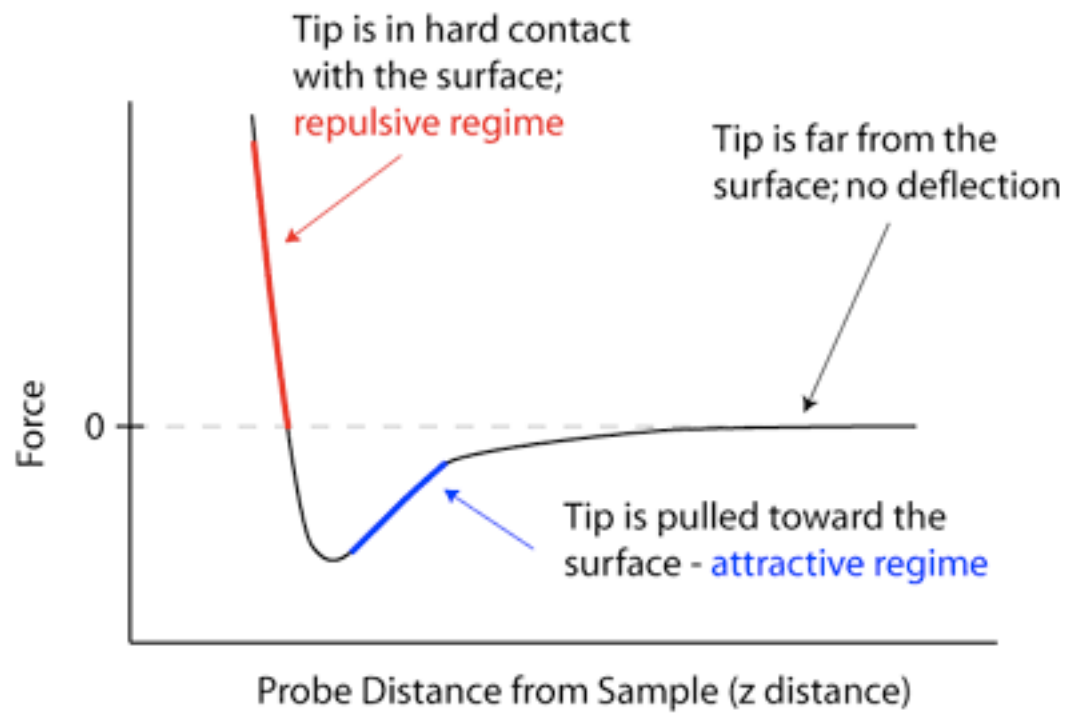
ration

AFM Cantilevers and Tips

Cantilever Geometry

Tip height h is to the middle of the beam
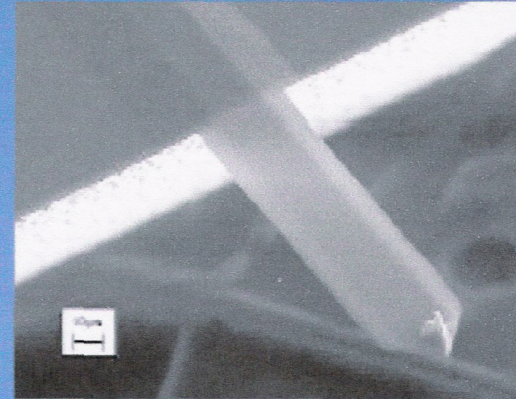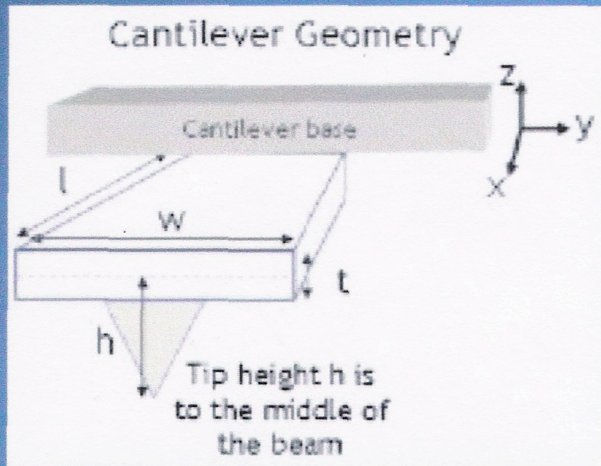

SEM image of cantilever

- Microfabricated cantilevers with integrated tips
  - Silicon nitride, silicon oxide, silicon
  - Spring constants: 0.1-1 N/m (contact), 10-100 N/m (non-contact)
  - Resonance frequencies: 1-50 kHz (contact), 100-300 kHz (non-contact)
  - Coatings depend on application: eg. conducting, magnetic, functionalized (specific molecules)

http://physics.usask.ca/~chang/course/phys404/STMandAFM.pdf
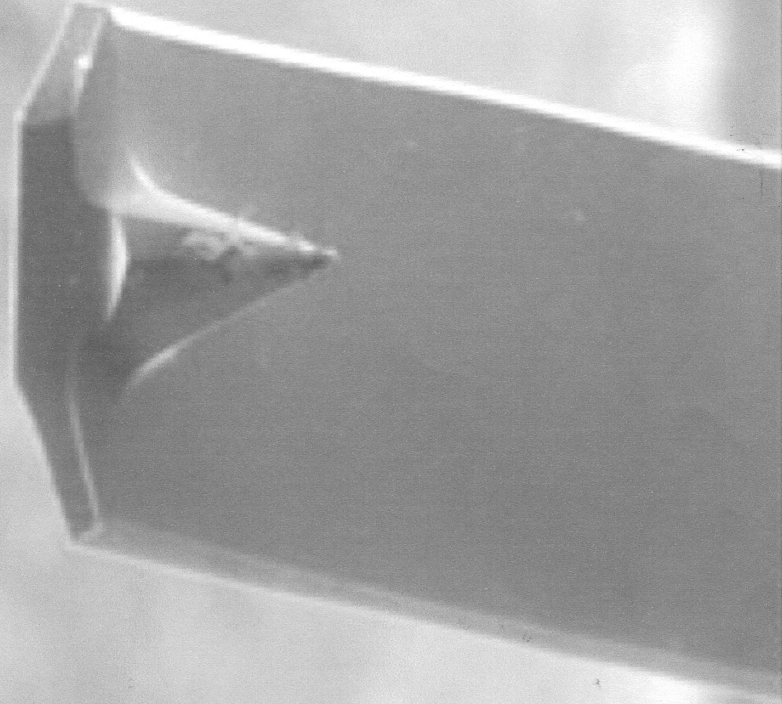
AFM (cont)

different forces

mech. contact force
van der Waal's force
capillary forces
chem. binding
electrostatic forces
magnetic forces (MFM)
~~etc~~ shear forces
etc...

all scanning done piezoelectrically.
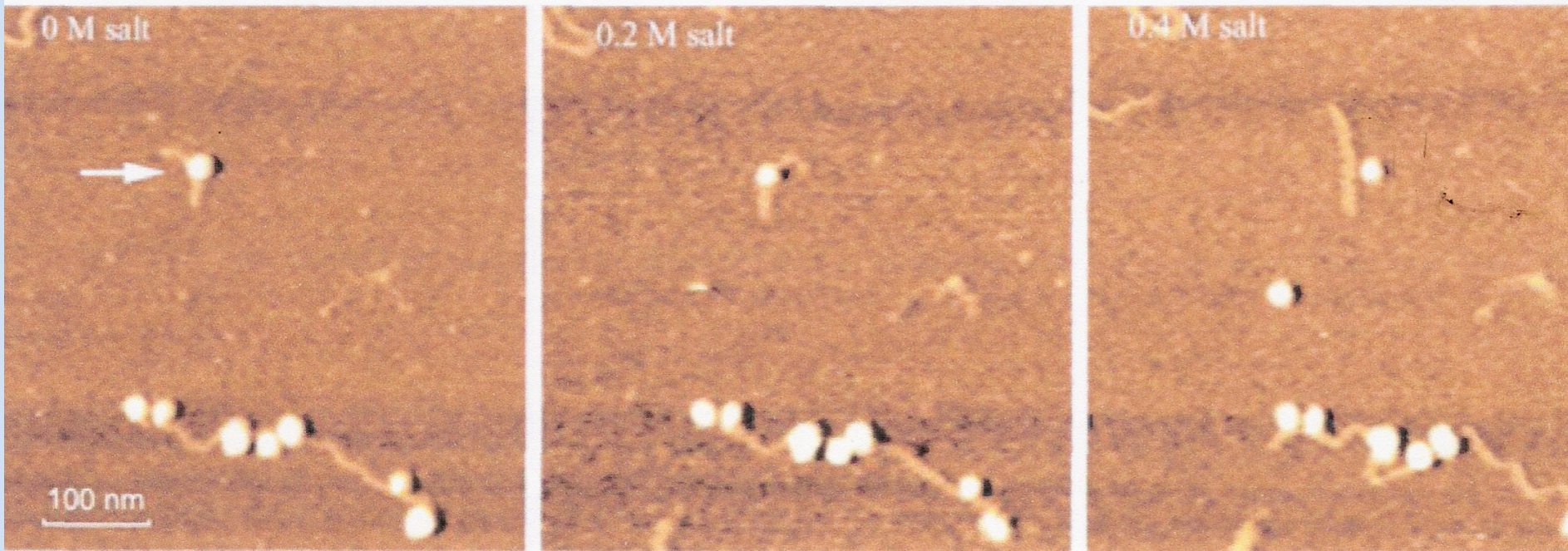
two modes

1. static
   deflection used as feedback signal/~~mechanism~~
   — probs. near surf, attractive forces can
     be large — such tip to sample
   — usually done "in contact" in repulsive mode
     force kept constant by maintaining
     const. defl.

2. dynamic
   tip "oscillates" (rather cantilever oscillate)
   — at freq. near fundamental resonance
     cont

Single Nucleosome Molecule

Scan Size 100 nm

In-situ observation of DNA and histone separation from a single nucleosome molecule due to increased salt concentration using a flow-thru cell.

AFM/

non contact model   cantilevers oscillated just above
             resonance. (< 10nm)
             Van der Waali forces predominate
             (1-10nm above surface)
             there decrease ~~osc. ampl~~ resonance
             freq of cantilever
             → goes to feedback to keep osc. constant
             thus, measure tip dist (avg).
             — best for "soft samples"

one generally uses freq mod under UHV conditions.
   (under low temp, thermal fluctuations reduced
     also)

A good reference for applications /
   Bushan and Kawata, eds.
      "Applied Scanning Probe Methods VI,
        Characterization. 2006 (Springer).

AFM //

oscillations ampl, phase and freq change
by tip-sample interaction forces.

— changes compared to ext. ref. oscillation and
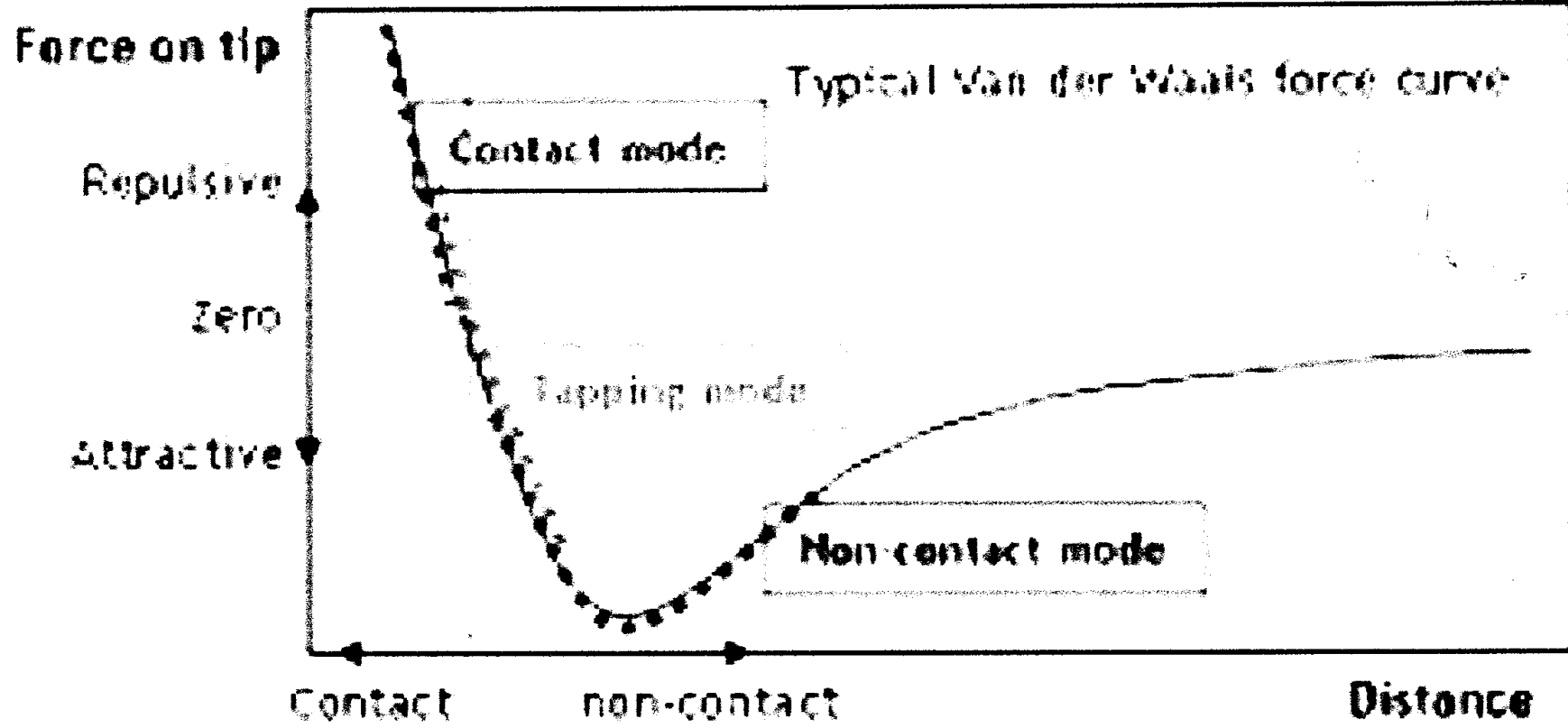give measure of force

In ampl. modulation, changes in osc. ampl u phase
used to provide imaging fr feedback.
- changes in phase can provide info on material
- whereas ampl. just gives us the topog.

freq modulation //
also
detect freq changes
which are demodulated
with an FM detector
- hi sensitivity
allows fr atomic
res at UHV

ampl. modulation: contact or non-contact

but in air or fluid to keep tip from
sticking to surface, one modulates the
distance between tip-surf. by oscillating
cantilevers — "tapping" — typical ~ 100 nm

tapping /
mode /

— as tip approaches surface, forces increase,
ampl osc decreases — piezo changes ht
to keep same ampl. osc /
o less destructive than pure "contact"
dragging over surface.

Typical Van der Waals force curve

Force on tip

Repulsive

Zero

Attractive

Contact mode

Tapping mode

Non-contact mode

Contact   non-contact   Distance
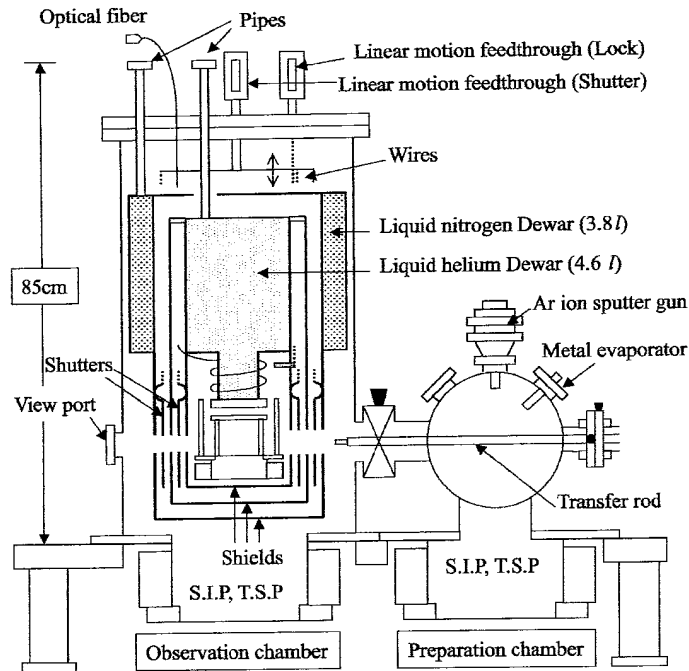
AFM forces/regions

⟨K. Mitchell⟩

Fig. 18.2. Side view of the observation and the preparation chambers for a low-temperature NC-AFM system

sample and cantilever exchange is performed even at low temperatures. The optimal and reproducible positioning of the optical fiber with respect to a cantilever can be performed with a specially designed three-dimensional micropositioner within 10 min.

As the force sensor, we used a conductive silicon cantilever with a sharpened tip. The spring constant and mechanical resonant frequency were 40–60 N/m and 150–170 kHz, respectively. The nominal radii of curvature for the tip apex were 5–10 nm. The silicon tip was cleaned by sputtering with Ar ions. There are the dangling bonds out of the silicon tip apex. The NC-AFM image was obtained under the constant frequency shift.

18.3
Identification of Subsurface Atom Species

NC-AFM has the capability to identify or recognize atom species on a sample surface, if we can control the atomic species at the tip apex. That is, we succeed in identification of Si and Ge atoms by imaging the Si/Ge intermixing Si(111) surface
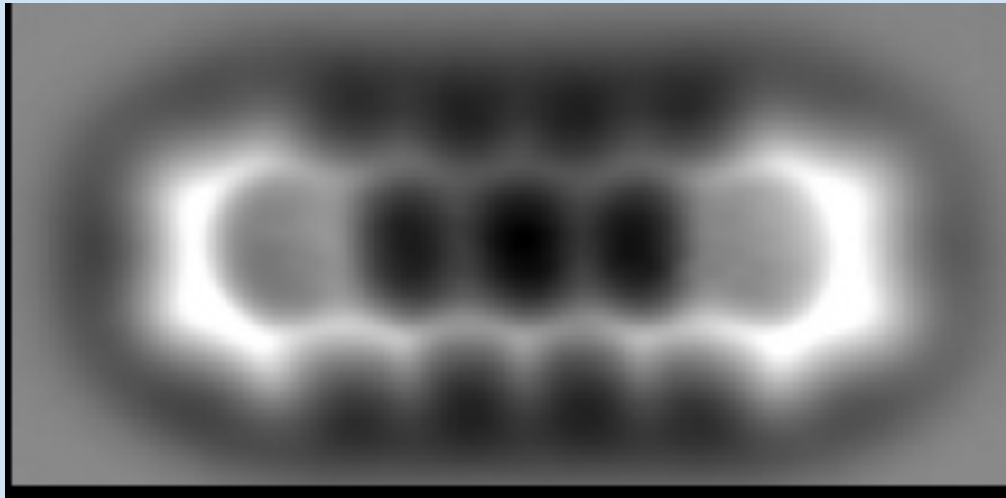
Pentacene molecule

Gross, L.; Mohn, F.; Moll, N.; Liljeroth, P.; Meyer, G. (2009). "The Chemical Structure of a Molecule Resolved by Atomic Force Microscopy". Science 325 (5944): 1110–1114.

EE213.

AFM modes of operation

contact mode :- maintain constant deflection
- hard contact with surf.
- lever stiffness < effective force holding atoms together $(1-10\,nN/nm)$
levers are $< 1\,nN/mm$

non-contact mode : oscillating cantilever
(in attractive regime)
low forces between tip-sample (pN)
- changes in res freq or ampl
$\quad$ (FM) $\quad$ (AM)

"tapping" mode : cantilever closer than in NC mode
- part of tip gets into "repulsive" regime.
- very stiff cantilevers (or tips stick in water contam layer)
- good for soft samples
- min. lateral force

force modulation : tip oscillated at lo freq into repulsive regime.
force vs dist correlates to elasticity.

phase imaging : measure phase shift relative to driving freq.—
measures. adhesion, viscoelasticity,

EE 213. Lecture 12

Near Field Scanning Optical Microscopy (NSOM)

E.H. Synge. Phil. Mag. 6 (1928). 356-362.
"A suggested method for extending
microscopic resolution into the
ultramicroscopic regime"

nephew of
JM Synge
"Playboy of
the Western
World"

Another scanned tip technique:

principles // —— resolution defined
by "opening"; within
λ from "opening" (near surface)
—— evanescent waves

trade-offs: resolution vs signal.

how do we make our optical probe? ⋁

tapered pipette or fiber //

throughput ?   fiber > pipette

throughput $(d)^4$ // ⟵ Power in/Power out

collimation ~ d, aperture ≥ size

9.5.28.

Co Dublin
Ireland.

Dear Professor Einstein.

I am much obliged for your letter. It was my original idea to have a very small hole in an opaque plate, as you suggest, and it was in that form that I had mentioned it to several people.

The employment of total reflection was an afterthought, and I fear I misunderstood a statement of Lord Rayleigh, from which I concluded that the object (Schicht S) could be brought as close as $\frac{1}{50}$ of a wave length from the quartz plate before the light came through from the plate generally, in the way you mention.

There remains the possibility of a _hole_ (ein winziges Loch). One actually finds such holes, ready to hand, in pieces of _badly_ silvered glass. A fragment from a cheap Thermos flask, for instance, contains countless small holes comparable in size with colloidal particles. No doubt they are due to the presence of colloidal particles on the surface of the glass, at the time of silvering. Unfortunately the silver rubs off very easily, and would be difficult to keep clean.

A better way would be, if one could construct a little cone or pyramid of quartz glass ◭ having its point P brought to a sharpness of order 10^{-6} c.m. One could then coat the sides and point with some suitable metal (e.g. in a vacuum tube) and then remove the metal from the point, until P was _just_ exposed.

I do not think such a thing would be beyond the capacities of a clever experimentalist. I know that needles can be made of quartz glass with exceedingly minute points, and there does not seem any reason why a point as sharp as 10^{-6} c.m. might not be secured.

If you should happen to know any experimental physicist who would care to try

NSOM (cont)

we can look at the probe size we form
in NSOM and far field optics

Far Field $I(r) = PSF(r) = |\mathcal{F}[A(\rho)]|^2$ square of
Fourier
Transform
of aperture
function

Near Field $I(r) = PSF(r) = |A(\rho)|^2$ square of
aperture
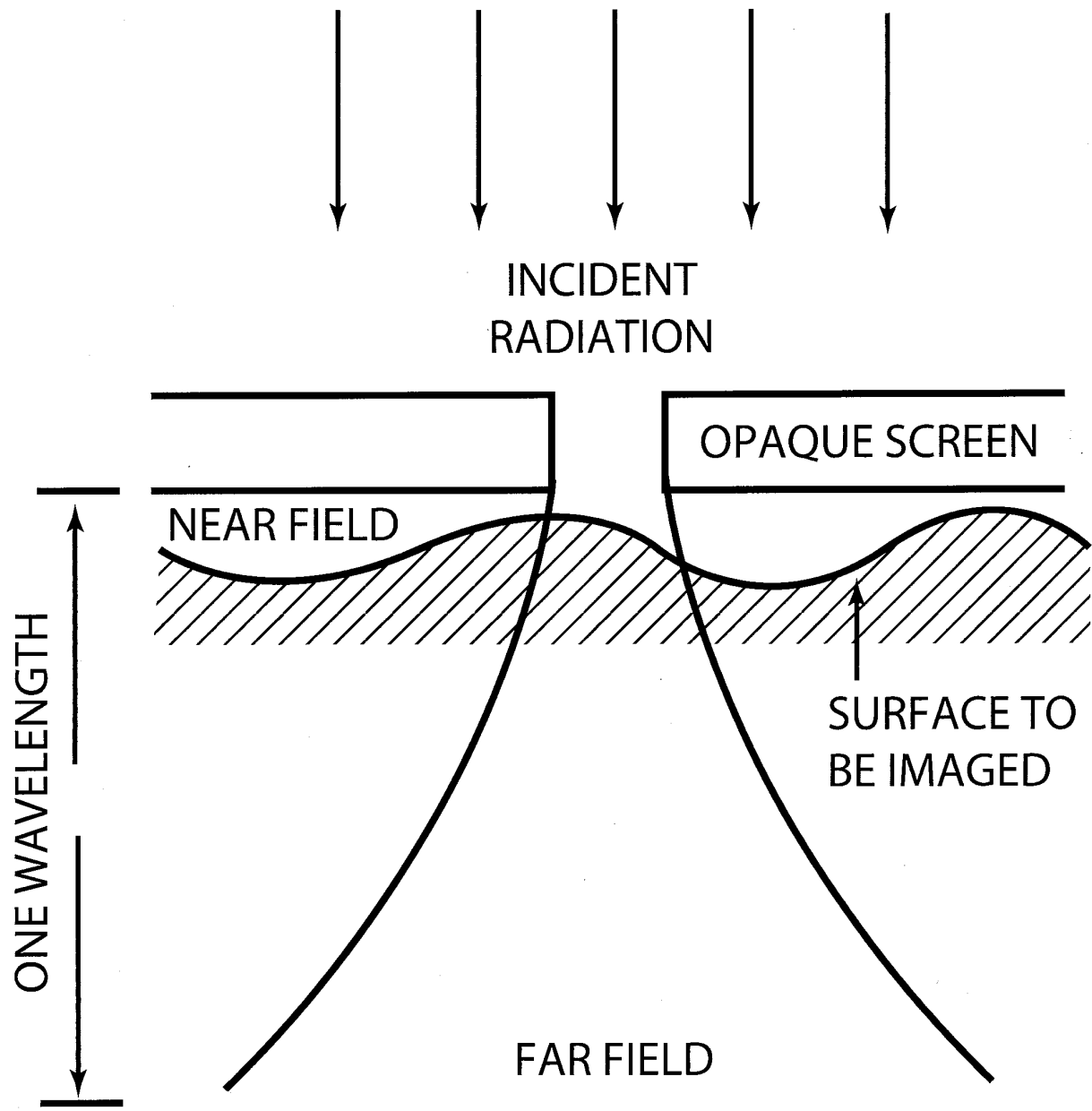function

"effective" aperture
depends upon how
much "leakage" thru the "screen"

different imaging modes /   with different "throughputs"

one can enhance "throughput" using a
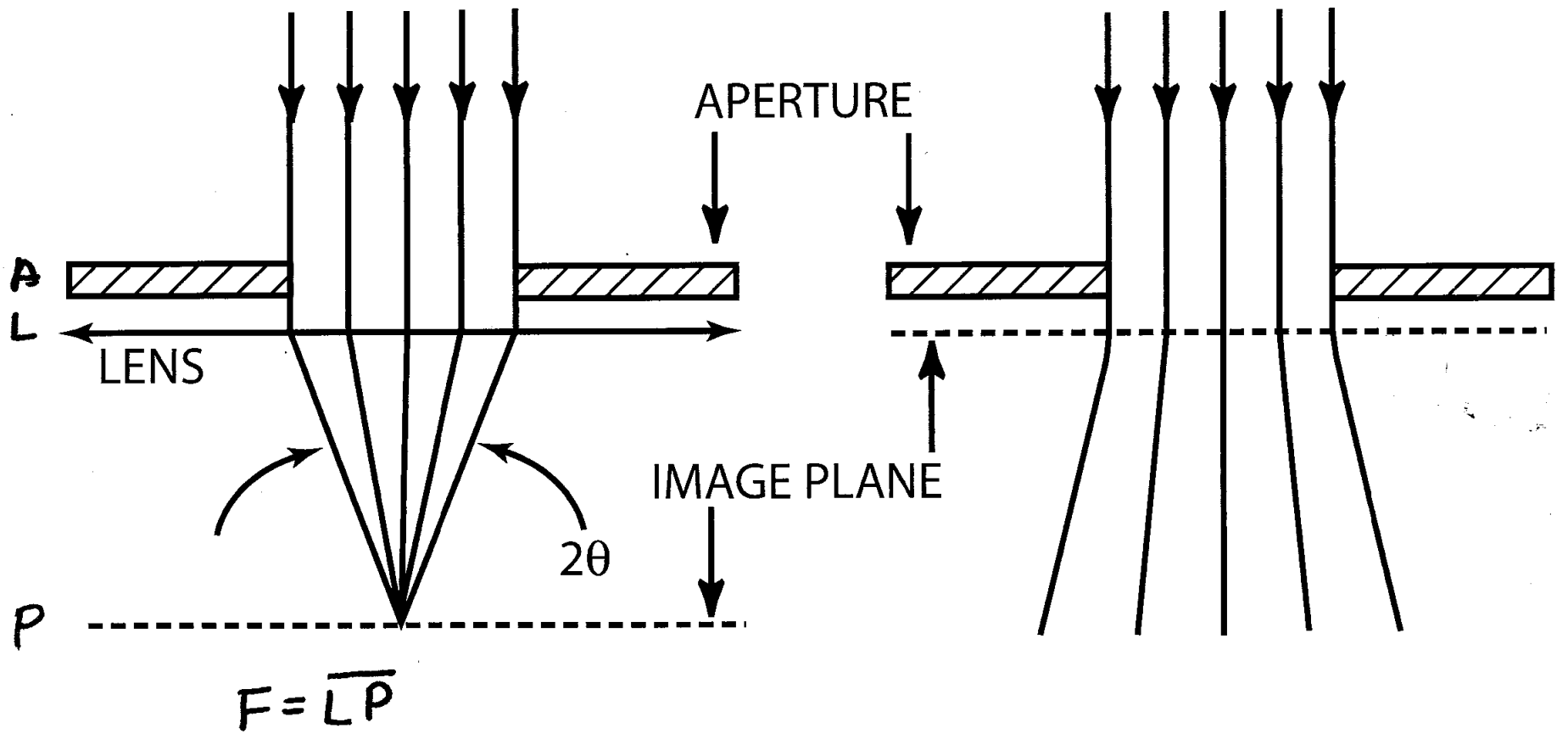metal tip to provide local excitation
ie, field enhancement

ref. Novotny and Stranick. Ann. Rev. Phys. Chem. 57
(2006). 303-331
"near field optical microscopy & spectroscopy
with pointed probes"

INCIDENT
RADIATION

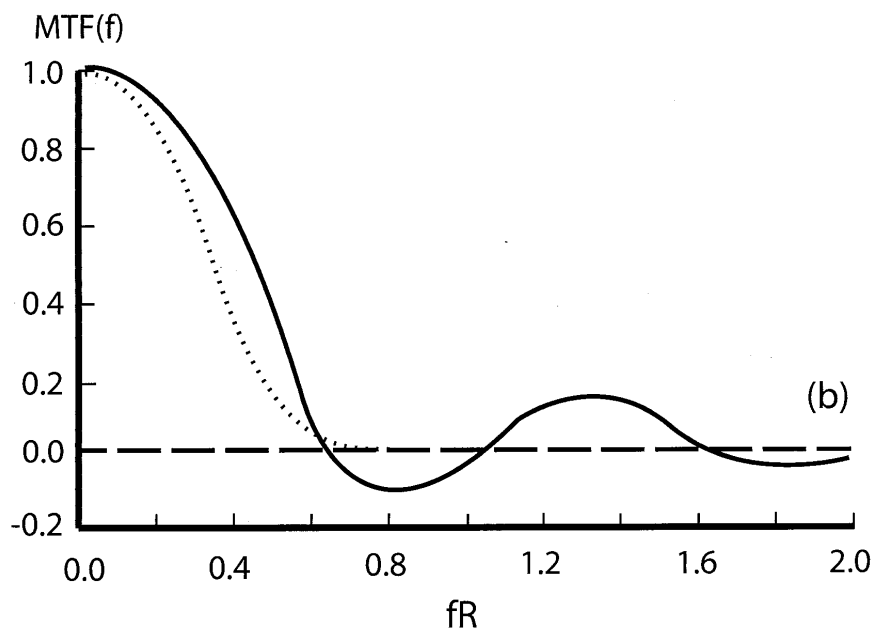OPAQUE SCREEN

NEAR FIELD

ONE WAVELENGTH

SURFACE TO
BE IMAGED

FAR FIELD

FAR-FIELD

NEAR-FIELD

APERTURE

A

L

LENS

2θ

IMAGE PLANE

P

$F = \overline{LP}$

FAR-FIELD

PSF(r)

(a)

r·(R/λF)

MTF(f)

(b)

f·(λF/R)

NEAR-FIELD

PSF(r)

opaque screen.

(a)

r/R

MTF(f)

(b)

fR

o metal coated glass pipette
□ metal coated single mode fiber

2R

↕ 10nm

measurement

FAR-FIELD

PSF(r)

(a)

r·(R/λF)

MTF(f)

(b)

f·(λF/R)

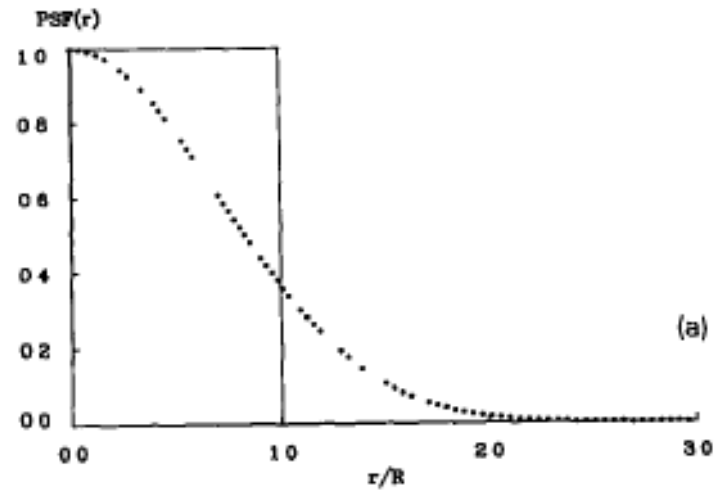Isaacson, J.Cline and H.Barshatsky. Ultramicroscopy.47.(1992).15-22.
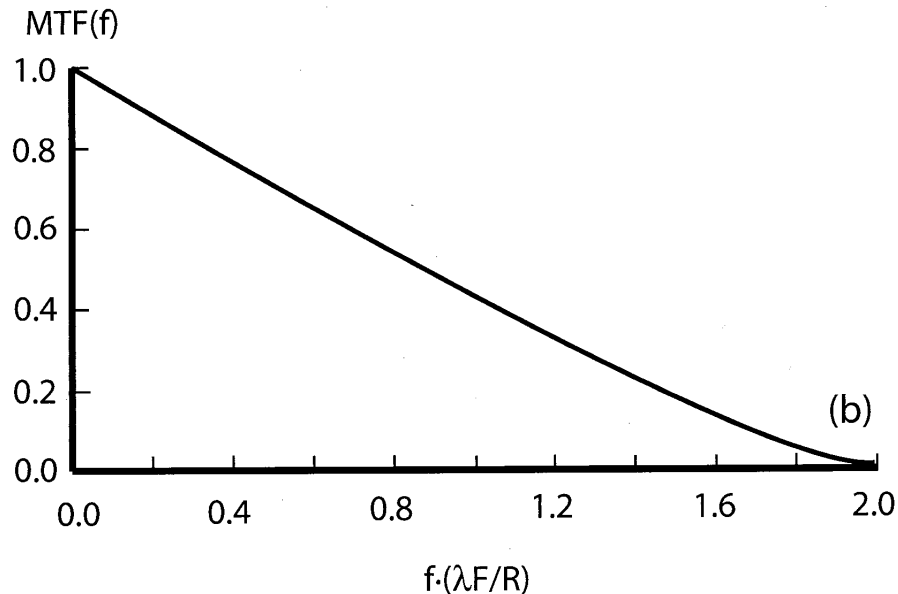
PSF(r)

(a)

r/R

MTF(f)

(b)

fR
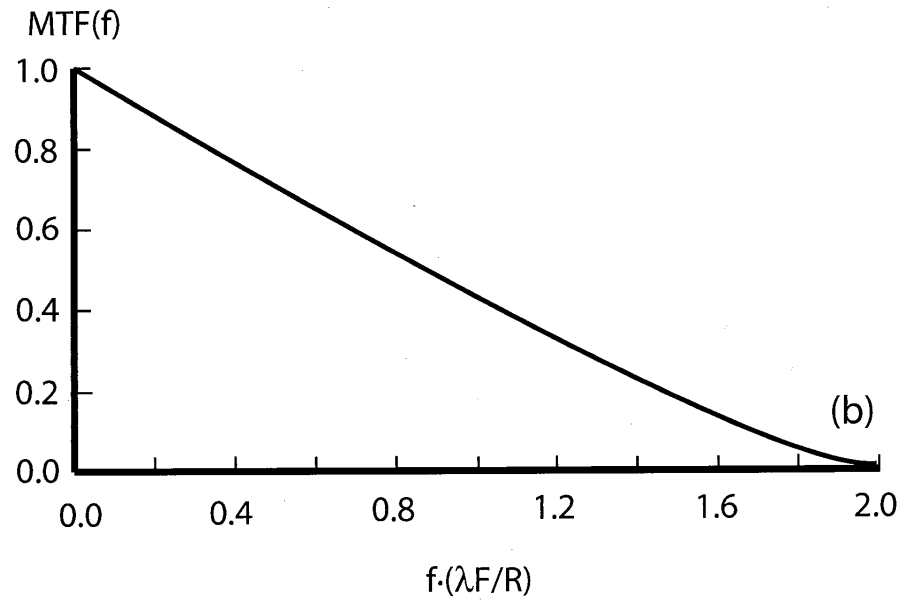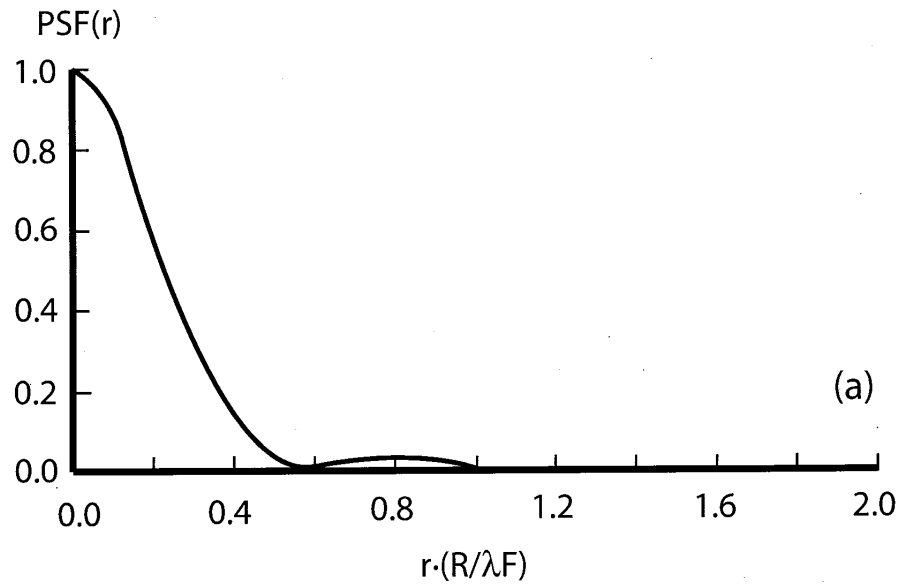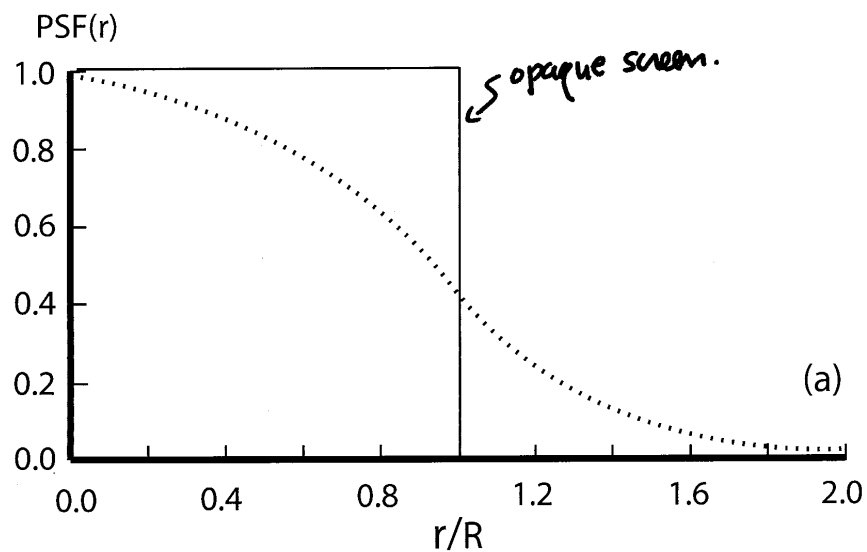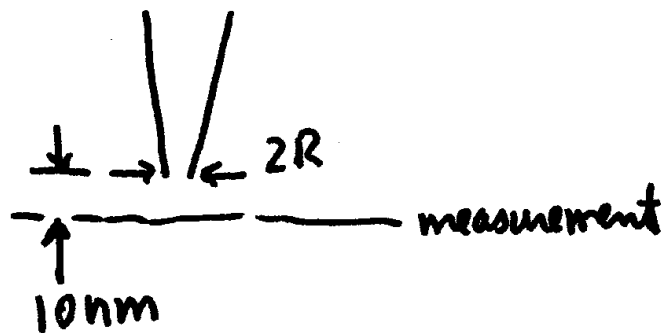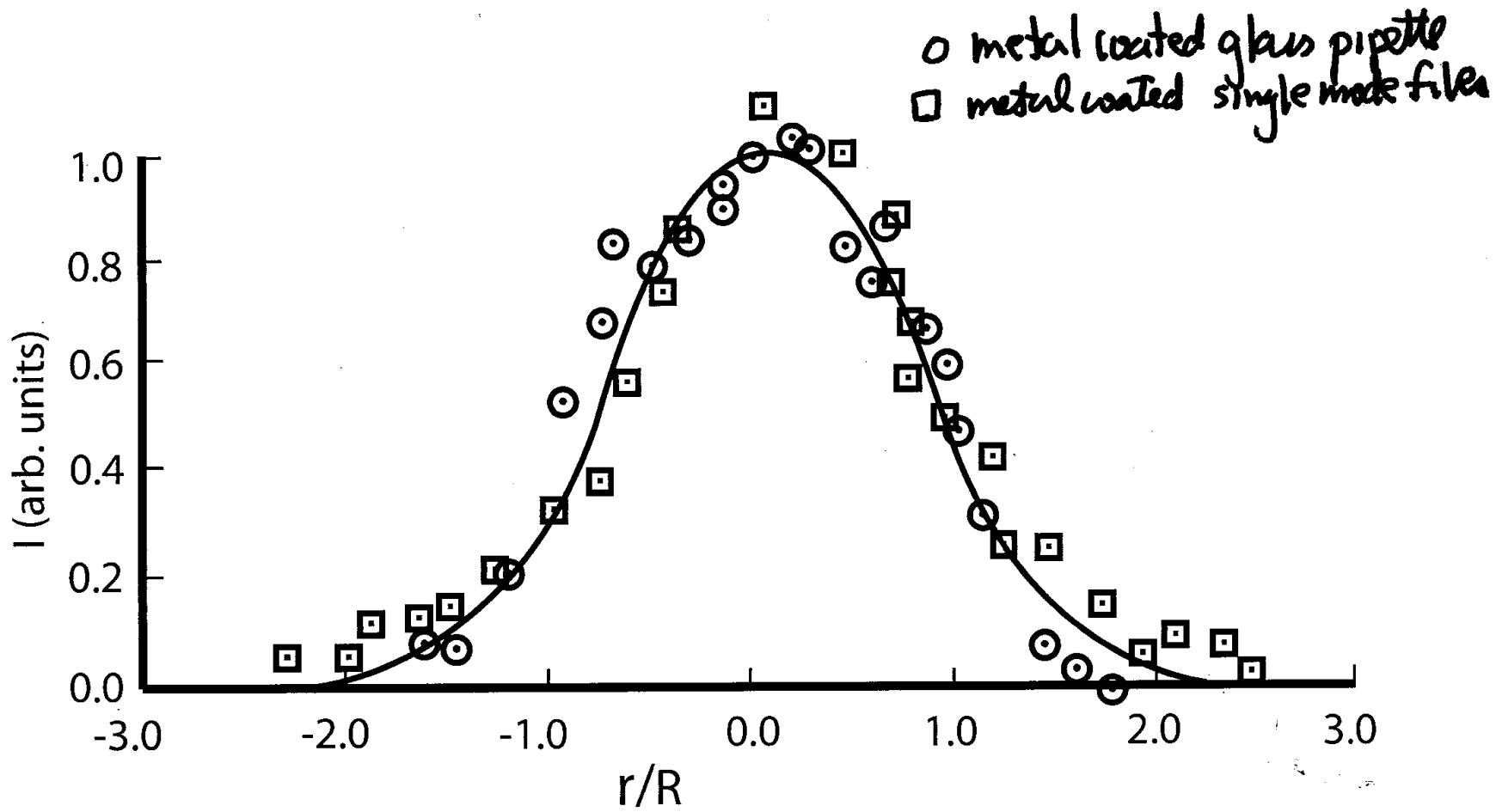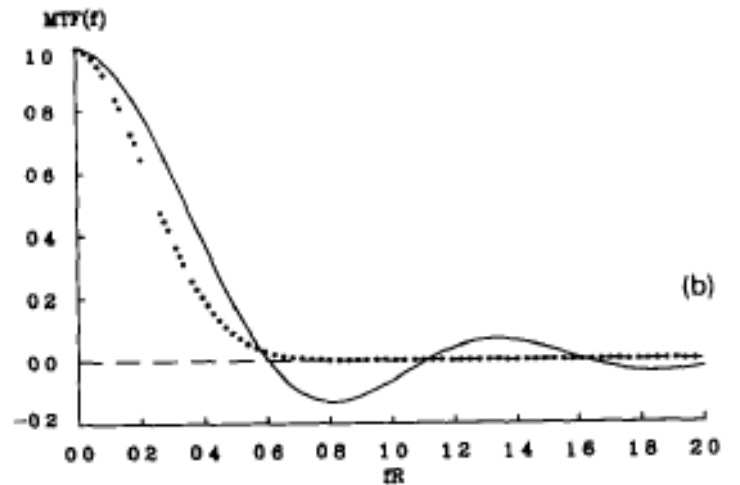
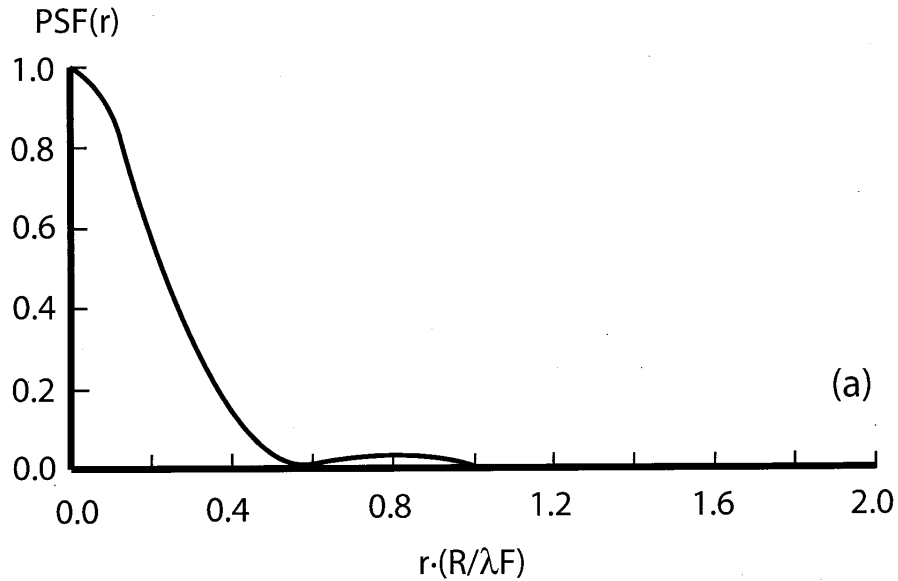Fig 6 (a) The near-field point spread function, PSF(r) due to an aperture of radius R The solid line is for an aperture in a perfectly conducting screen (neglecting the intensity increase at the aperture edge), the dashed line is for an aperture in an aluminum screen with finite dielectric constant assuming λ = 488 nm The point spread function is evaluated at the exit of the aperture (b) The modulation transfer functions of the near-field imaging systems giving the point spread functions shown in (a) Again, the dashed line is for an aluminum screen of finite dielectric constant

INCIDENT
RADIATION

OPAQUE SCREEN

NEAR FIELD

ONE WAVELENGTH

SURFACE TO
BE IMAGED

FAR FIELD
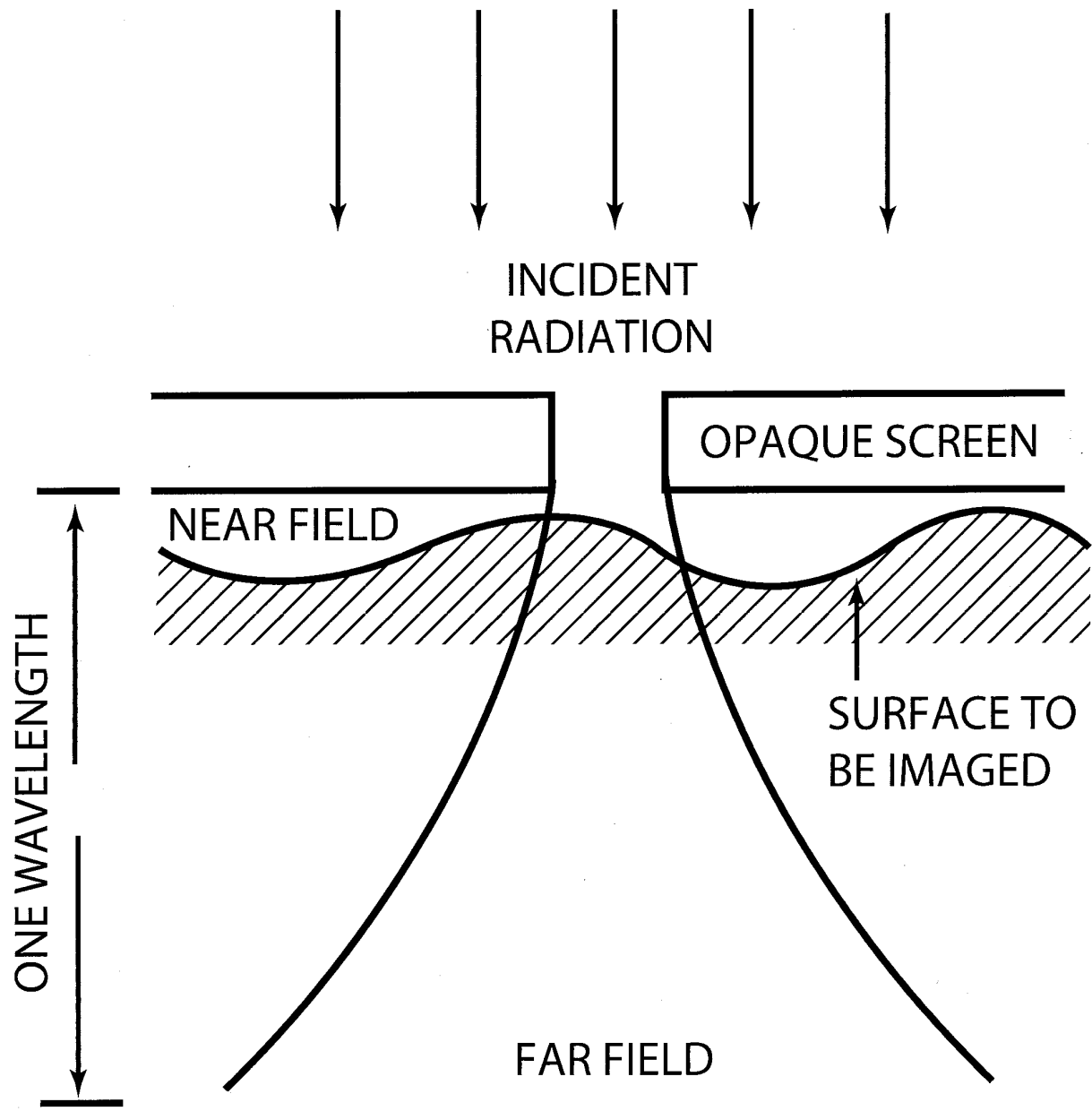
with a contrast of the MTF of 9%. On the other hand, the Sparrow criterion (in which the second derivative at the center of the intensity sum from two point objects is zero) [23] gives a resolution of

$$r = 0.47\lambda/n\sin\theta \qquad (2b)$$

with an MTF contrast of zero. One should note that the resolution criteria given above are somewhat arbitrary and the practical resolution limit is related to a minimum detectable contrast, which is related to the signal to noise ratio of the imaging system. In addition, it should be stressed that in all cases, the MTF of the far-field incoherent imaging case depends upon the wavelength of the radiation used. All we can do to improve resolution is somewhat reduce the proportionality constant in eq. (2), reduce λ or increase the numerical aperture $n\sin\theta$.

3. Near-field optics

If we relax the far-field condition, and allow ourselves to investigate the spatial distribution of the radiation in the near field, we can use the same treatment as before to obtain a point spread function and a modulation transfer function for near-field imaging. It should be pointed out that to properly deal with the near-field case we must solve the 3D vector diffraction problem. Here we will consider a simplified case assuming the Kirchoff formulation [24] and will consider the more rigorous case in a later paper.

Consider the schematic shown in fig. 4. Here, plane wave radiation again illuminates an aper-
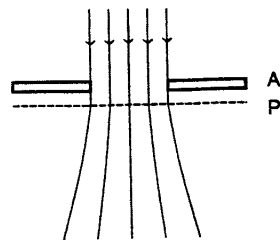
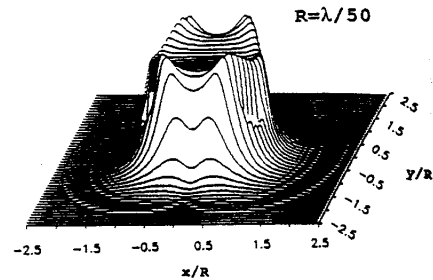Fig. 4. Schematic representation of light probe formation without a lens.

Fig. 5. Calculation of the power transmitted through an aperture in an infinitely thin, perfectly conducting screen. The incident radiation is assumed to be a polarized plane wave incident normal to the aperture plane. The electric field is parallel to the x-axis and the magnetic field is parallel to the y-axis. The intensity plot shows the power at a distance of $R/10$ from an aperture of radius R where $R = \lambda/50$, $\lambda = 500$ nm (from ref. [16]).
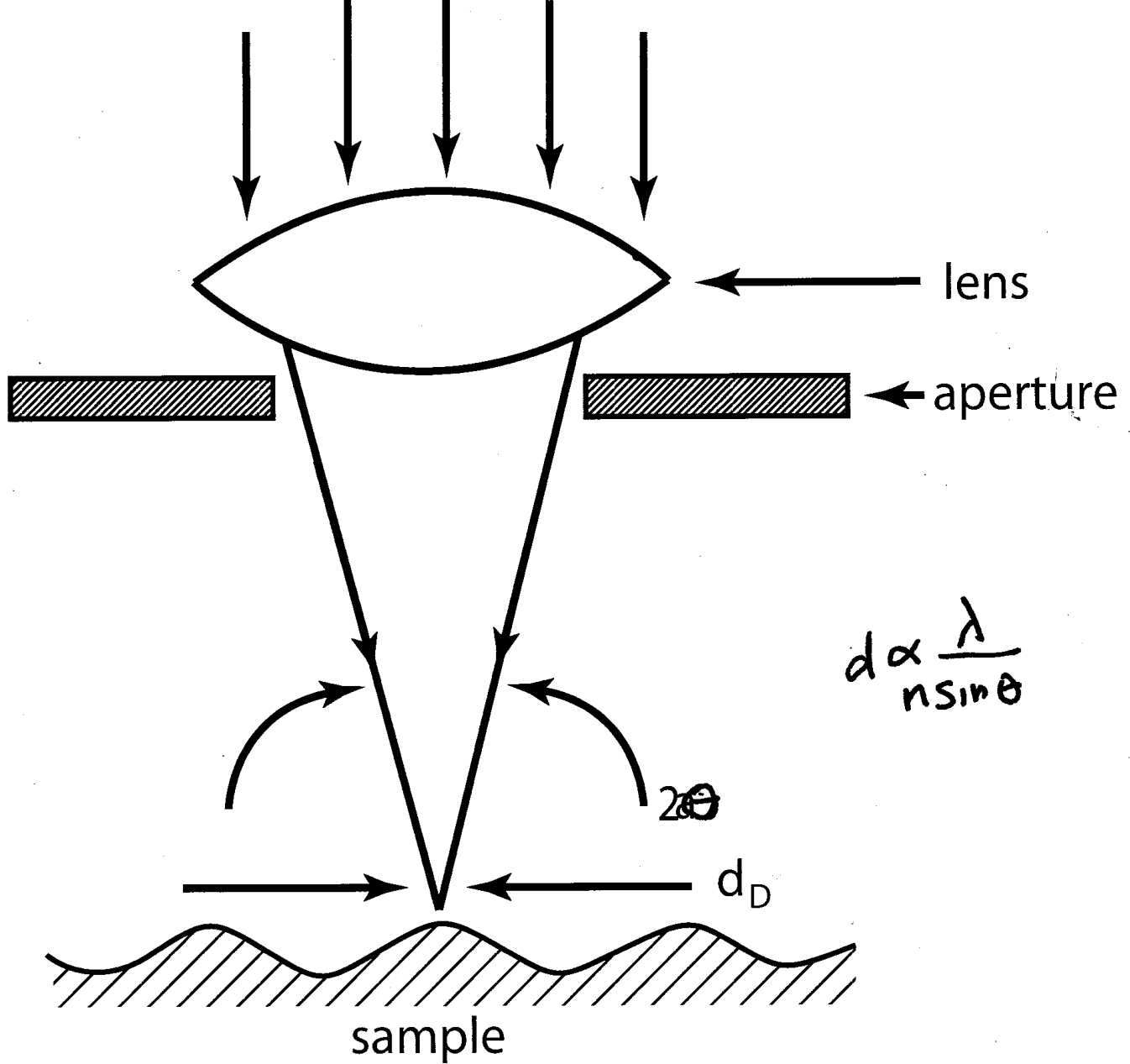
ture in an opaque screen. Only now we consider the spatial distribution of radiation in the immediate proximity of the exit side of the aperture. The intensity of radiation here is just given as

$$I_{NF}(r) = |A(\rho)A(\rho)^*| = \mathrm{PSF}_{NF}(r) \qquad (3a)$$

where r is again the coordinate in the sample plane (which here is at the aperture exit and is the same as ρ) and $A(\rho)$ has the same meaning as before. Thus, the intensity distribution in the near field is essentially the geometric projection of the aperture (or more accurately the modulus squared of the aperture function). Note that this is not exactly true, since a more rigorous calculation indicates an increase in the intensity at the aperture edge. This has been shown before for the case of apertures in thin perfectly conducting screens and the result of such a calculation by Harootunian [16] is shown in fig. 5. In fig. 6a we plot a representation of eq. (3a) where R is the aperture radius.
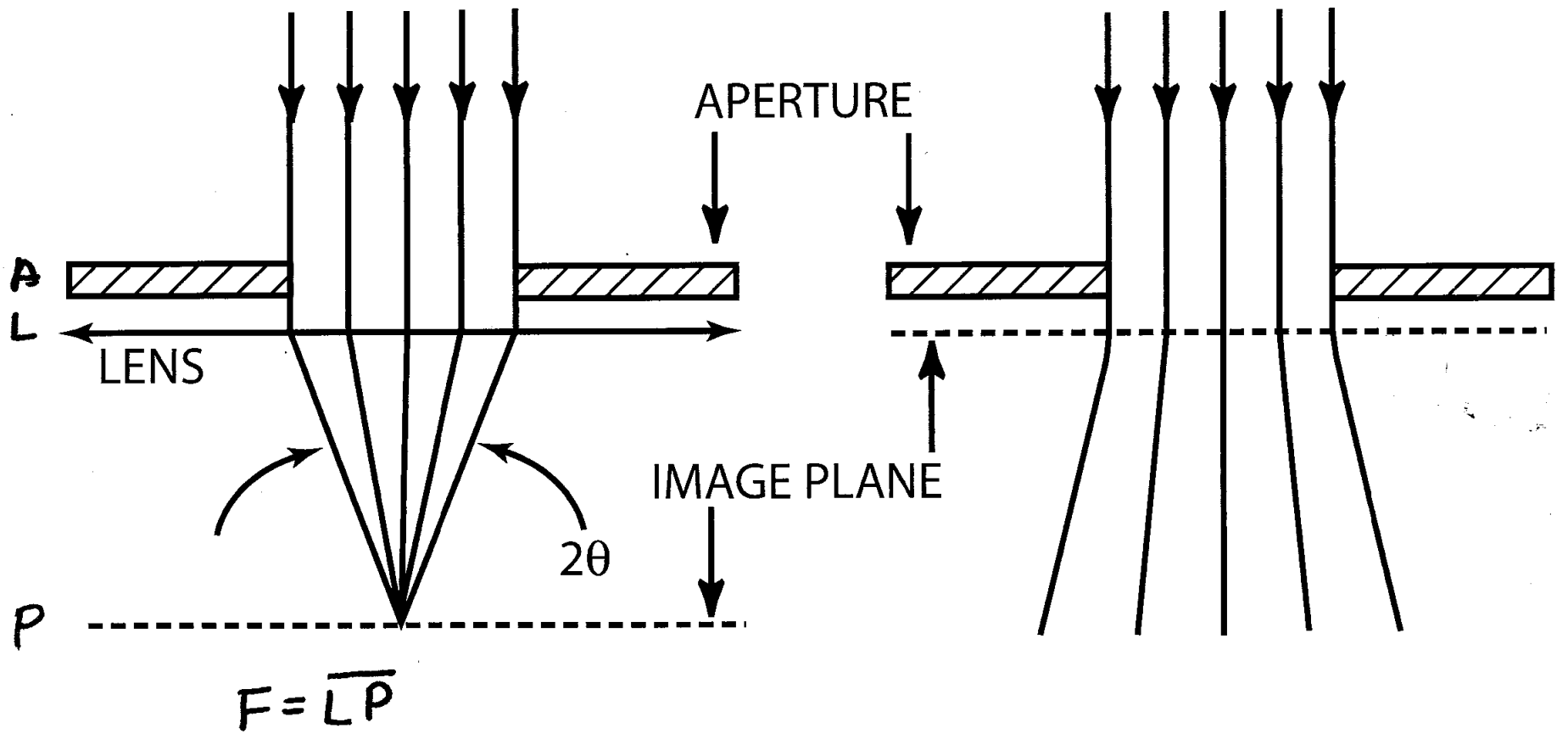
The modulation transfer function for the point spread function given by eq. (3a) is again the Fourier transform of the PSF.

$$
\begin{aligned}
\mathrm{MTF}(f)_{NF} &= \mathscr{F}[I_{NF}(r)] \\
&= \mathscr{F}[A(\rho)A(\rho)^*] \\
&= \mathscr{F}[A(\rho)] \otimes \mathscr{F}[A(\rho)]^* \qquad (3b)
\end{aligned}
$$

lens
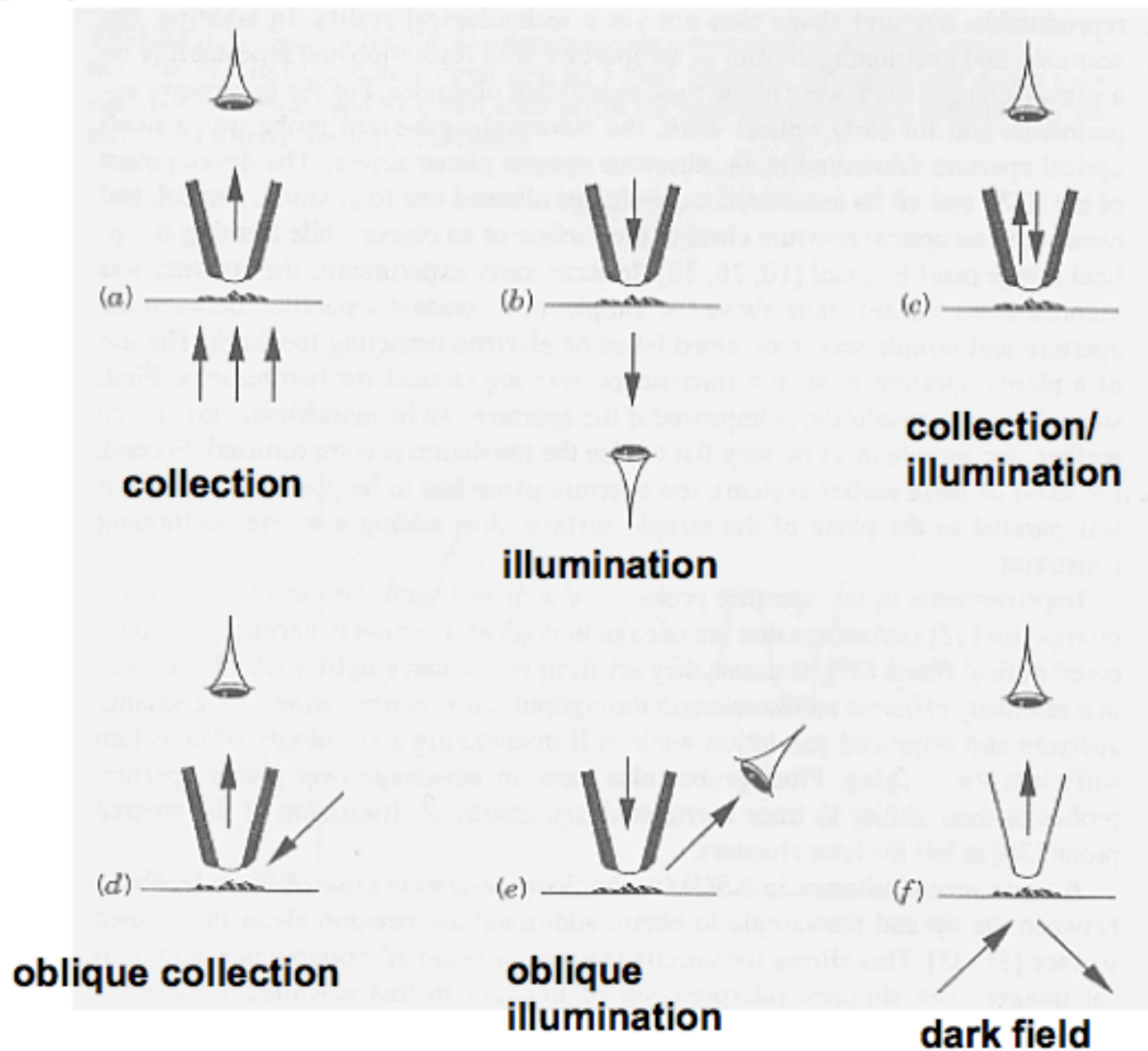
aperture

$$d \propto \frac{\lambda}{n \sin \theta}$$

2θ

d_D

sample

FAR-FIELD

NEAR-FIELD

APERTURE

A

L

LENS

IMAGE PLANE

2θ

P

$F = \overline{LP}$

Near Field Scanning Optical Microscopy

Imaging modes:

(a) collection

(b) illumination

(c) collection/illumination

(d) oblique collection

(e) oblique illumination

(f) dark field

Shear Force Microscopy

$\leftrightarrow$ dither

Betzig et.al.
App Phy Lett. 60(1992).
2484

feed back to split detector
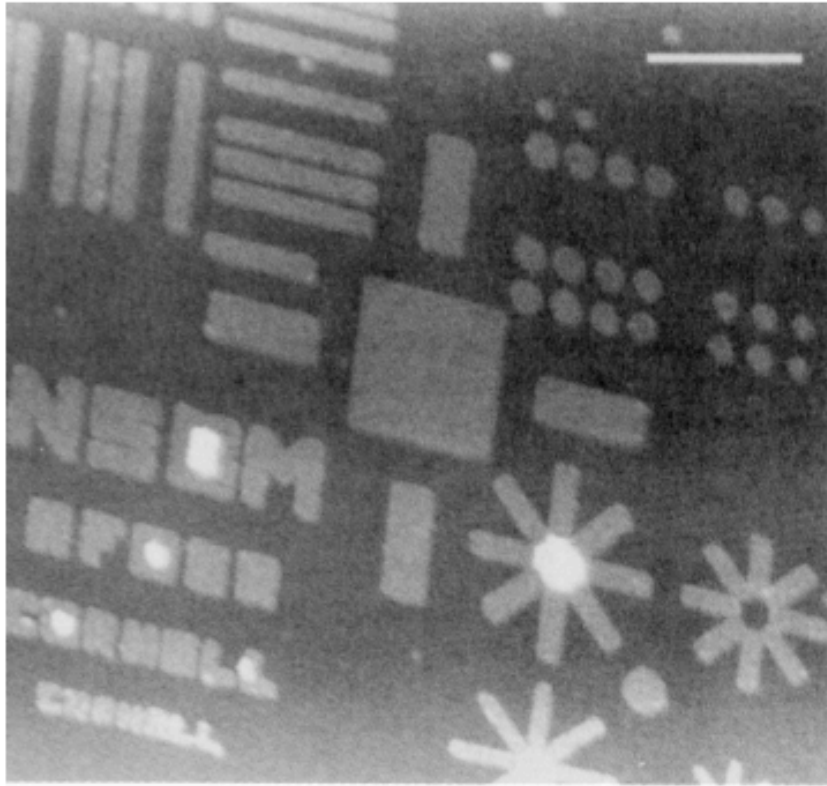for shear signal.

Near Field Scanning Optical Microscopy (Reflection)
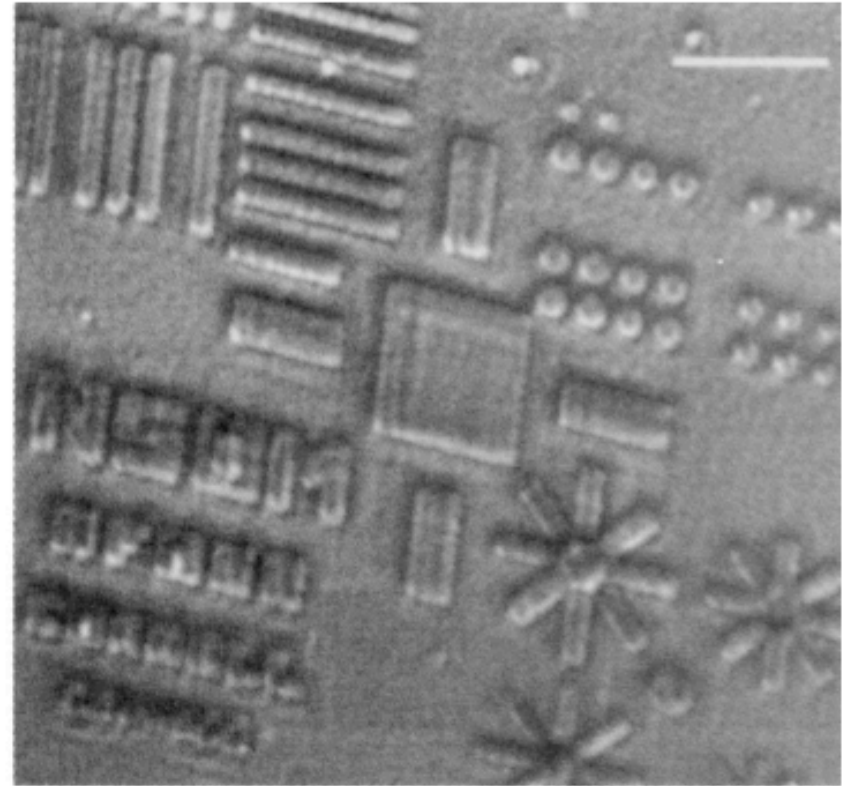
aluminum on silicon

400nm

Shear force

NSOM

Cline and Isaacson, Ultramicroscopy
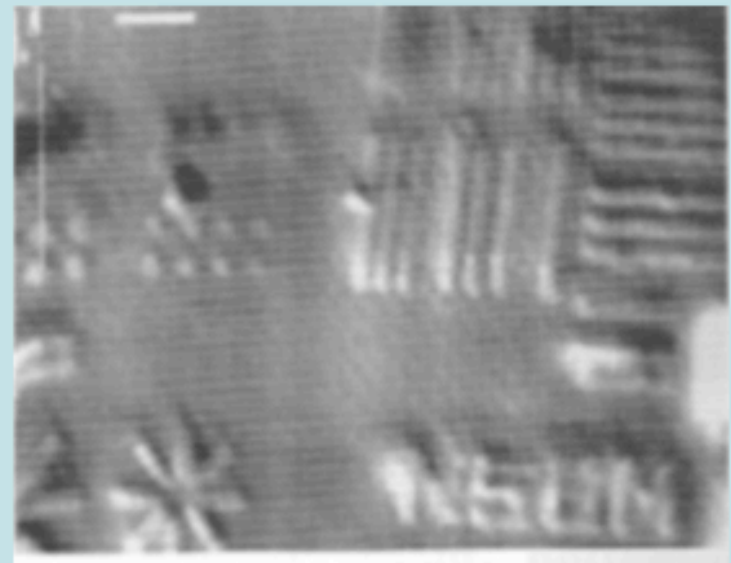
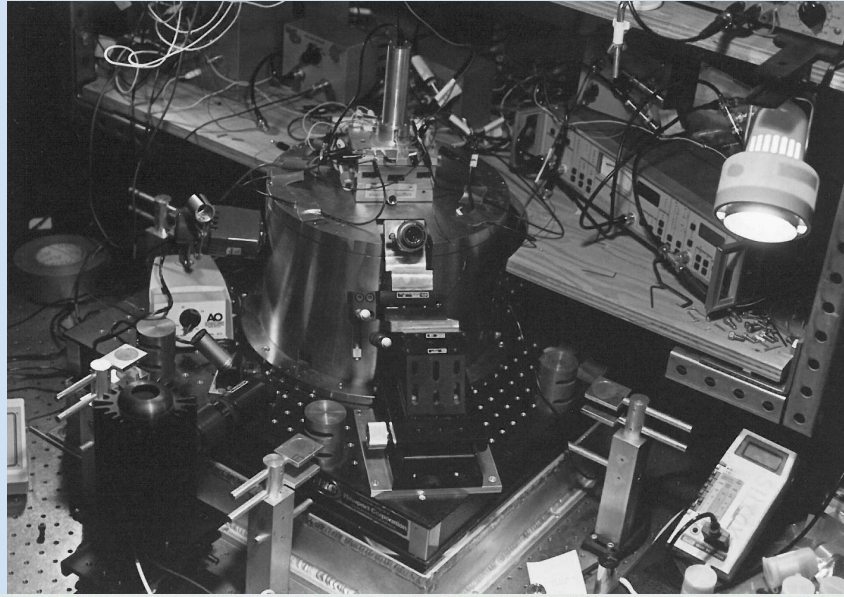**SHEAR FORCE**   **REFLECTION**

Fig. 8. Shear force and reflection images of an aluminum-on-aluminum pattern. The images display the effect of the topography on the imaging. The white scale bars are 2-μm bars, and the detector is oriented on the bottom on the image.

    J. Cline and M. Isaacson

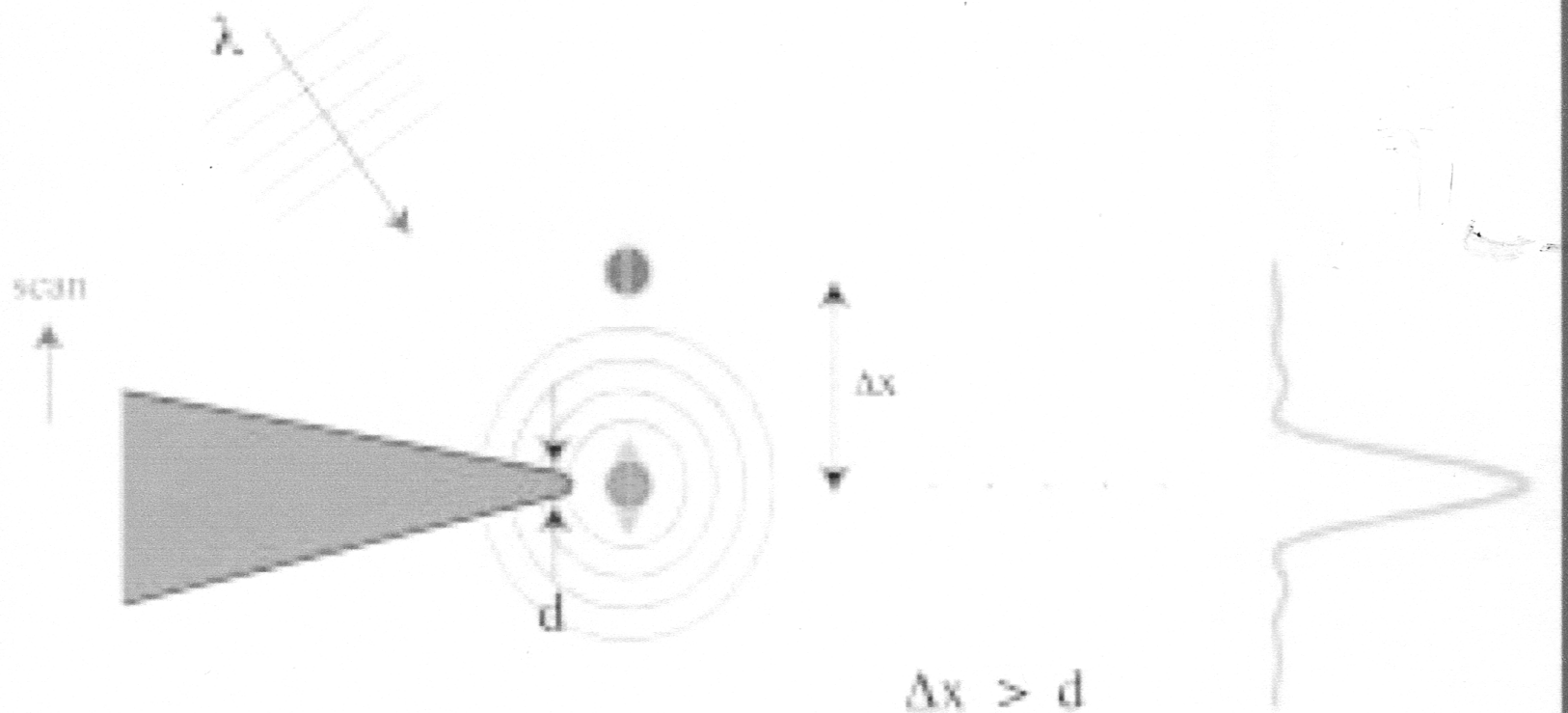# NSOM Instrument Constructed at Cornell
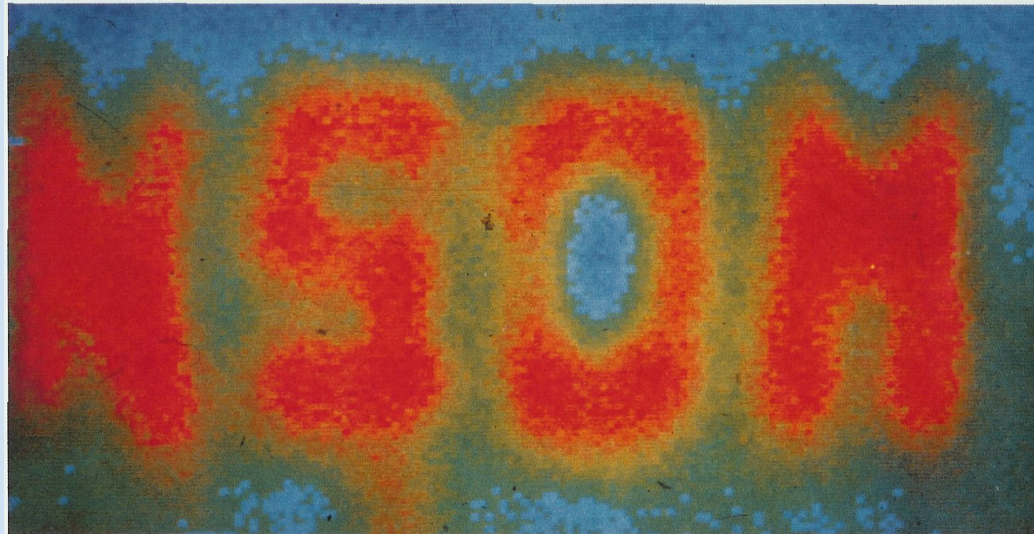
ALUMINUM LETTERS fabricated on a silicon nitride substrate imaged with a near field optical microscope. The full horizontal scale is 550 nm, the wavelength of the light being used.

M. Isaacson and E. Betzig, Cornell University

M.Isaacson, 8/3/10

FIELD ENHANCEMENT MICROSCOPY

λ

scan

Δx

d

$\Delta x > d$

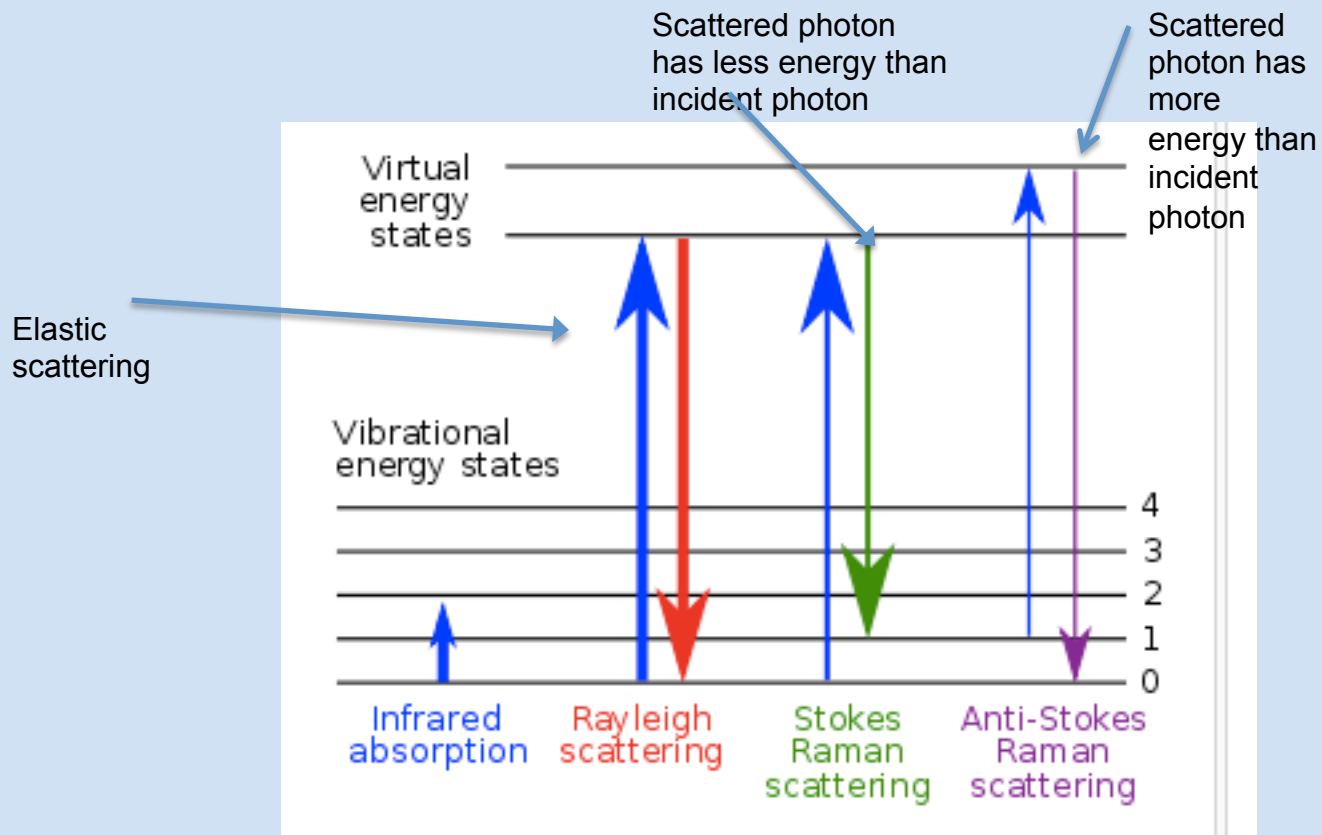H. Furukawa and S. Kawata, Opt. Commun. **148**, 221, 1998

L. Novotny et al., Ultramicroscopy **71**, 21, 1998

metal tip

local field enhancement

RAMAN SCATTERING (a chemical fingerprinting tool)

Scattered photon
has less energy than
incident photon

Scattered
photon has
more
energy than
incident
photon

Elastic
scattering

Virtual
energy
states

Vibrational
energy states

4
3
2
1
0

Infrared
absorption

Rayleigh
scattering

Stokes
Raman
scattering

Anti-Stokes
Raman
scattering

Fluorescence is limited by the need to label and photobleaching.
> **Raman spectroscopy** provides molecular information

Raman: inelastic light scattering

$E_i = h\nu_i$

$E_s = h\nu_s$

$\Delta E = E_i - E_s$
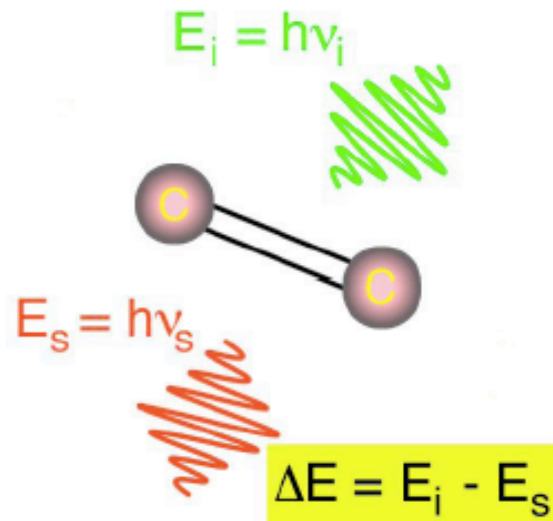
Raman spectrum of a single bacterial spore
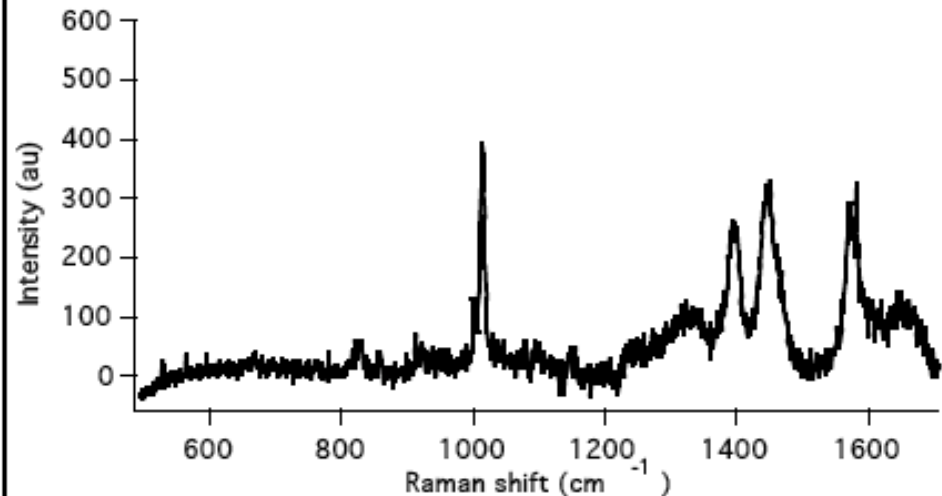
Raman spectroscopy provides
- Fingerprint spectra (molecular identity)
- Information about 3d structural changes (orientation, conformation)
- Information about intermolecular interactions
- Dynamics

Raman scattering, however, is extremely inefficient
Only 1 in 10^8 incident photons are Raman scattered
Typical scattering cross-sections ~ 10^{-30} cm² (15 orders of magnitude lower than fluorescence excitation)

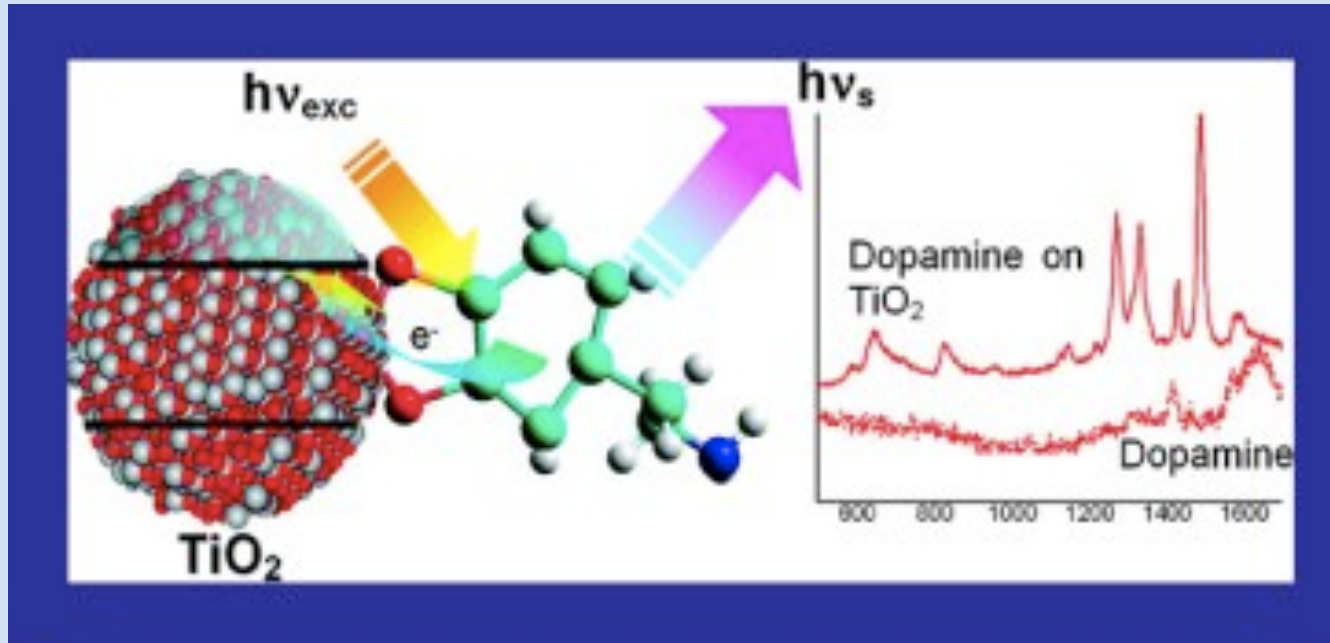In 1977, an interesting finding was reported, starting the "age of surface-enhanced Raman spectroscopy"

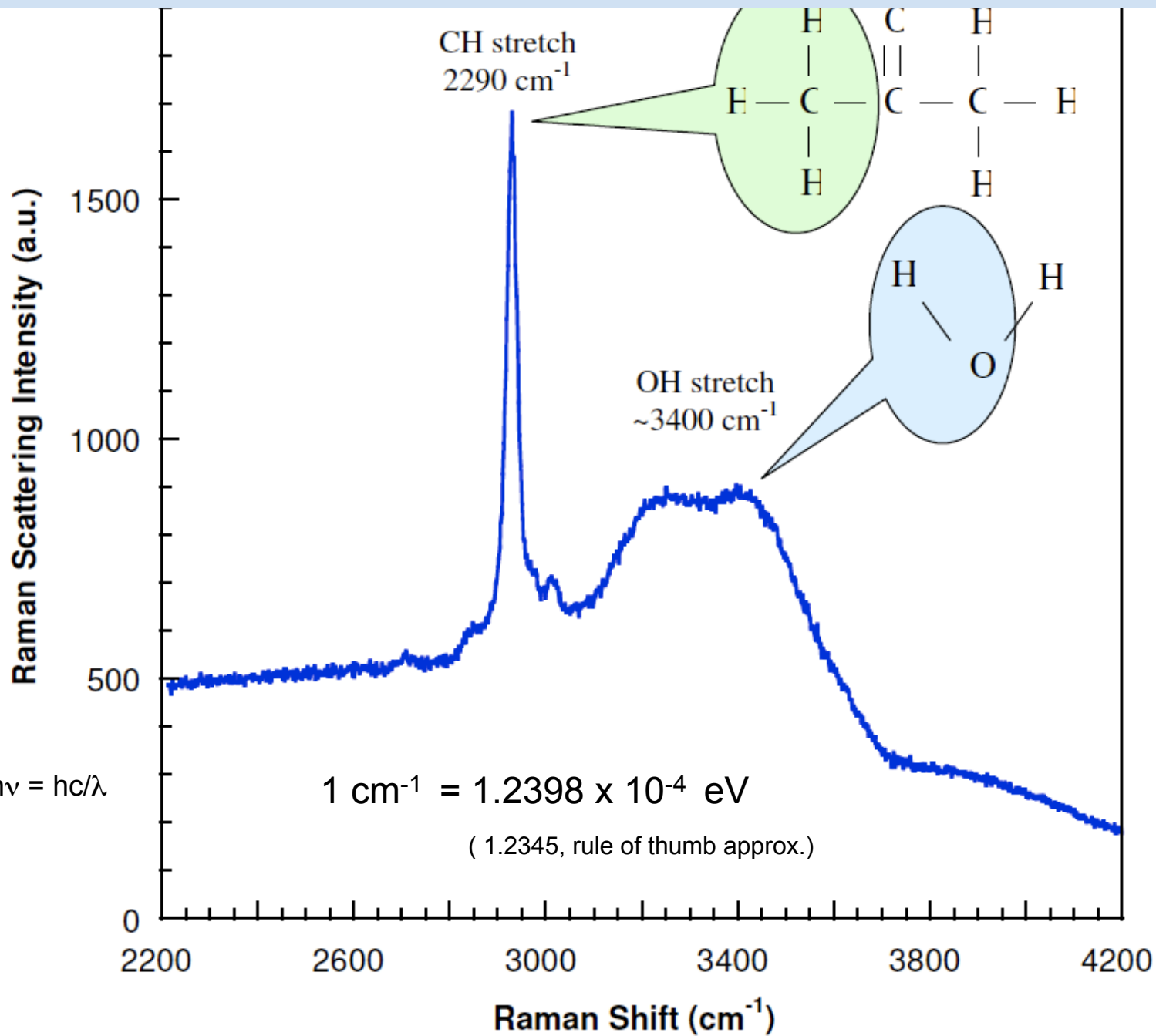- **Flat surfaces give Raman enhancements in the range of** $10^3 - 10^6$
  - **Jeanmaire and Van Duyne,** *J. Electroanal. Chem.*, 84, 1 (1977)
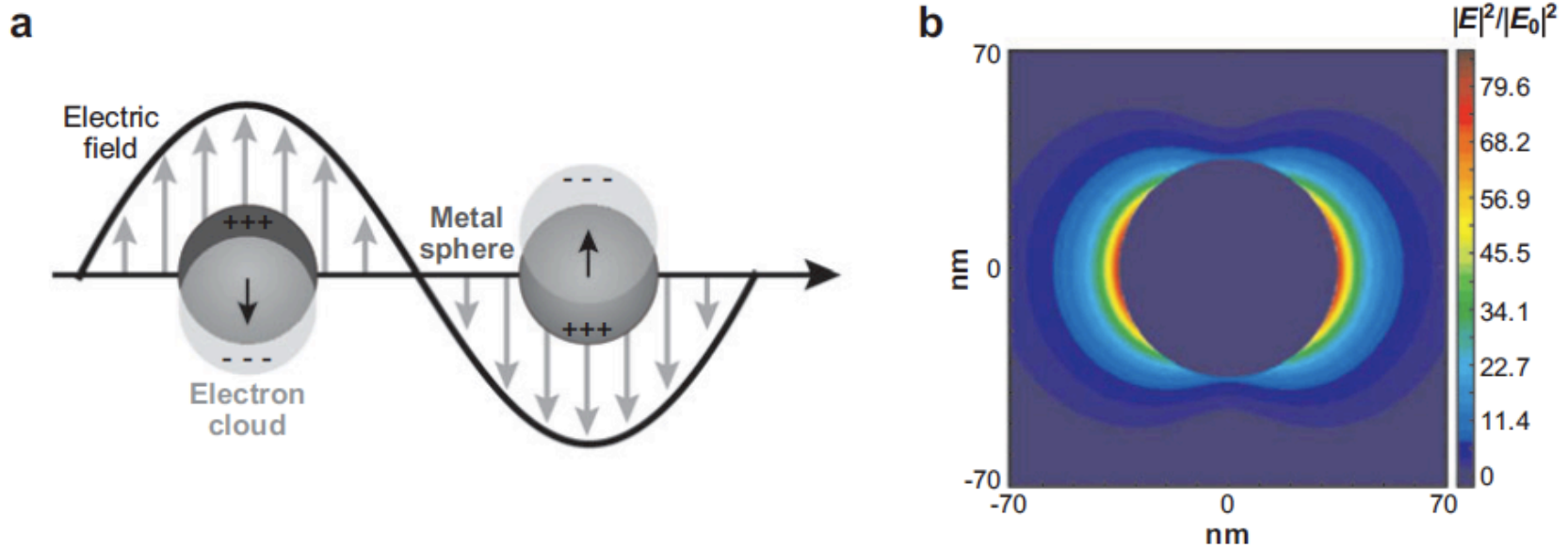 - **Albrecht and Creighton,** *J. Am. Chem. Soc.*, 99, 5215 (1977)

Ag
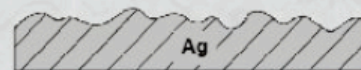
Surfaced Enhanced Raman Scattering

Orders of magnitude increase in signal over regular Raman Scattering

a Electric field · Metal sphere · +++ · - - - · +++ · - - - · Electron cloud

b $|E|^2/|E_0|^2$ · 79.6 · 68.2 · 56.9 · 45.5 · 34.1 · 22.7 · 11.4 · 0

Figure 1

(*a*) Illustration of the localized surface plasmon resonance effect. (*b*) Extinction efficiency (ratio of cross section to effective area) of a spherical silver nanoparticle of 35-nm radius in vacuum $|E|^2$ contours for a wavelength corresponding to the plasmon extinction maximum. Peak $|E|^2 = 85$.
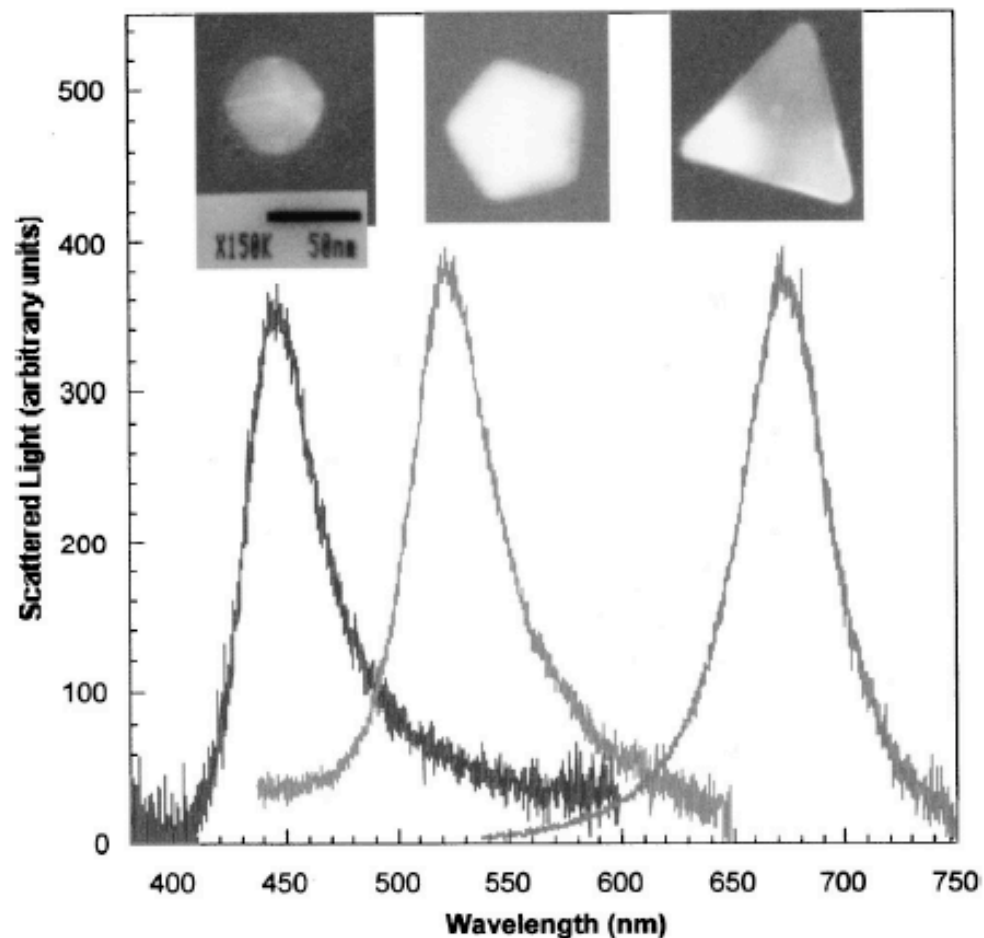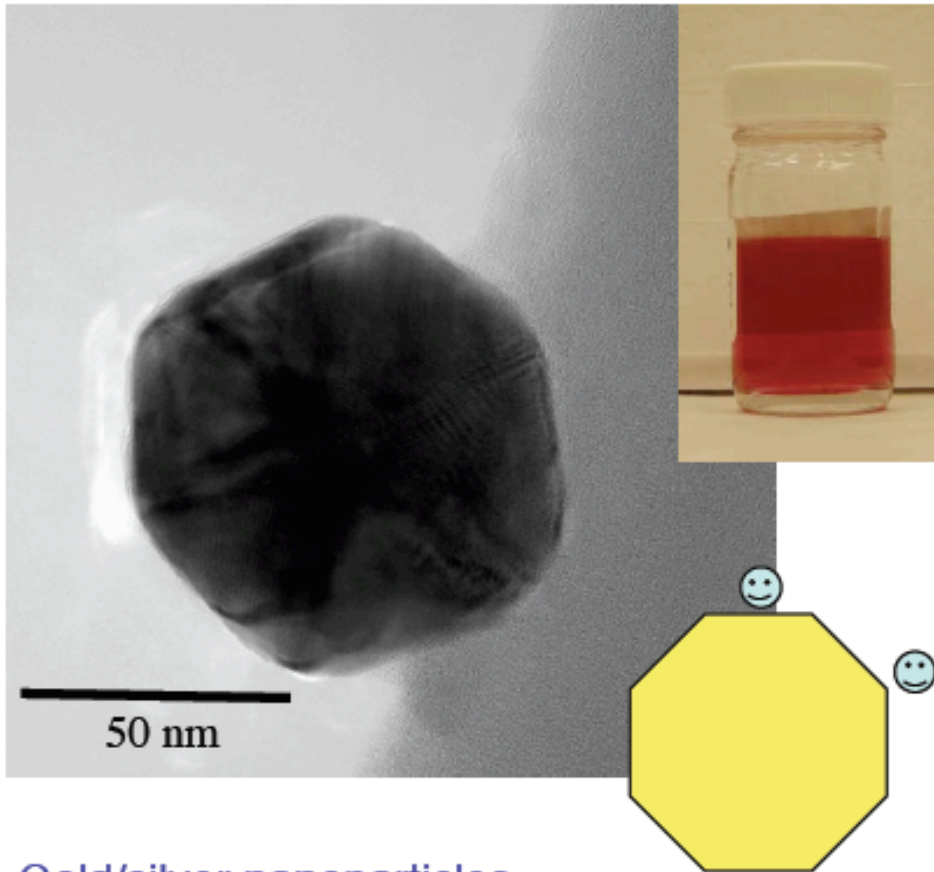
FIG. 2. Typical optical spectroscopy measurements of individual silver nanoparticles. The figure shows the spectrum of an individual red, green, and blue particle, and the high-resolution TEM images of the corresponding particle are shown above their respective spectrum. This example is a representative of the principle conclusion that the triangular shaped particles appear mostly red, particles that form a pentagon appear green, and the blue particles are spherical.

The plasmon resonance of metal nanoparticles depends on their size, shape and composition
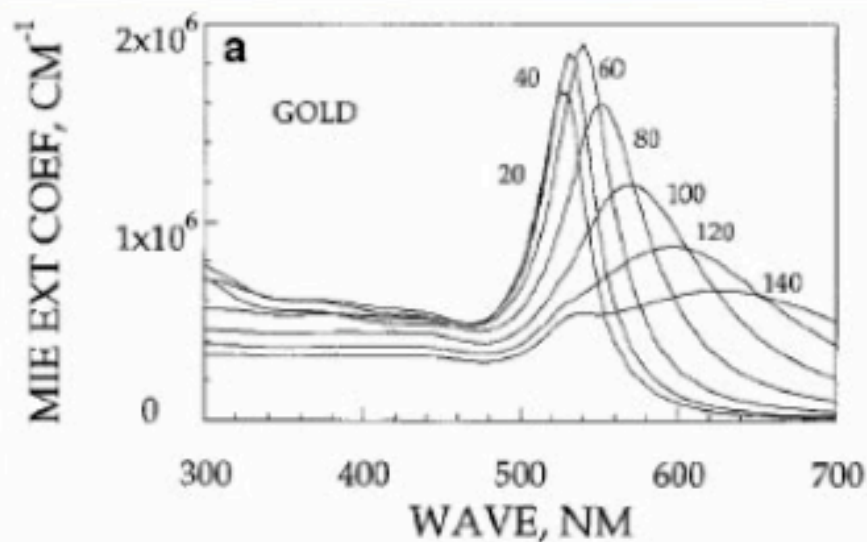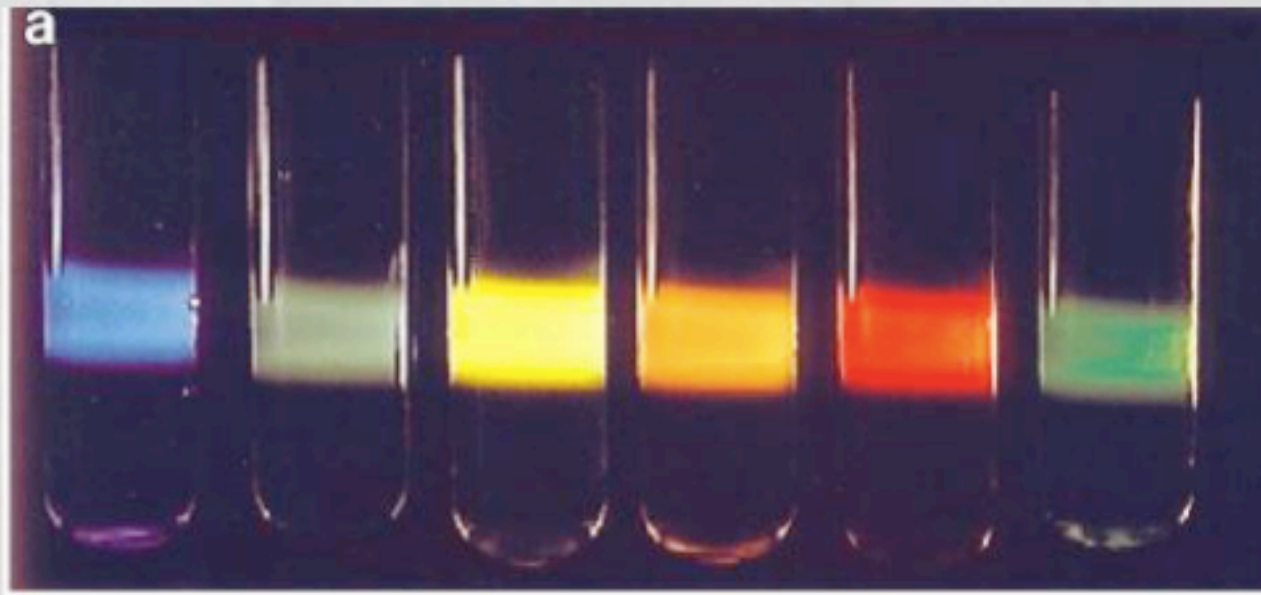
Yguerabide, et al.,
Anal. Biochem.,
262, 17, 137 (1999)

Computer model of E-fields at triangular silver tip
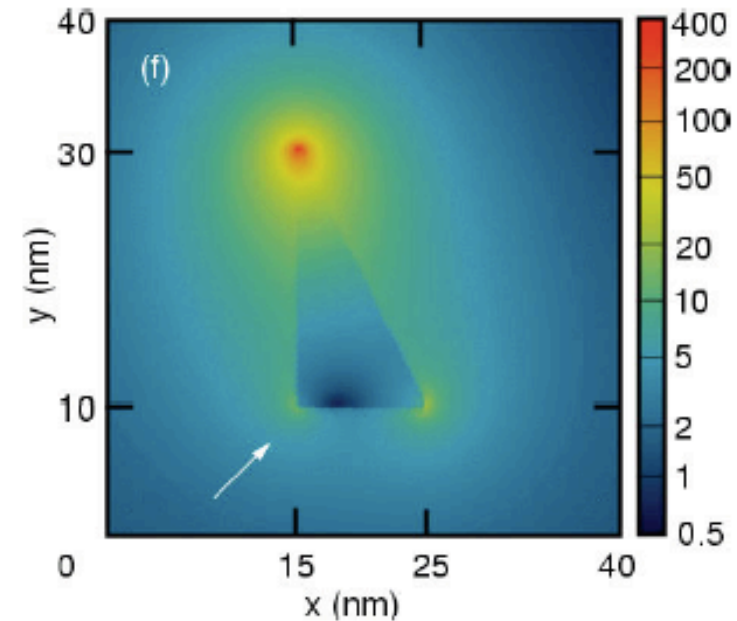
Figure courtesy O.J. F. Martin
Ref.: Chem. Phys. Lett. **341**, 1 - 6 (2001)

Gold/silver nanoparticles

- are polycrystalline and faceted
- support surface plasmons excited with visible light
- leakage radiation has evanescent nature at surface irregularities
- exponential decay leads to highly localized fields

Fig. 3. Surface-enhanced Raman spectra of R6G obtained with a linearly polarized confocal laser beam from two Ag nanoparticles. The R6G concentration was 2×10^{-11} M, corresponding to an average of 0.1 analyte molecule per particle. The direction of laser polarization and the expected particle orientation are shown schematically for each spectrum. Laser wavelength, 514.5 nm; laser power, 250 nW; laser focal radius, ~250 nm; integration time, 30 s. All spectra were plotted on the same intensity scale in arbitrary units of the CCD detector readout signal.

Xie and Emory
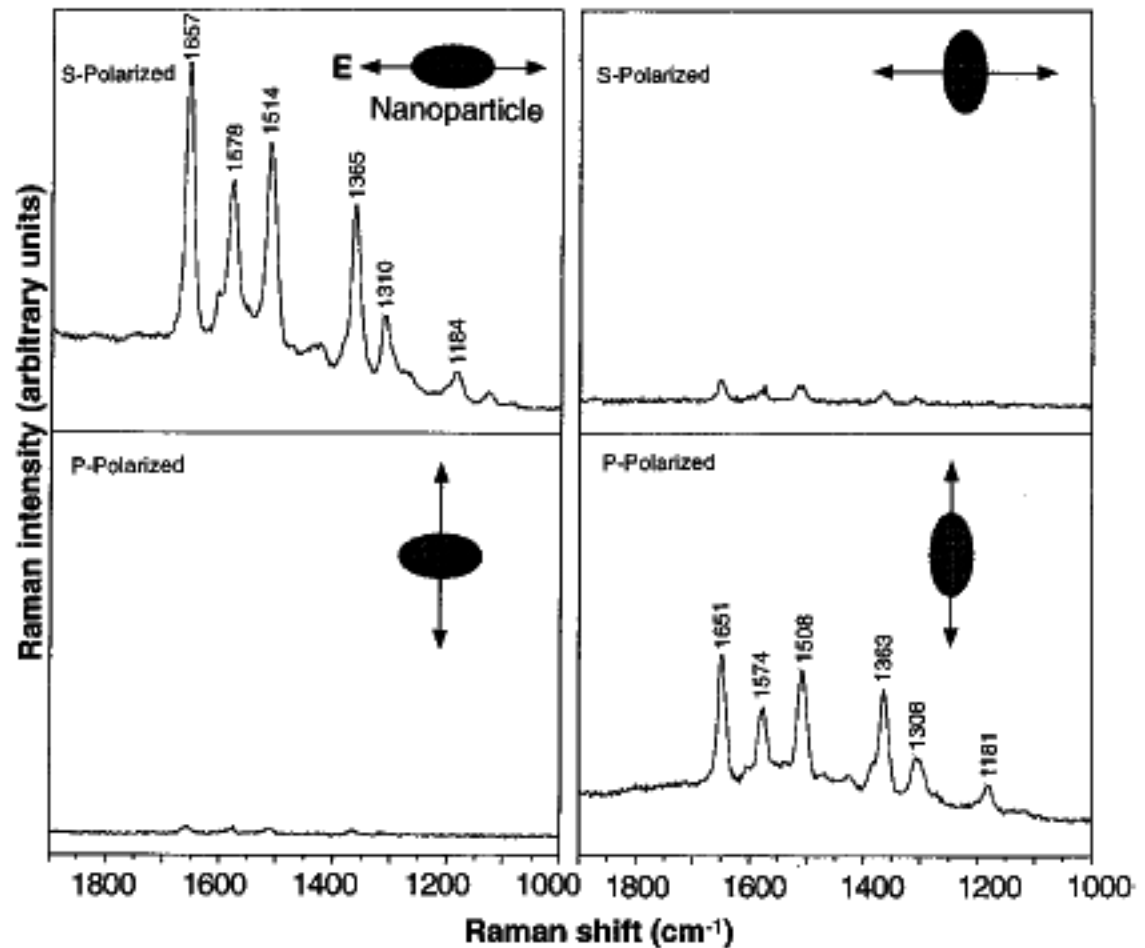
Nanoscale Probing of Adsorbed Species by Tip-Enhanced Raman Spectroscopy

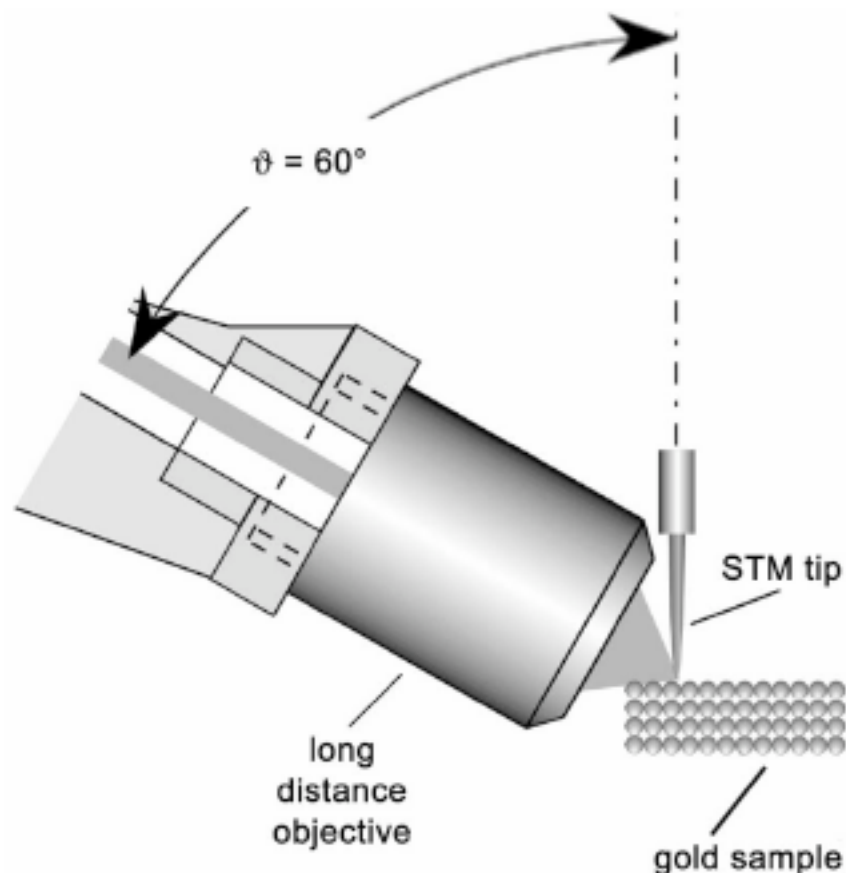Bruno Pettinger,[1,*] Bin Ren,[1,2] Gennaro Picardi,[1] Rolf Schuster,[1] and Gerhard Ertl[1]

FIG. 1. Experimental setup for TERS using the 60° arrangement. Olympus long distance microscope: 50× magnification, NA = 0.5. He-Ne laser: 5 mW at the sample, $\lambda_{ex} = 632.8$ nm.
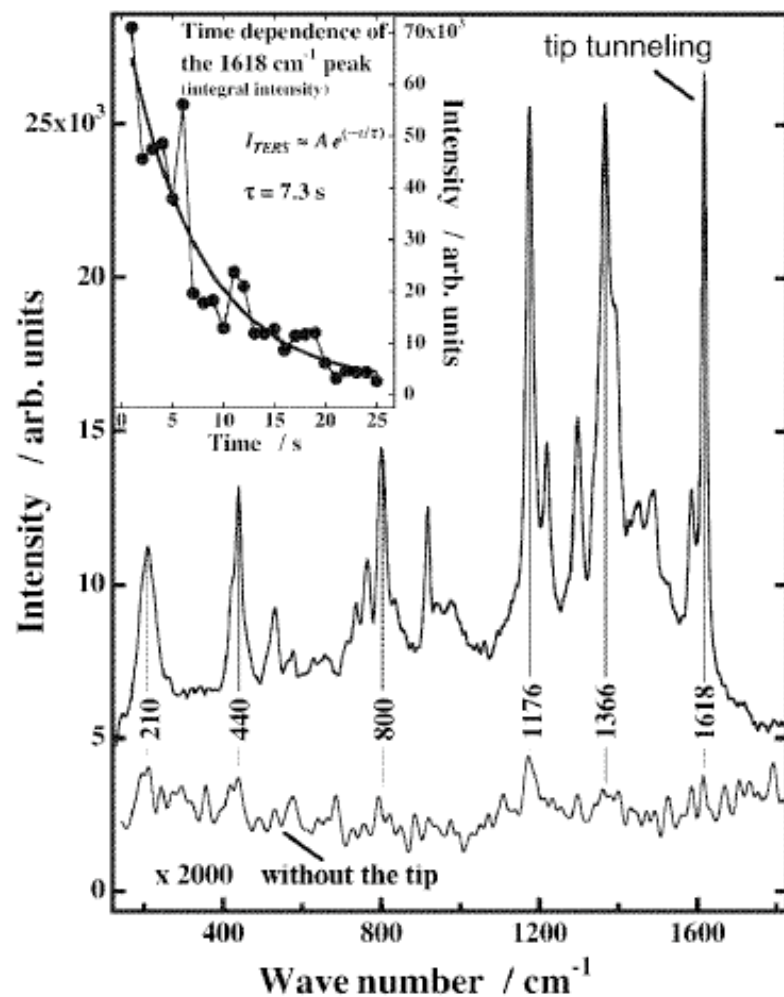
FIG. 4. Comparison of RRS and TERS spectra for malachite green isothiocyanate adsorbed at a Au(111) surface. The laser power in the TERS case is reduced to 0.5 mW; the spectral intensities are normalized to full laser power (5 mW) and acquisition time 1 s. The actual acquisition times were TERS, 1 s and RRS, 60 s. The MGITC dye is adsorbed from a $10^{-7} M$ ethanol solution for 30 min. Tunneling current: 1 nA; voltage: -150 mV. Inset: Time dependence of the integral intensity of the 1618 cm^{-1} band for the reduced laser power.
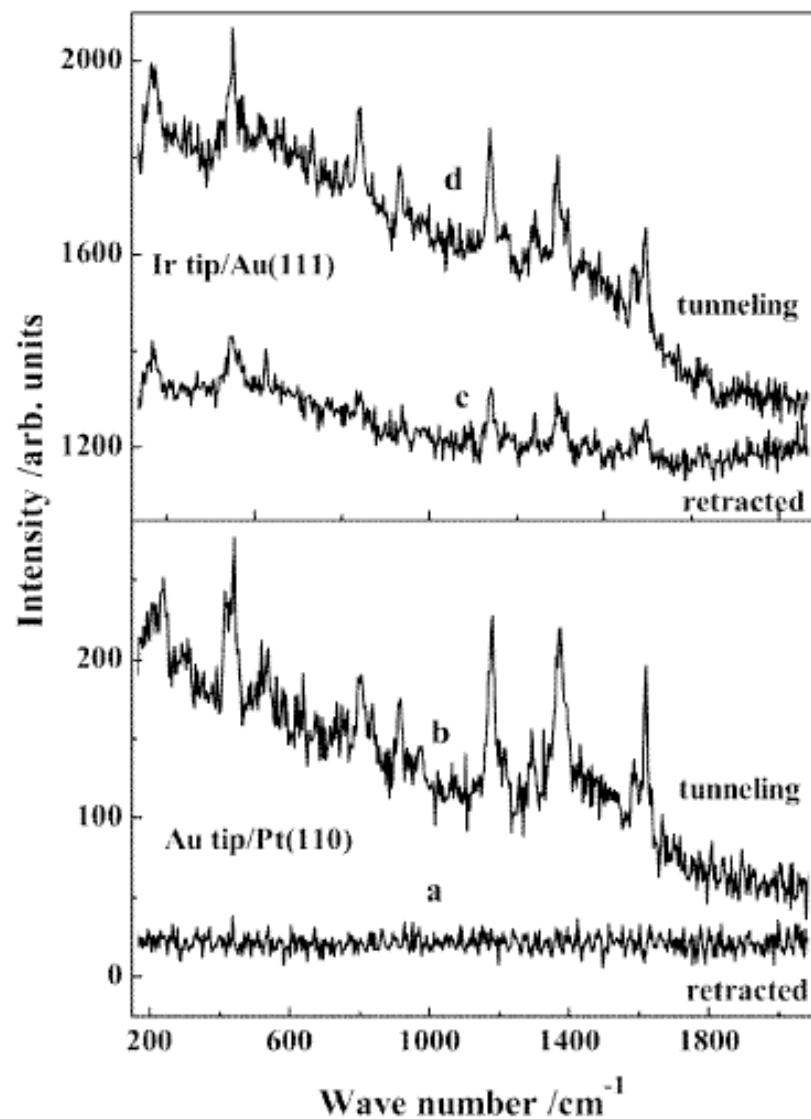
FIG. 3. TERS and RRS for other tip-metal configurations. Top panel: Ir tip/Au(111); acquisition time 30 s. Bottom panel: Au tip/Pt(110); acquisition time 2 s. For both configurations, the MGITC dye is adsorbed from a $10^{-6} M$ ethanol solution for 30 min. Laser power: 5 mW. Tunneling current: 1 nA; voltage: -150 mV.

Tip enhanced Raman spectroscopy for chemical characterization of nano-structures

Mischa Nicklaus[1], Andreas Ruediger[1]

[1]INRS-EMT, Université du Québec, 1650, Boul. Lionel-Boulet, Varennes J3X 1S2

Keywords : Near field microscopy, Raman spectroscopy, scanning probe microscopy, ferroelectrics

Nano-electronics and biotechnology call for analytical methods with nanometer precision. Common techniques that provide such high resolutions are electron microscopy (SEM) and scanning probe microscopy (e.g. STM and AFM). Although some of these techniques can probe the topography of the sample with atomic resolution, the chemical and structural information remains unknown. Chemically-sensitive methods like Raman or IR-spectroscopy are physically limited by the diffraction limit of light and thus do not provide access to the nano-scale. With the goal of making chemical characterization available at nanometer resolution, we are working on tip enhanced Raman spectroscopy (TERS). This aperture-less near-field scanning microscopy is based on an atomic force microscope that uses localized surface plasmons at the apex of the microscopy tip (Figure 1) to generate an optical near-field of a few nanometers in diameter. While scanning the surface of the sample, the plasmons at the tip act as light source for the Raman spectroscopy (Figure 2) and the chemical structure of the sample can be mapped with molecular sensitivity. Our system is specifically designed to allow the characterization of insulating and opaque samples. We are therefore using a tuning fork AFM operated in shear force mode with electro-chemically etched gold tips. The optical access for the confocal Raman measurement is established from the side. We are presenting scans of carbon nanotubes with 15 nm optical resolution and first TERS spectra of $PbTiO_3$ nano structures.
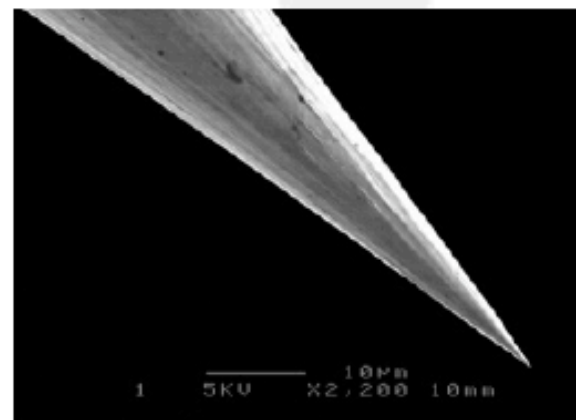

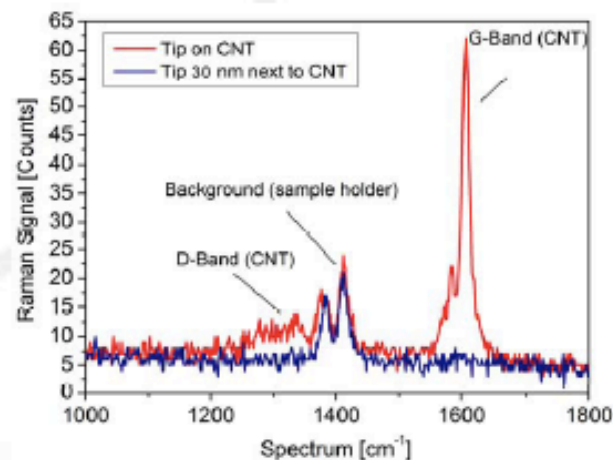Figure 1 – SEM image of an electro-chemically etched gold tip for tip enhanced Raman spectroscopy.

Figure 2 – Tip enhanced Raman spectrum of a carbon nanotube (red). The blue curve shows the loss of the G-band when the carbon nanotube is positioned 30 nm away from the tip. This demonstrates the position dependence and thus the high lateral resolution of TERS.
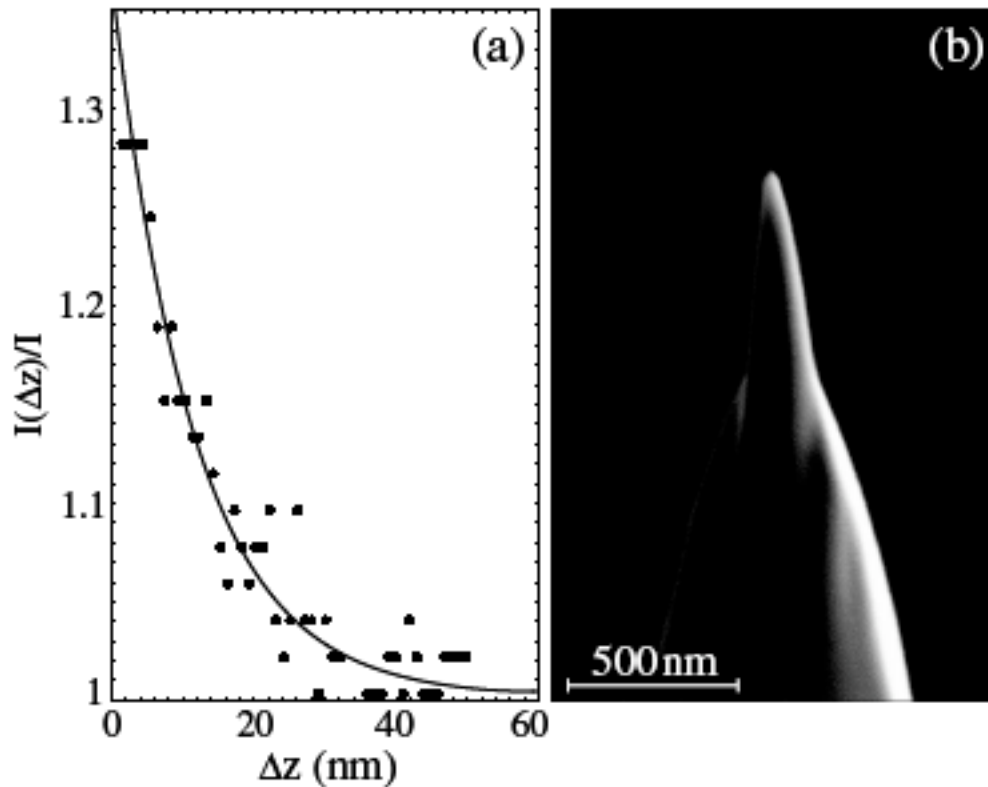
Decay of SERS Signal away from Object

FIG. 3. (a) Dependence of the Raman scattering strength of the G' band (I) on the longitudinal separation (Δz) between a single SWNT and the tip. The solid line is an exponential fit with a decay length of 11 nm. The signal is normalized with the far-field signal. (b) Scanning electron micrograph of a sharp silver tip fabricated by focused ion beam milling.

From Hartschuh, et.al. 2003

Scanned Tip Microscopies: Selected references

Tip Enhanced Raman Microscopy/Spectrosopy (TERS)

Sanchez, et.al. Phys. Rev. Letters. 82(20)1999.4014.

Hartschuh et.al. Phys. Rev. Letters. 90(9).(2003).095503

Xie and Emory. SCIENCE. 275. (1997).1104

Scanning Thermal Microscopy

A.Majumdar. Ann. Rev. Mat. Sci. 29.(1999).505-585.

C. Williams and K. Wickramasinghe. Appl. Phys. Lett.49 (1986).1587.

Hammiche, et.al. Measurement Science and Technol. 7(2).(1996).142.
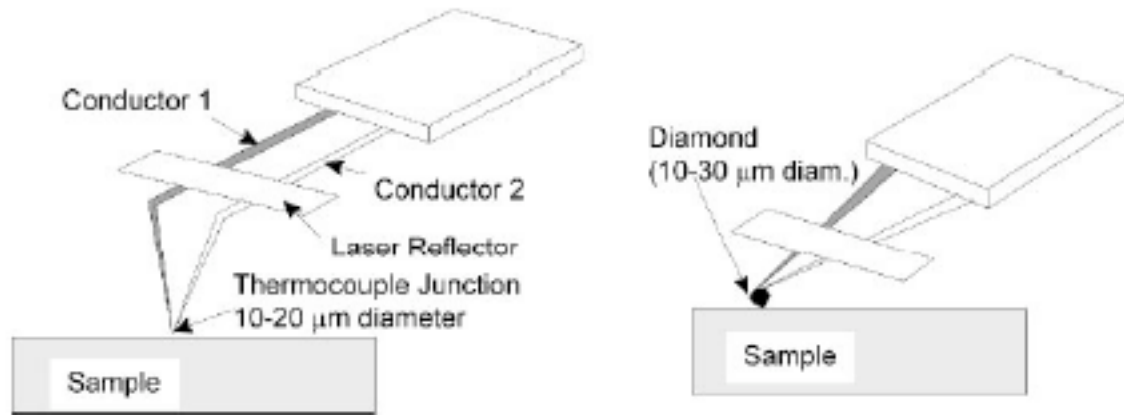
Hammische et.al. Applied Spectroscopy. 53(7).(1999).810.

Scanning Ion Conductance Microscopy (SCIM)

P. Hansma, et.al. Science.243 (1989).641.

Korchev et.al. Biophys. J. 73 (1997).653.

Rheinlaender et.al. J. Appl. Phys. 105 (2009)094905.

Thermal Conductance Microscopy

Figure 8 Experimental apparatus and details of the cantilever thermocouple probe used for SThM (22).

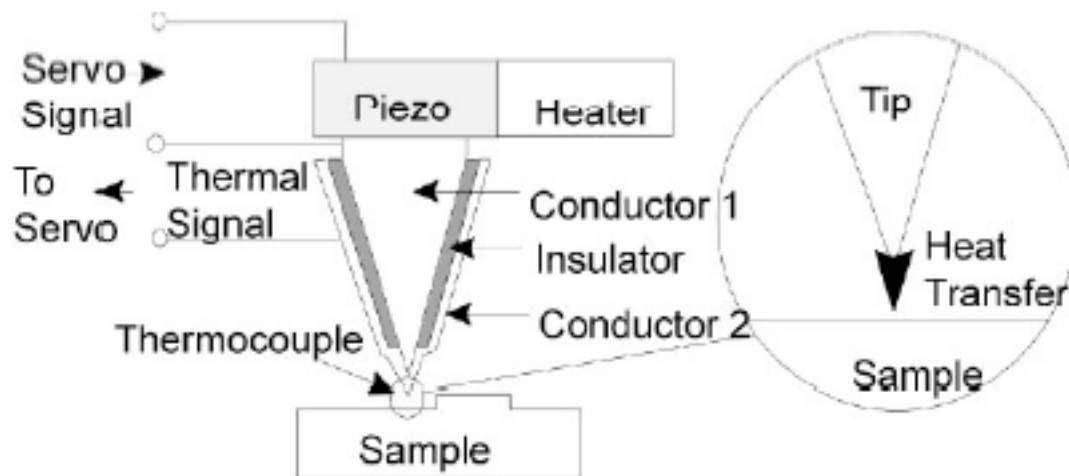Majumdar A, Carrejo JP, Lai J. 1993. *Appl. Phys. Lett.* 62:2501–3

Figure 1 Schematic diagram of the scanning thermal profiler (13).

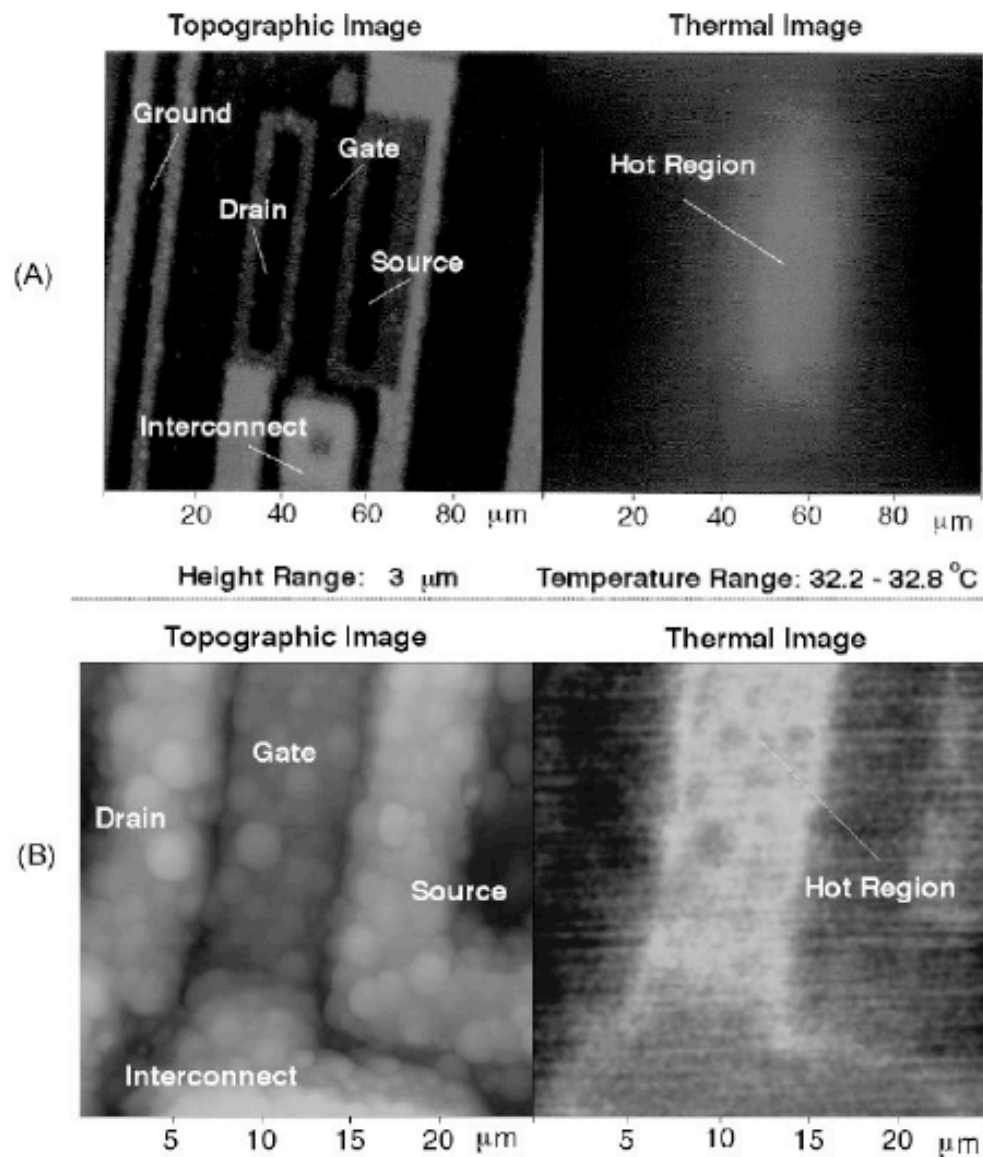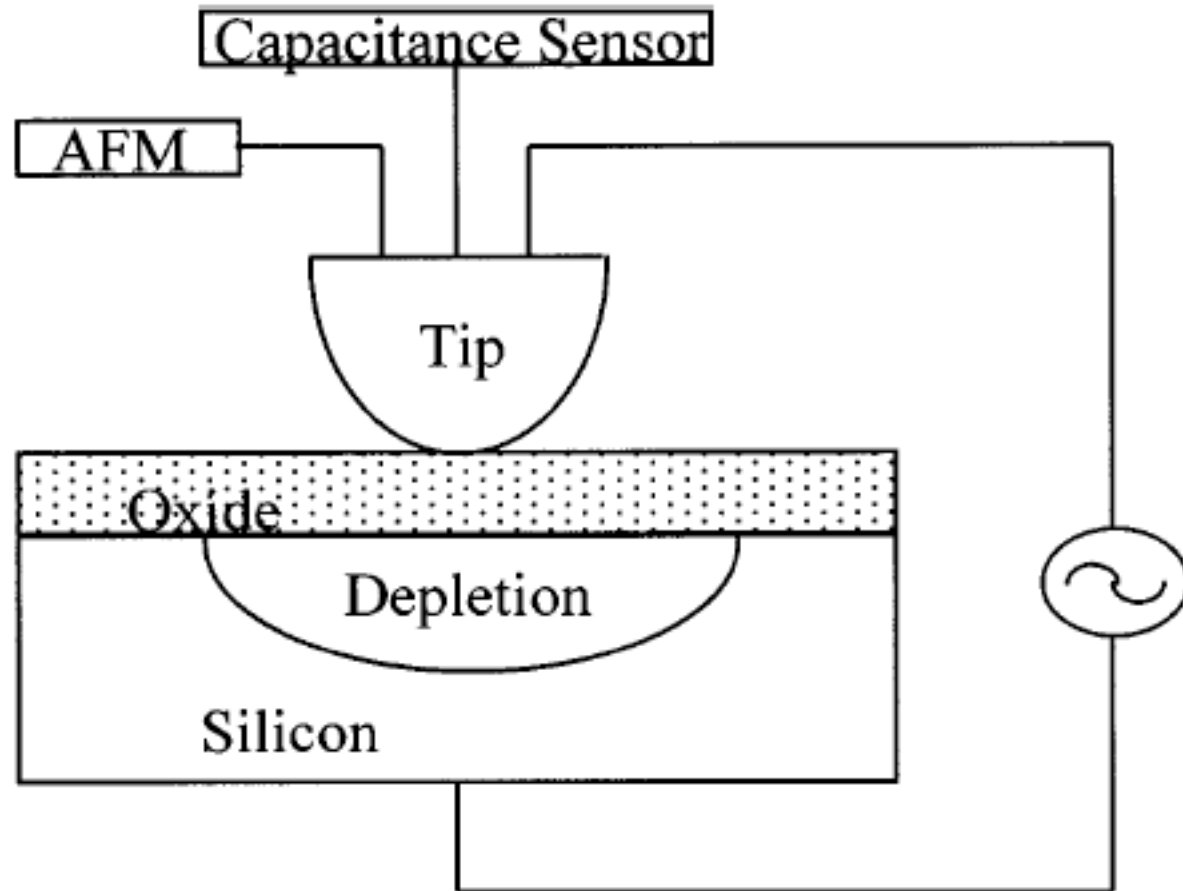Williams CC, Wickramasinghe HK. 1986.
Appl. Phys. Lett. 49:1587–89

Figure 14 Topographical and thermal images of a Si-MOSFET obtained with a diamond-tip wire thermocouple cantilever SThM probe: (a) 100 μm × 100 μm scan size and (b) 25 μm × 25 μm scan size (25).

Nakabeppu O, Igeta M, Hijikata K. 1997.
Microscale Thermophys. Eng. 1:201–13
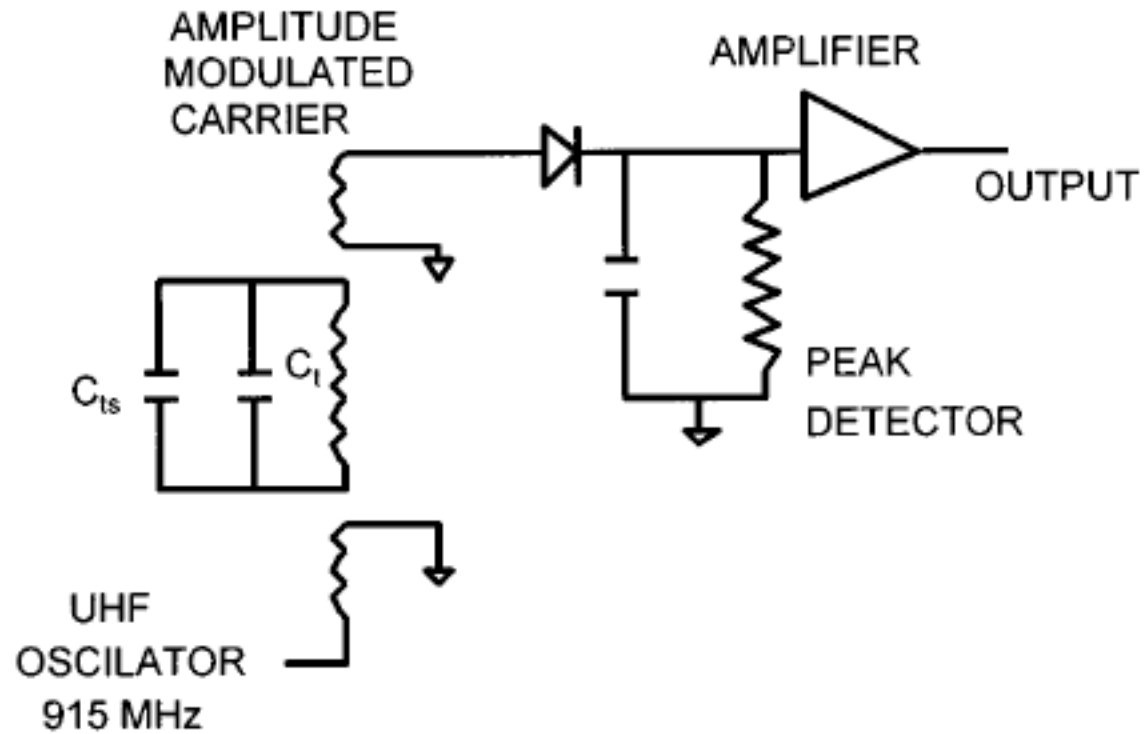
Scanning Capacitance Microscopy

Figure 2 System drawing of a generic SCM with AFM topographic control.

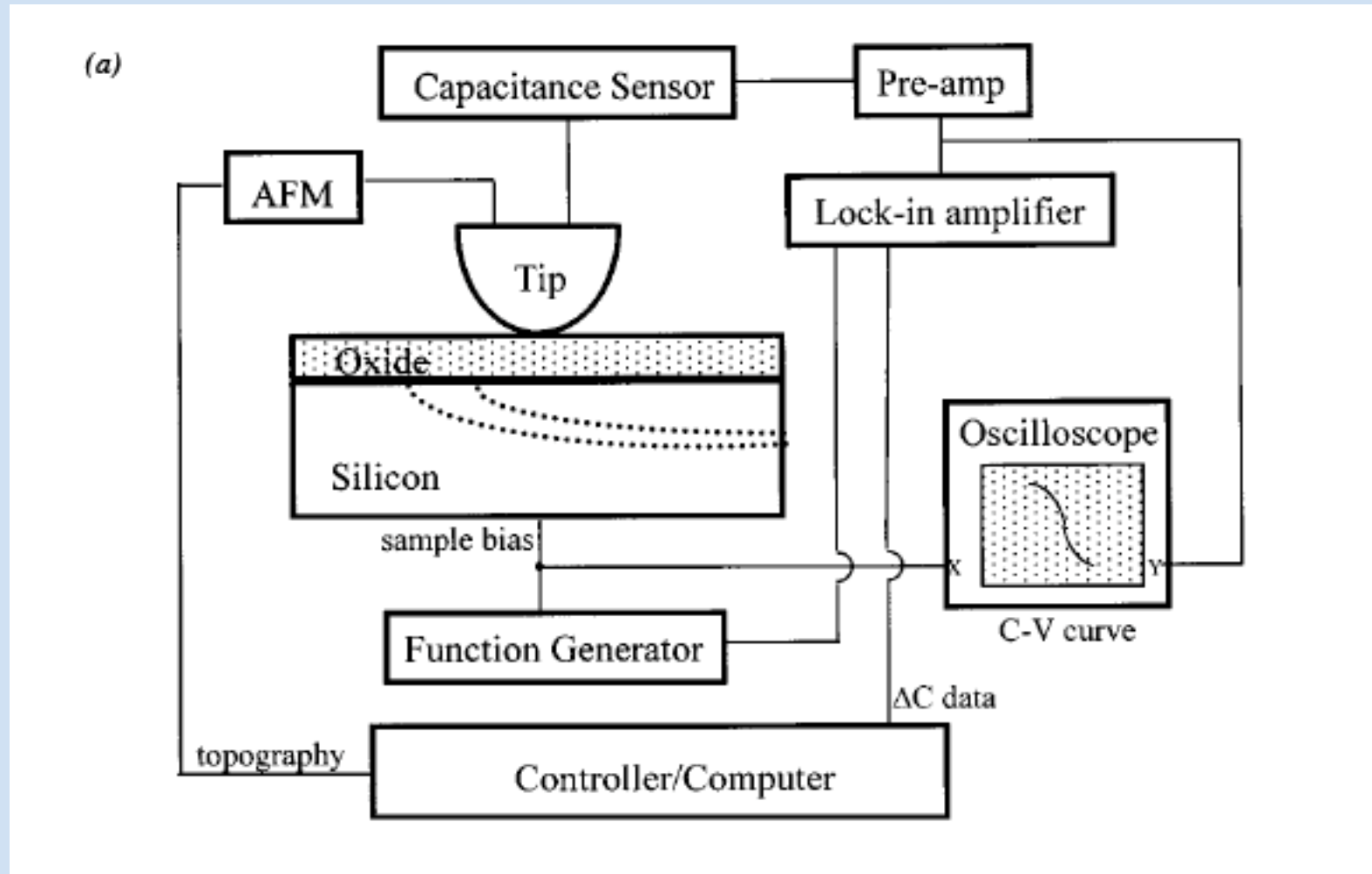C.C. Williams (Ann. Rev. Materials Science.29(1999).474-504.

Capacitance sensor

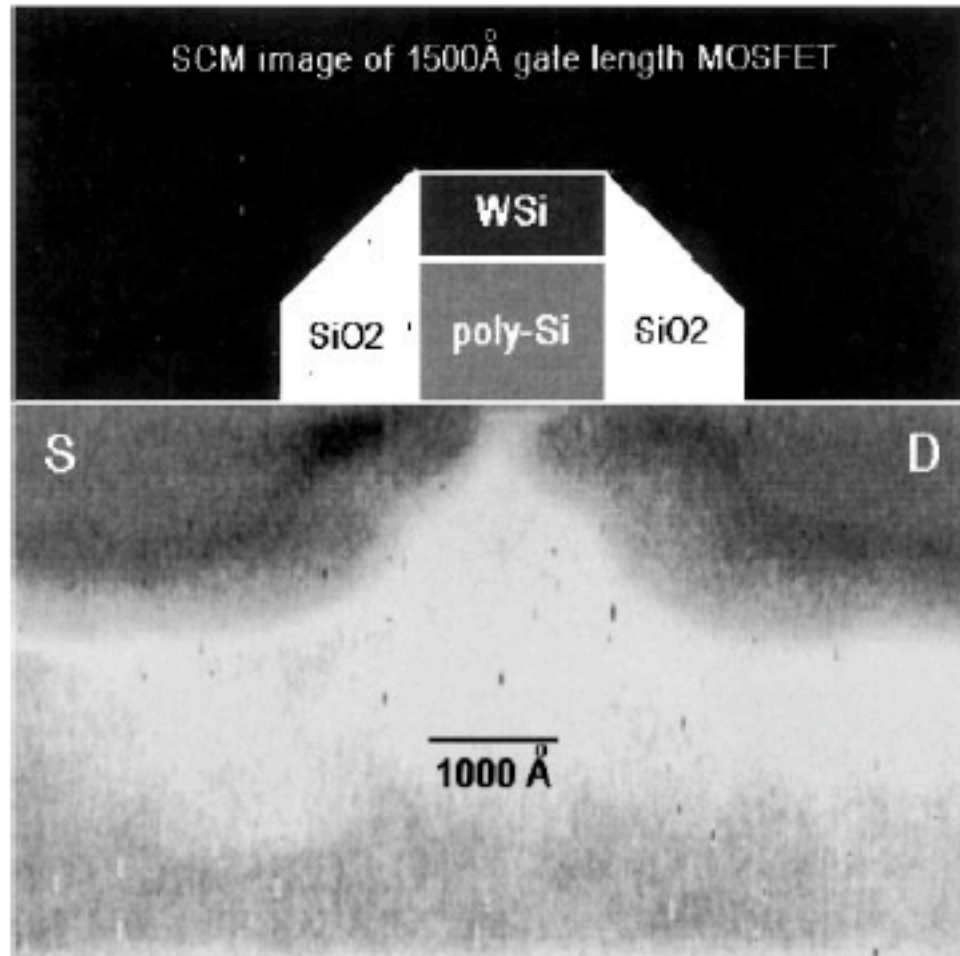Figure 3   Schematic diagram illustrating the RCA capacitance sensor.

From Palmer et.al. RCA Review.43(1993)194

Capacitance Microscopy

From Clayton Williams. 1999

(b)

SCM image of 1500Å gate length MOSFET

WSi

SiO2 poly-Si SiO2

S D

1000 Å
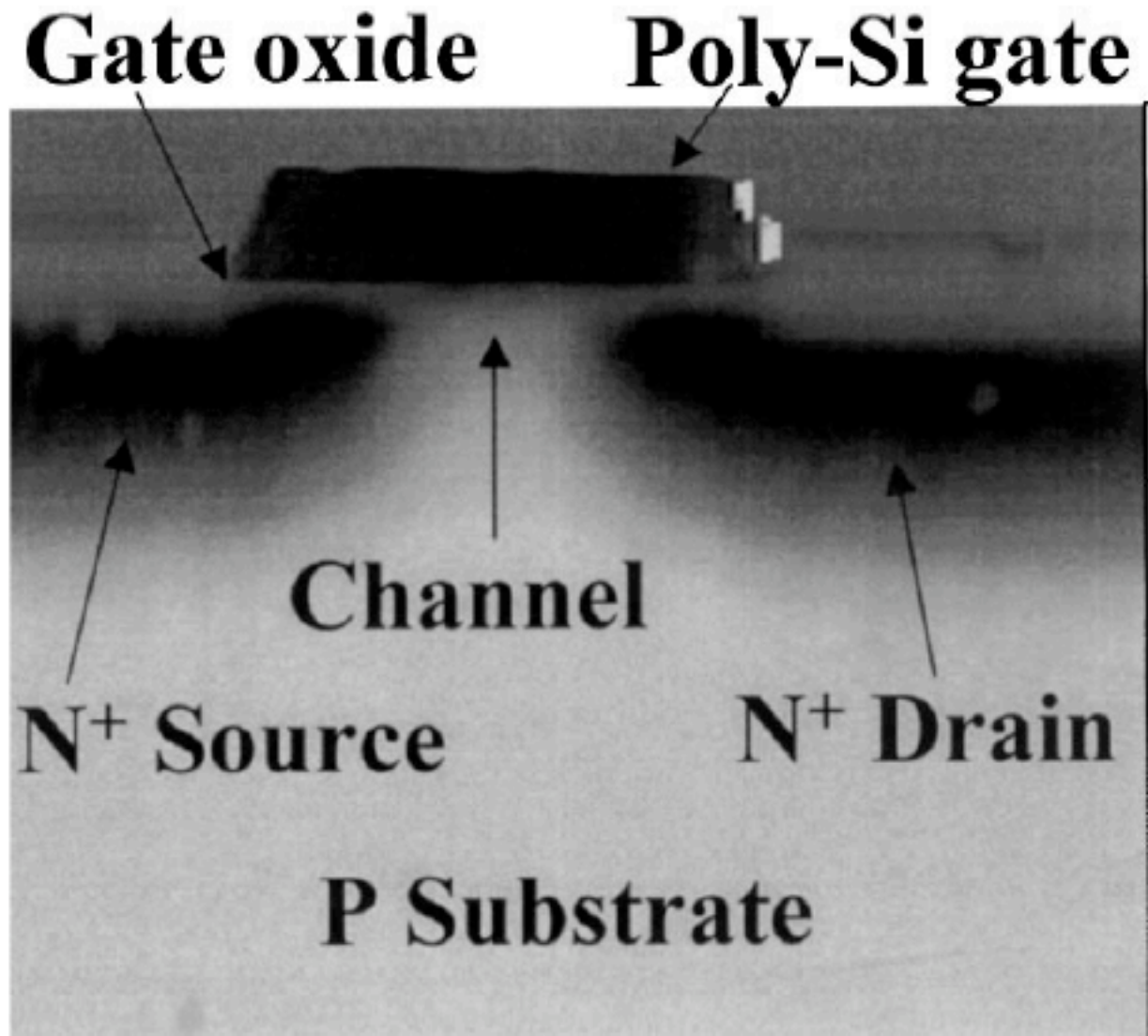
Figure 1 SCM image of a cross-sectioned MOSFET device structure showing the key elements

From C.C. Williams. 1999

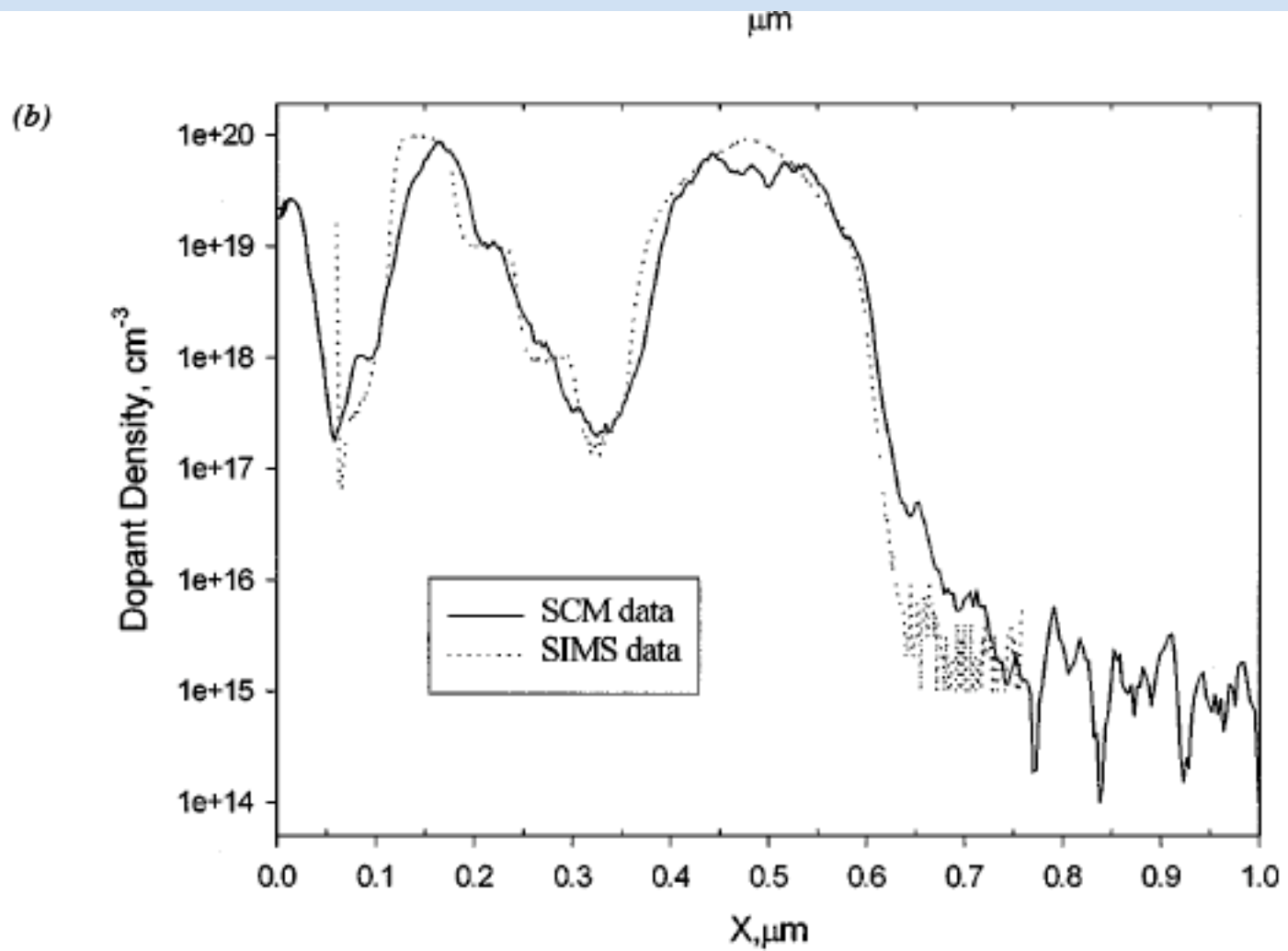Figure 17 (a) Comparison of a converted SCM profile with a spreading resistance profile (SRP) on a large stepped dopant structure. (b) Comparison of a converted SCM profile with a SIMS measurement on a much smaller scale dopant profile with 50-nm steps.
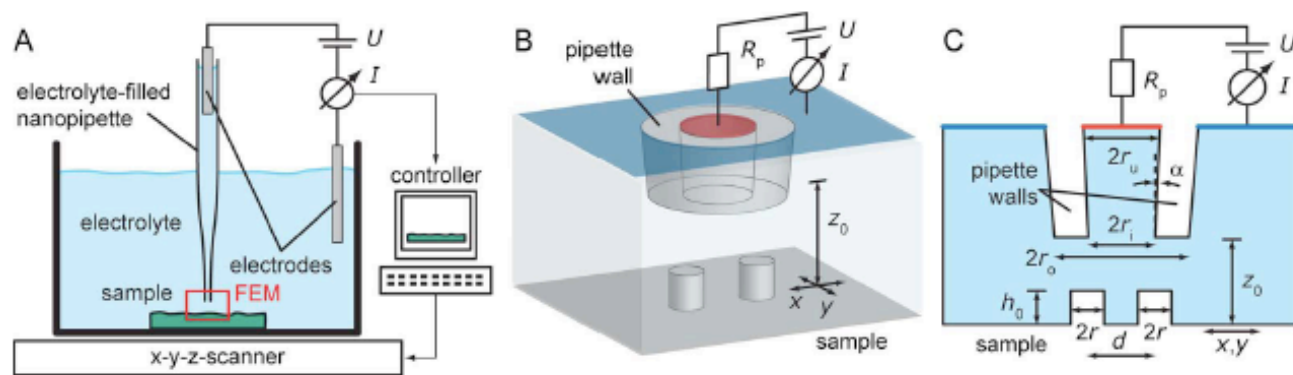
From C.C. Williams, 1999

FIG. 1. (Color online) (a) Schematic of a SICM setup, which is based on an electrolyte-filled nanopipette. The ion current, I, induced by an applied voltage between the two electrodes, U, is measured by a nanoampere amplifier and used for feedback via a computer-based controller and an x-y-z-scanner. (b) Three-dimensional schematic and (c) two-dimensional cross section of the pipette tip region that are modeled with finite element analysis, indicated by a red box in (a), here shown for a planar sample with two cylindrical particles (radius r, height h_0, and distance d). The scanning process is simulated by changing the relative pipette-sample orientation (x,y,z_0). A series resistance R_p suffices to model the remaining upper part of the pipette.

Scanning Ion Conductance Microscopy (SICM)
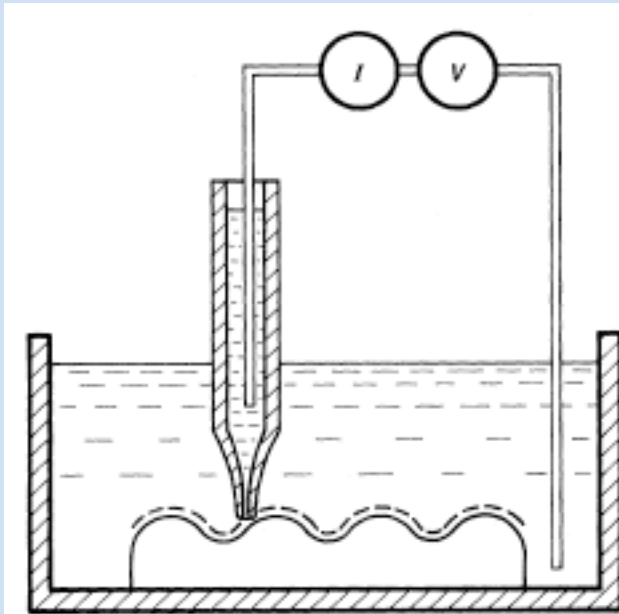
Fig. 1. The SICM scans a micropipette over the contours of a surface by keeping the electrical conductance through the tip of the micropipette constant by adjusting the vertical height of the probe.
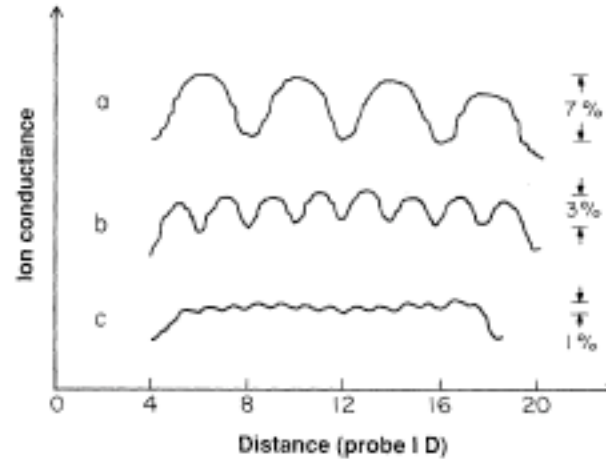
Fig. 2. Resolution test for the SICM. A pipette with an ID of 0.71 mm and an OD of 1.00 mm was scanned at constant height over three grooved plastic blocks with spacing of (a) four times, (b) two times, and (c) the same as the ID of the pipette. A 0.1M NaCl solution covered the blocks and filled the pipette. Note that even the grooves spaced by the ID of the pipette could be resolved.

From P. Hansma, et.al.
SCIENCE.243 (1989).641
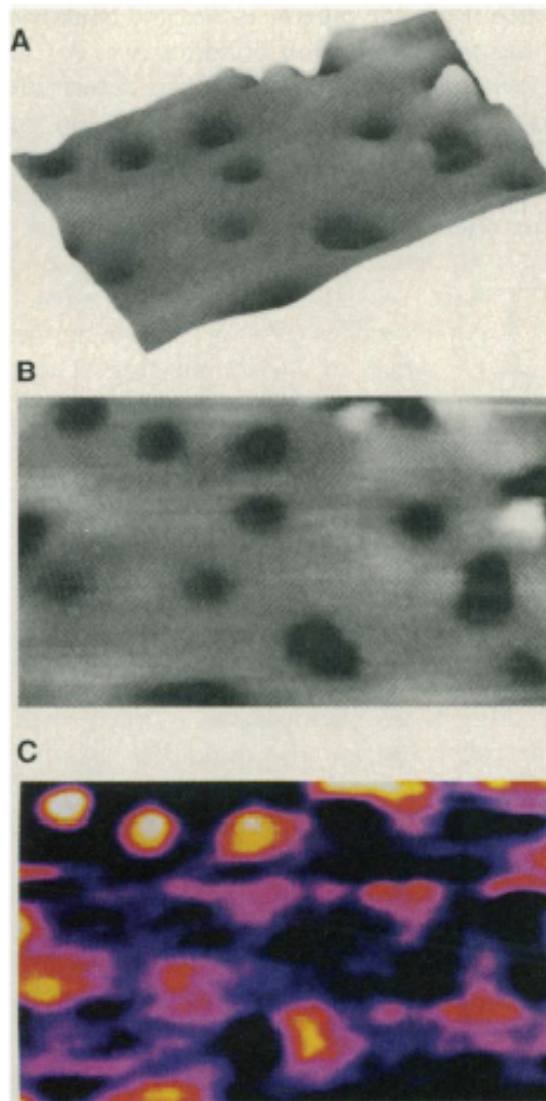
Fig. 4. (**A**) A SICM topographic image of the 0.8-μm diameter pores in a Nuclepore membrane filter (24). (**B**) The same image presented in a top view. (**C**) A SICM image of the ion currents coming out through the pores. The false colors go from black at the background level of current, 8 nA, up to white at the maximum level of ≈40 pA above the background. The imaged area is 7.8 μm by 4.5 μm for all three images.
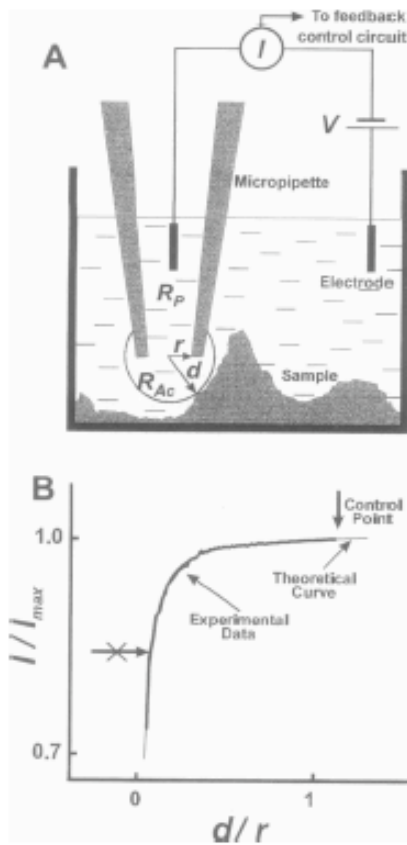
From p. Hansma, et,al. 1989

FIGURE 1 Diagram of sensing mechanism of the scanning ion conductance microscope. (A) The micropipette tip/surface interaction. The position of the micropipette tip relative to the sample surface strongly influences the access resistance (R_{Ac}) and, consequently, the ion current (I) flowing through the pipette. The current value at a distance (d) that exceeds the radius (r) can be used to control the vertical position of the tip to sense neighboring structures that are higher than the vertical sample/probe separation. During the scan, the tip of the pipette, with its "spherical current sensor" of radius d, "rolls" over surface irregularities of the specimen without damaging it. (B) Comparison of expected and actual values of tip current (I) as a function of the sample/tip separation (d). The theoretical curve was calculated for a simplified model of a frustum (truncated cone)-shaped tip of known geometry approaching a flat, nonconductive surface. The experimental data show the approach characteristic of a tip of similar geometry. The vertical arrow indicates the value of current (control point) used for the scanning protocol in the feedback control circuit.
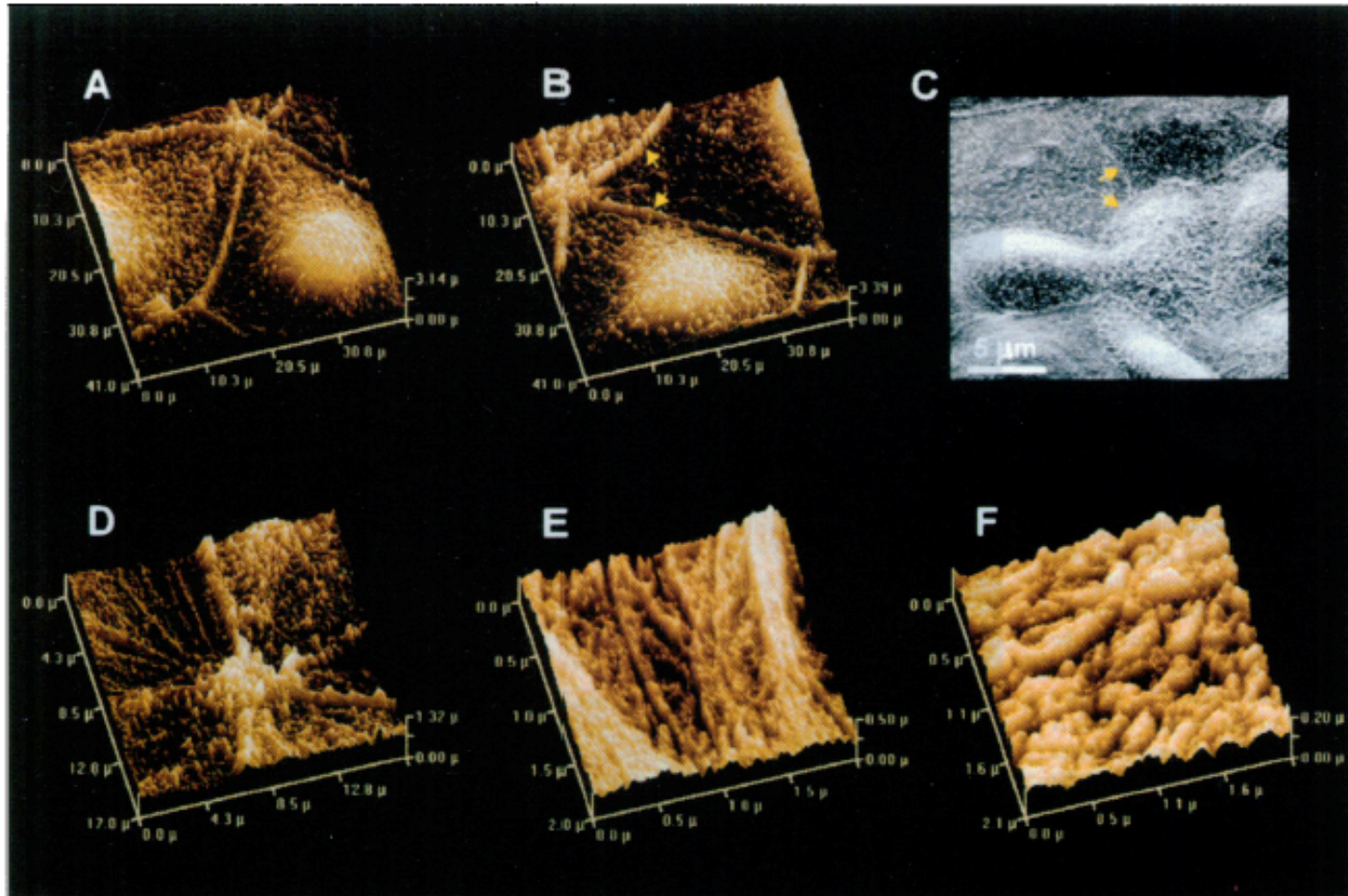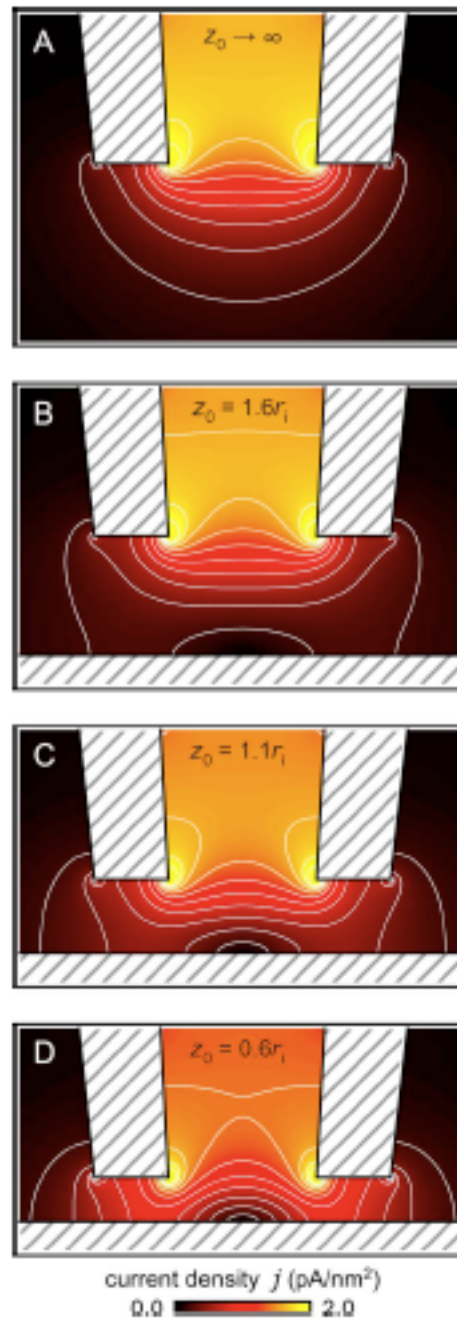
Korchev, et.al. 1997

Korchev, et. al. Biopphys.J.73(1997)653.
SICM

FIGURE 3 (*A, B, D–F*) Scanning ion-conductance microscope images, in real time, of a confluent monolayer of a human colon cancer cell line (Caco-2) in a 1:1 mixture of phosphate-buffered saline and medium (RPMI 1640 with 20% fetal calf serum). During the 8-h period of continuous scanning (monitoring), the cells remain viable and motile. *A* and *B*, separated by 140 min, show movement of the "junction" between five cells. The nuclear regions of two cells are discernible under the membrane as the lighter areas, and the boundaries between cells (*arrows*) appear to be raised. At higher magnification a variety of surface morphologies were observed in the five adjacent cells (*D–F*). One cell (*top left in D,* and at higher magnification, *E*) showed filamentous structures, reminiscent of microfilaments, converging on the "junction." Other cells had numerous surface projections, possibly microvilli. The projections (*top right in D,* and at higher magnification, *F*) can represent a developing brush border. (*C*) Scanning electron micrograph of Rama 25 mammary carcinoma cells in culture. The cells were grown on plastic in culture medium with serum (Bennett et al., 1978). Microvillous cell surfaces, with denser microvilli marking cell boundaries (*arrows*), can be observed. These cells grow in culture as a single layer (monolayer), similar to the human colon cancer cells. (This scanning electron micrograph was kindly provided by Dr. D. C. Bennett.)
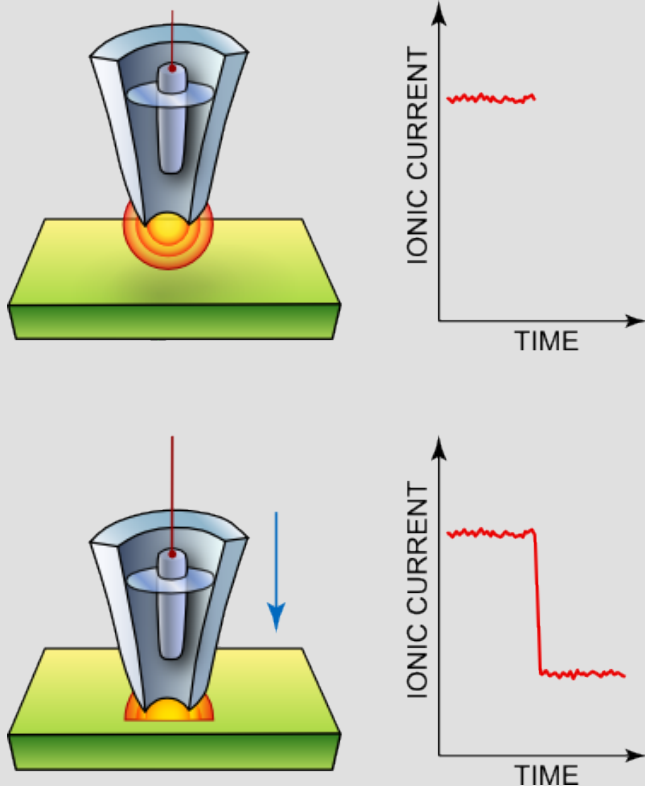
Scanning Ion Conductance Microscopy

FIG. 2. (Color online) Cross section through the pipette showing the calculated distribution of the ion current density in the tip region. (a) When the pipette-sample distance is much larger than the inner pipette radius ($z_0 \gg r_i$), the current density below the tip has approximately spherical isosurfaces (white lines: equally spaced contour lines at $0.2, 0.4, \ldots, 2.0$ pA/nm^2). (b) When the tip comes into the vicinity of a planar sample ($z_0 = 1.6 r_i$), these isosurfaces start deforming. [(c) and (d)] At even smaller pipette-sample distances ($z_0 = 1.1 r_i$ and $z_0 = 0.6 r_i$, respectively), a ring-shaped area of high current density is formed below the pipette walls. Parameters used for this figure: inner pipette radius $r_i = 25$ nm, outer pipette radius $r_e = 2 r_i$, conductivity $\sigma = 1$ S m^{-1}, and applied voltage $U = 1$ V.
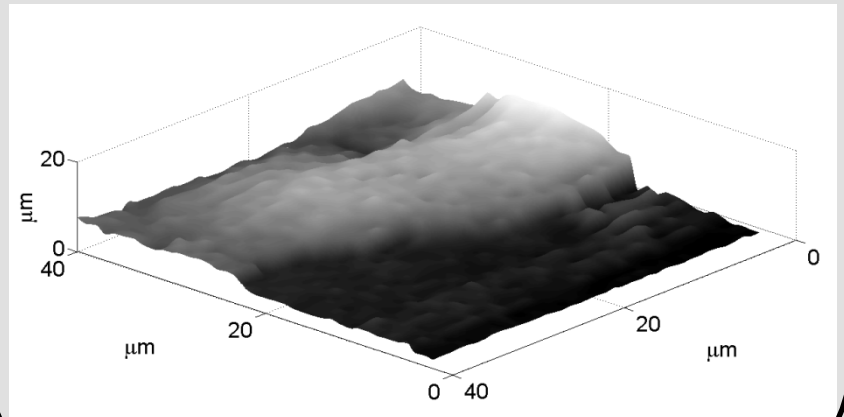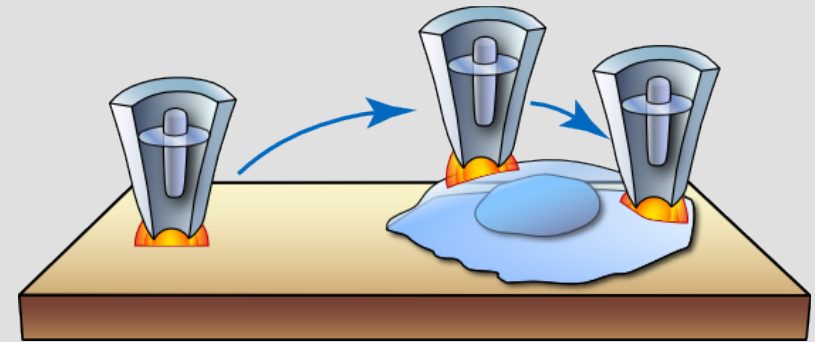
From Rheinlaender, et al. J.Appl. Phys. 105(2009)

Scanning Ion Conductance Microscope (SICM)

Electrical Feedback

Topographical Mapping

IONIC CURRENT

TIME

IONIC CURRENT

TIME

HeLa Cell

Pourmand, Seger et.al. Nanoscale. 2012